Technische Universität München
Lehrstuhl für Kommunikationsnetze

Strategic Network Planning for Converged Optical Networks

Elena Grigoreva M. Sc.

Vollständiger Abdruck der von der Fakultät Elektrotechnik und Informationstechnik der Technischen Universität München zur Erlangung des akademischen Grades eines

Doktor-Ingenieurs (Dr.-Ing.)

genehmigten Dissertation.

Vorsitzender:		Prof. Dr.-Ing. Norbert Hanik
Prüfer der Dissertation:	1.	Priv.-Doz. Dr.-Ing. habil. Carmen Mas Machuca
	2.	Prof. Lena Wosinska, Ph. D.

Die Dissertation wurde am 13.11.2019 bei der Technischen Universität München eingereicht und durch die Fakultät für Elektrotechnik und Informationstechnik am 25.03.2020 angenommen.

Strategic Network Planning for Converged Optical Networks

Elena Grigoreva M. Sc.

July 18, 2020

Abstract

Declining revenues, increasing network costs, new stringent and heterogeneous user requirements place a set of challenges for the Network Providers (NPs). An example of new requirements could be ultra-reliable communications with 0.99999 availability requirement for mission critical services, 1ms delay for tactile Internet or 10 Gbps capacity per sector for the centralized 5G cloud Radio Access Network (RAN). The traditional approach of building an individual optical networks for every application, i.e., residential access and mobile backhaul in 4G, would be cost prohibitive in this case. This means that the NPs have to find the ways to reduce the network costs and maximize revenues. The strategic business decisions on the network implementation and upgrade are made based on the results of strategic network planning.

In this dissertation, we take a holistic approach on strategic network planning for converged optical networks. By converged networks we refer to sharing of the physical infrastructure (ducts, sites, etc.) and technologies for different network types that traditionally would be independent (optical access and backhaul networks). The strategic network planning work-flow was implemented in a Automated Map-Based Strategic Fixed Network Planning Tool (AMS) to allow reproducibility and comparability of the results, as well as future extensions.

We start from investigating the possible generalizations of the strategic network planning results by using graph-based road topology models instead of specific area maps. Then, we look into implications of providing for the reliability requirements of the ultra-reliable communication heterogeneous wireless protection for the mission critical communication. The studies are done for the converged Optical Distribution Network (ODN) and for a wireless access network. We continue with analyzing the energy consumption of converged ODNs, its influence on reliability and delay. To enable energy-saving methods, we propose a network-initiated equipment wake-up method (to switch the equipment back to the active state from the sleep or dooze state) for packet switched networks. We compare the delay and energy performance of our proposed method to the measure the state-of-the-art circuit switched method.

Finally, we investigate network migration planning, i.e., multi-period strategic network planning problem. To guarantee the network profitability, we maximize the Net Present Value (NPV) under the condition that user's requirements are satisfied. We further deal with user uncertainty, i.e., users leaving the NP or user churn, with the rational agent based algorithm.

Kurzfassung

Die Telekommunikationsanbietern werden vor eine Reihe von Herausforderungen gestellt: abnehmende Einnahmen, steigende Netzwerkkosten, neue strenge und heterogene Benutzeranforderungen. Z. B., die extrem zuverlässige Kommunikationen erfordern Verfügbarkeit von 0,99999; taktiles Internet erfordert eine Latenz von 1 ms, und für zentralisierte 5G-Cloud RAN wird eine Kapazität von 10 Gbps pro Sektor benötigt. Normalerweise, wird für jede Anwendung ein separates optisches Netzwerk wird aufgebaut, z. B., optische Zugangsnetz und mobiles Backhaul. Für die vielfältigen neue Anwendungen wäre dies nicht wirtschaftlich. Die Telekommunikationsanbietern müssen die Netzwerkkosten senken und die Einnahmen maximieren. Das sind die Aufgaben der strategischen Netzwerkplanung.

In dieser Dissertation, verfolgen wir einen ganzheitlichen Ansatz zur strategischen Netzwerkplanung für optische Netzkonvergenz. Unter Netzkonvergenz ist die gemeinsame Nutzung der physischen Infrastruktur (Kabelkanäle, Standorte, usw.) und Technologien für verschiedene Netzwerktypen, die traditionell unabhängig waren (optische Zugangs- und Backhaul-Netzwerke) gemeint. Der Workflow für die strategische Netzwerkplanung wurde in einem AMS implementiert, um die Reproduzierbarkeit und Vergleichbarkeit der Ergebnisse sowie zukünftige Erweiterungen zu ermöglichen.

Wir fangen mit der Untersuchung möglicher Verallgemeinerungen der Ergebnisse der strategischen Netzwerkplanung an, indem wir Graph-basierte Straßentopologiemodelle anstelle spezifischer Gebietskarten verwenden. Anschließend untersuchen wir die Auswirkungen der Bereitstellung der Zuverlässigkeitsanforderungen für die heterogenen extrem zuverlässigen Kommunikation. Die Studien werden für das konvergierte ODNs und für ein drahtloses Zugangsnetzwerk durchgeführt. Wir fahren mit der Analyse des Energieverbrauchs von konvergiertem ODNs fort, und evaluieren dessen Einfluss auf Zuverlässigkeit und Latenz. Um energiesparende Methoden zu ermöglichen, schlagen wir für paketvermittelte Netzwerke eine netzwerkinitiierte Aktivierungsmethode für Geräte vor (um die Geräte aus dem Schlaf- oder Schlummerzustand in den aktiven Zustand zurückzusetzen). Wir vergleichen die Latenz und die Energieeffizienz unseres vorgeschlagenen Verfahrens mit der Messung des Standart schaltungsvermittelten Verfahrens.

Schließlich untersuchen wir die Netzwerkmigrationsplanung, bzw. ein strategisches Netzwerkplanungsproblem mit mehreren Planungsperioden. Um die Wirtschaftlichkeit des Netzwerks zu gewährleisten, maximieren wir den NPV unter der Bedingung, dass die Anforderungen des Benutzers erfüllt werden.

Contents

Abbreviations

ADSL2+ Asymmetric Digital Subscriber Line 2+

AI Artificial Intelligence

AMS Automated Map-Based Strategic Fixed Network Planning Tool

AP Access Points

ARPU Average Revenue Per User

AWG Array WaveGuide

BS Base Station

BTS Base Transceiver Station

C.U. Cost Unit

CapEx Capital Expenditures

CO Central Office

CSM Critical Safety Messaging

DBA Dynamic Bandwidth Allocation

DD Distribution Duct

DF Distribution Fiber

DLEP Dynamic Link Exchange Protocol

DRX Discontinuous Reception

DSL Digital Subscriber Line

DSLAM Digital Subscriber Line Access Multiplexer

DSRC Dedicated Short Range Communication

DXT Digital Switch

ECM Evolved packet system Connection Management

EMM Evolved packet system Mobility Management

eNB evolved Node B

EPC Enhanced Packet Core

FD Feeder Duct

FF Feeder Fiber

FTTA Fiber-To-The-Antenna

FTTB Fiber-To-The-Building

FTTCab Fiber-To-The-Cabinet

FTTH Fiber-To-The-Home

FTTx Fiber-To-The-X

GG Gabriel Graph

GPON Gigabit Passive Optical Network

GSM Global System for Mobile communications

HPON Hybrid Passive Optical Network

HT Hybrid Terminal

HVAC Heating Ventilation and Air Conditioning

IMS IP Multimedia Subsystem

IoT Internet-of-Things

ITS Intelligent Transportation System

LOS Loss of Signal

LTE Long Term Evolution

MBS Macro Base Station

MDU Multiple Dwelling Unit

MNO Mobile Network Operator

MTC Machine Type Communication

NAT Network Address Translator

NGOA Next Generation Optical Access

NP Network Provider

NPV Net Present Value

ODN Optical Distribution Network

OLT Optical Line Terminal

ONU Optical Network Unit

OpEx Operational Expenditures

OSM Open Street Maps

OSW Optical SWitch

OTT Over-The-Top

P2P Point-to-Point

P-Active Disjoint Fiber Protection

P-AS Energy-Efficient Disjoint Fiber Protection

PGT Procedural Generated Topology

PoC Proof-of-Concept

PON Passive Optical Network

PS Power Splitter

PV Present Value

RAN Radio Access Network

RBD Reliability Block Diagram

RHS Right Hand Side

RN Remote Node

RP Reflective Disjoint Fiber Protection

RRC Radio Resource Control

RSU Road Side Unit

RxMon Monitoring Receiver

SC Small Cell

SDCCH Standalone Dedicated Control CHannel

SIP Session Initiation Protocol

SLA Service Level Agreement

SMS Short Message Service

SMS-SC SMS Service Center

SR Splitting Ratio

SS Service Server

SSD Sleep Slot Duration

TBS TETRA Base Station

TCO Total Cost of Ownership

TDM Time Division Multiplexing

TETRA Terrestrial Trunked Radio

TxMon Monitoring Transmitter

UDP User Datagram Protocol

UDWDM Ultra Dense Wavelength Division Multiplexing

UE User Equipment

UP UnProtected

VDSL Very high speed Digital Subscriber Line

VIO Vertically Integrated Operator

VoIP Voice over IP

VoLTE Voice over Long-Term Evolution

WDM Wavelength Division Multiplexing

WLAN Wireless Local Area Network

XGPON 10-Gigabit Passive Optical Network

1. Introduction

With the growing popularity of the bandwidth-hungry services as high definition video streaming or gaming, the user requirements to the telecommunication networks are becoming more demanding. These requirements result in the need of network upgrades, for example migrations from copper to fiber for the fixed networks or 2G-3G-4G-5G upgrades for mobile networks, and thus imply higher costs for an NP. In order for the NP to stay profitable, there are two potential ways: increase the Average Revenue Per User (ARPU) and/or decrease the Total Cost of Ownership (TCO) of the network.

Traditionally, the fixed access network market was characterized by no or limited competition, e.g., there was a single national telephone company providing the connectivity and the service. The increase in the ARPU was easily achieved through the increase of the respective user tariffs. With the market development and appearance of competitors (supported by the regulators to avoid monopoly), the increasing of the ARPU by a single NP is not possible anymore as the customers can switch to a cheaper NP alternative. Hence, the revenues of the traditional NPs are not increasing at best [14]. On the other hand, the costs of the network maintenance and upgrade are growing due to the increasing network complexity. To be able to decrease the overall network costs or the TCO, an NP has to understand and analyze its components. The network TCO or costs of the network implementation, upgrade and operation are divided into Capital Expenditures (CapEx) and Operational Expenditures (OpEx) [15].

Capital Expenditures (CapEx) [63] are the investments that are depreciated over time. CapEx comprise the cost of physical infrastructure (e.g., buildings, land), network infrastructure (e.g., ducts, fiber, equipment, supporting software) and planning costs. CapEx is always taken into account when making financial decisions.

The **Operational Expenditures (OpEx)** [17] do not contribute to the infrastructure and are not depreciated over time. OpEx includes all the costs associated to keep the company operational: energy costs, rent or lease costs for the equipment sites, maintenance costs, salaries and marketing costs, etc. Due to their complexity, OpEx were neglected or significantly simplified in the TCO evaluation, which led to unpredictable TCO under- and overestimations. The accurate TCO estimation is vital for a correct project profitability evaluation. The unpredictable difference of the estimated TCO to the real one can cause wrong business decisions and potentially loosing millions of Euro in lost investments or revenues.

Long-term business and technical decisions are made during the **strategic network**

planning based on the project profitability evaluation. Strategic network planning includes market forecasting, techno-economic modeling and the identification of the most economically attractive technologies that satisfy user requirements. The strategic network planning operates with the estimated TCO that includes the results of the approximated network planning and equipment dimensioning. Although TCO estimation is complex and time consuming, it is unavoidable for profitability estimation as $Profits = Revenues - Costs$.

Strategic network planning depends not only on the planning algorithms, but also on the quality of the input data. The input data in the strategic network planning is the information about the network deployment area (for example a consistent map of an area), demands' capacity and their locations, and a set of prospective technologies with respective techno-economic models for CapEx and OpEx calculation.

The current industrial state-of-the-art for the NPs is to deploy and operate in the same geographical area completely separate optical access network for the fixed users and the optical backhaul network of the mobile access network, e.g., with the Macro Base Stations (MBSs) as demands for the optical backhaul. This separation results in high CapEx and OpEx. An intuitive solution to this TCO problem, is to find a possibility of reusing the existing infrastructure to reduce CapEx and making use of the new available technologies to reduce OpEx. A network that combines traditionally separate networks (e.g., fixed access and backhaul, multiple technologies or heterogeneous demands) in one is called a **converged access network** and the planning of such networks is **converged network planning**. Converged network planning is sometimes referred to as joint network planning, but for consistency purposes we use the term converged planning. In this dissertation, when we refer to "network planning", we refer to strategic network planning. In the next section, we introduce the research challenges that stem out of the introduced here state-of-the-art status.

1.1. Research Challenges

NPs face technological and business challenges due to the introduction of the new users, e.g., Internet-of-Things (IoT), and services, e.g., ultra-reliable communications. Depending on the concrete use case, the emerging requirements can be as stringent as 1 ms delay [127], 0.99999 availability [126], or 10 Gbps capacity per sector per MBS [18]. Deploying an individual single purpose fixed network for each use case, would satisfy the requirements of each use case at a cost of prohibitive TCO. The NPs have to face these new requirements, and evaluate their challenges, benefits and opportunities in order to stay in the market and grow. The problem for the NPs is two fold: satisfy the customers' needs while reducing the TCO to increase profitability. Satisfying the wide range of increasing and emerging customer demands in fixed connectivity can be achieved with ODNs. ODNs architectures, technologies and costs have to be evaluated accordingly.

In general, strategic network planning aims at minimizing the costs, while satisfying the user requirements. Significant CapEx reduction, can be achieved by reusing the existing network infrastructure as much as possible. The scenario where there exists a reusable infrastructure is called **brownfield**. Otherwise, the planning has to be done from the ground up, which is referred to as **greenfield** scenario. One example of a brownfield scenario is planning a Passive Optical Network (PON) in an area with an existing copper network, e.g., fixed telephone line. Regarding OpEx, reusing an older technology, normally results in higher OpEx due to equipment aging and higher energy consumption. It was shown that the energy costs are a major cost driver of the OpEx [95]. Moreover, the energy consumption grows with the expanding capacity of the networks, as more equipment is needed. There is a need in evaluation of the energy-saving options as addressed in this dissertation.

There are many approaches in network planning differing on planning algorithms and possible sets of input data [19]. The planning algorithms can be broadly divided into heuristic, e.g., [43], and optimal, e.g., [16]. The trade-off between the heuristic and optimal solutions is scaling versus precision guarantees. A typical scale of a strategic network planning problem is large: high number of demands (for example, more than 1000 per km^2 in an urban area), high number of road segments in a road graph and their non-Euclidean distances for the path finding. In the planning problems over network life-time, i.e., network upgrade or migration, the scale grows with the problems' dimensions, i.e., time. This makes usage of optimization limited to rather small-scale and mainly non-strategic cases of final planning, where precision is the main goal. Heuristic network planning algorithms allow planning for more relevant in scale problems of strategic planning, where the goal is the estimation of the prospective technologies and the precise planning cannot be done due to the large number of assumptions, uncertainties and limitations due to the early stage of a project. This is why, in this dissertation we concentrate on heuristics and the optimization is left for the future work. Finally, the planning algorithms' implementations are generally not publicly available and often cannot be fully reconstructed from the publicly available publications.

The input data for any network planning algorithm consist of the area models, e.g., geometrical model or geographical map [64], demands, prospective technologies, architectures and respective cost models. This data is generally not publicly accessible and is often case-study specific (especially when maps and area specific geometric models are used). This creates a problem of not reproducible, not comparable scientific results that in the end cannot be generalized or applied to another set of input data. In general, the accurate modeling of the input data is crucial for obtaining meaningful results.

Finally, the new users of the converged networks, e.g., MBSs, demand the availability levels that cannot be guaranteed in ODNs without protection mechanisms, i.e., more than five nines (0.99999) for the ultra-reliable communications. The reliability of an ODN depends on the equipment availability, fiber and duct availability [45]. The

availability of the fiber and ducts is proportional to their length. The lengths are the result of the network planning. An increase in availability can be achieved through redundant components for the weak equipment, while the ducts protection could be achieved by link-disjoint ducts. All the availability increase measures result in additional costs. These additional costs are often prohibitive for the residential access networks due to their low failure impact. The research challenge here is to define efficient protection re-using the existing infrastructure and different protection options suitable for the technology.

1.2. Main Contributions

In this dissertation, we take a holistic approach to strategic network planning for converged optical networks. We start investigating the input data for the planning, i.e., appropriate geography models for initial network planning. Then we define the reliability requirements and the reliability improvement methods, including their evaluation. We further look into the energy consumption minimization and enabling it through the wireless wake-ups. Finally, we include the techno-economic analysis of the planning and planning of network upgrades over time, i.e., migrations. The main contributions of the dissertation are:

- **Automated fixed network planning tool [1].** We developed and published at [1] a geography-based fixed network planning tool. It was based on the ESRI ArcGIS [129] for effective work with maps as SQL-databases and the heuristic algorithm from [43]. The tool provides a strategic network planning implementation for different planning scenarios, details on which are available in Section 2.2 of Chapter 2. It was used to calculate the equipment locations, as well as required fiber and duct lengths for the abstract topologies evaluation (Chapter 3), reliability and energy consumption evaluations in Chapters 4.1 and 5.1, migration planning (Chapter 6). The tool can be extended and modified according to the planning needs. Providing a publicly available tool guarantees that the results are reproducible.

- **Abstract topologies for strategic network planning [4].** In this dissertation, two graph-based models, i.e., Gabriel Graph (GG) [30] and Procedural Generated Topology (PGT) [25], were implemented, analyzed and compared against the analysis results on a real geography map, i.e., Open Street Maps (OSM) [135]. A systematic, expendable and reproducible analysis is presented. The abstract topologies are evaluated based on the graph and planning evaluation results. The planning evaluation was conducted for three urban areas, for different demands and architectures, i.e., Point-to-Point (P2P) and one-stage Gigabit Passive Optical Network (GPON). Based on the evaluation and analysis, recommendations on the models use are given. A generation tool is publicly available [2].

- **Analysis of the existing GPON network reliability for ultra-reliable communications support [6].** We show a reliability analysis of the state-of-the-art pro-

tection schemes in comparison with the unprotected case and evaluate their applicability for the ultra-reliable communications. We also evaluate the cost of protection in terms of additional fiber length.

- **Heterogeneous RAN protection [7].** We present a proof-of-concept of the wireless protection options for the heterogeneous RAN. Our implementation case study considered a RAN containing Terrestrial Trunked Radio (TETRA), Long Term Evolution (LTE) and Wireless Local Area Network (WLAN). We measured the packet loss rates, defined the empirical availability metric and analyzed with the Reliability Block Diagrams (RBDs). Here, we showed based on the Dynamic Link Exchange Protocol (DLEP) testbed that the ultra-reliable levels of availability are achievable in the RAN.

- **Network planning heuristics for energy consumption minimization [6].** We show the adaptation of the network planning heuristics to minimize the energy consumption of the active components, through taking into account the equipment (user) activity patterns. The analysis is done for the greenfield and brownfiled planning and includes the evaluation of additional resources that are needed to make use of the activity pattern.

- **Performance evaluation of wireless wake-ups [5].** The energy savings in the PON are defined by sleeping and doozing [20], it means that the equipment has to be waken-up. We provide, a measurement based proof-of-concept that the waking-up of the equipment can be done though the public mobile networks if the delay requirements are not stringent.

- **Converged optical network migrations model [9].** A rational agent-based migration model is developed and evaluated for residential and converged demand case. It takes into account user adoption uncertainty, as some users that have joined earlier can leave the network. The main contribution of the migration algorithm is the identification of the final migration step based on the maximized NPV or profitability of the project. In the current state-of-the-art, the migration state is normally considered to be fixed, e.g., [34, 39]. Finally, the assumptions of the problem are evaluated in a sensitivity analysis of the important model parameters.

1.3. Thesis Outline

Our umbrella topic is strategic converged network planning, specifically converged planning for optical access networks with fixed demands and optical backhaul for wireless access networks and converged wireless access networks (using multiple wireless technologies). With our holistic approach, we looked into planning, energy consumption, protection and migration aspects of the converged networks. Table 1.1 maps the papers of the author to the chapters and presents the dissertation structure.

Chapter 2 provides the necessary background for the dissertation understanding. First, we define the strategic network planning work-flow and follow its logical structure in our description. We start with defining the concepts for the planning scenario: input modeling (area and demands), network architectures and planning objectives (including protection, energy efficiency or migrations). Then, we discuss the network planning and introduce the AMS. Finally, we introduce the metrics for the techno-economic analysis. These are the necessary steps (and definitions) for a data-based business decision.

Chapter 3 concentrates on the evaluation of two graph-based road topology models for strategic network planning. The comparison is done with respect to the graph and planning analysis of the results obtained based on geographic maps. The graph-based models have the potential to speed-up the strategic network planning by reducing the time for input preparation while maintaining a reasonable estimation quality. Further, such models could allow removing the anomalies of a particular area, making the results more generic. The chapter is concluded with our recommendations on the use of the models.

Chapter 4 introduces the reliability analysis for the fixed and wireless access networks. First, we look into reusing the existing GPON access network for ultra-reliable communications. For this, we evaluate the available protection options in a reliability analysis and the additional resources needed. In the second part, we provide a Proof-of-Concept (PoC) for the wireless heterogeneous protection in a wireless access network. It is achieved through using the diversity of existing technologies and evaluated with a reliability analysis.

Table 1.1.: Thesis content structure and related publications of the author.

		Converged Access Networks	
		Optical networks Access or backhaul (Fixed demands or MBSs)	**Wireless network** Access (Mobile demands)
Chapter 2	**Background**	Strategic network planning tool [1]	
Chapter 3	**Planning**	Road topology modeling [4]	
Chapter 4	**Protection**	Link disjoint 1:1 [6]	Heterogeneous RAN [7]
Chapter 5	**Energy**	Energy savings in PON [6]	Mobile wake-ups [5]
Chapter 6	**Migrations**	Rational agent based migrations [9]	

Chapter 5 covers energy-efficient converged access planning. The first part is dedi-

cated to the planning for the energy-saving in the PONs. The energy consumption is reduced by taking into account the users activity patterns and putting the inactive equipment to energy-saving sleep or dooze modes. In order to enable the energy savings in PON through equipment doozing and sleeping, an effective method of waking-up the equipment has to be used. In the second part of this chapter, we look into waking-up the user equipment with the state-of-the-art industry options.

Chapter 6 presents the rational agent based migration algorithm. It guarantees the maximum overall project profitability and it is the main criterion for the migration path definition. The final state of the migration, in this case, is not predefined from the beginning and is one of the results as well as the maximized NPV. We also take the user churn (users leaving the network) probability into account.

Finally, **Chapter 7** wraps-up the dissertation with a final discussion of the results and outlining the extension directions.

2. Background

This chapter introduces the main definitions and concepts that are within the scope of the dissertation. The chapter follows the strategic network planning work-flow as illustrated in Figure 2.1.

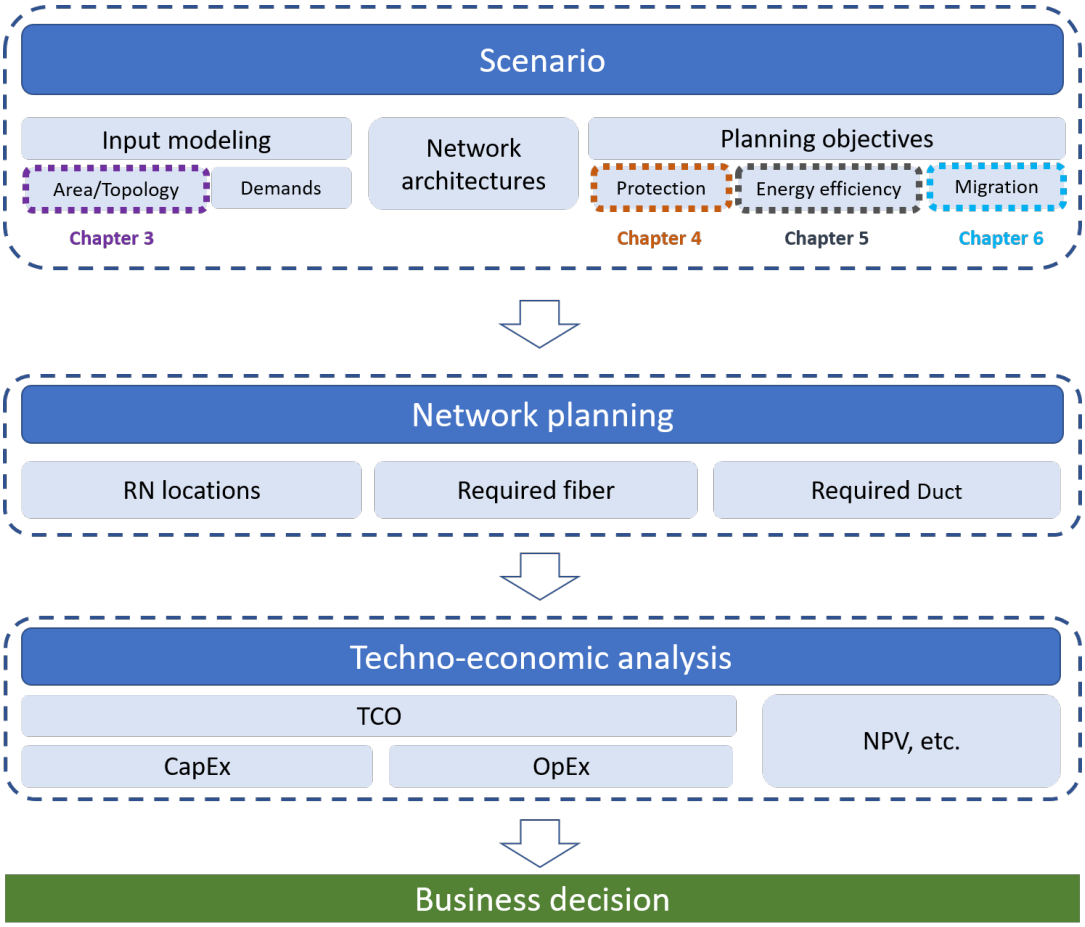

Figure 2.1.: Strategic network planning work-flow.

We define **strategic network planning** as a full pre-project study, which aims at evaluating the required investments to implement a given solution and a particular scenario. Based on the techno-economic analysis results, informed business decisions can be made [59]. Strategic network planning is used to identify the appropriate technology for a particular project, the most suitable strategy of its implementation or migration with the aim of maximizing the project profitability. Thus, the accuracy of the strategic network planning is a key success factor for the entire project.

We follow the strategic network planning work-flow as depicted in Figure 2.1. The chapter begins with the Section 2.1 on network planning scenario, including the necessary definitions for input modeling, network architectures, and main definitions for the planning objectives in focus, i.e., protection, energy efficiency and migrations. The planning objectives directly impact the results of network planning and subsequently the results of the techno-economic analysis. Section 2.1 is concluded with relevant scenario examples. Section 2.2 introduces the network planning methodology and the developed AMS network planning tool [1], which was used in obtaining all the planning results presented in this dissertation. Section 2.3 introduces the metrics for techno-economic analysis. The business decision making is the final goal of the strategic network planning, the business decision would be made based on the final techno-economic metric. For example, the technology with the lowest TCO is chosen for implementation or the project is not implemented if an NPV is lower than zero. The chapter is wrapped-up with the conclusions.

2.1. Scenario

This section describes the scenario of strategic network planning. The scenario consists of input modeling, network architectures and planning objectives. For the input modeling, we define what our planning area and demands models are. Network architectures are presented for optical networks and wireless networks. We also point out different possible convergence options. Finally, we look into possible strategic network planning goals: achieving a certain network reliability level, increasing the energy efficiency or planning the technology migration over time.

2.1.1. Input Modeling

Input modeling consists of planning area and demands modeling. In this dissertation, area model refers to the road model of a particular area size in km^2. In practice, fixed network infrastructure has to follow the roads, either installed in ducts that need to be trenched or in aerial cables supported by poles. The demands are also distributed along the roads. Thus, network planning results, techno-economic analysis and business decision making depend to a great extent on the input modeling.

Area Modeling

Area modeling is equivalent to road topology modeling on a certain surface (in km^2) as it is the road distribution that defines the area for strategic network planning. There are three approaches to area modeling: geographic maps, geometric models and graph-based models.

Geographic maps are the most exact models that include the information about all the known area properties. Digital maps include coordinates and attributes of the

three main data classes: points, lines and polygons. These data classes include not only the roads and buildings, but also endless additional information, for example points of interest (points), administrative boundaries (lines), districts (polygons). Due to the sheer amount of information, it is hard to work with maps and special software has to be used for effective work, e.g., ArcGIS. Moreover, collecting precise geographical data is challenging and expensive work. Therefore, the geographical maps are either expensive and proprietary, or open-source and thus often inconsistent. Finally, geographical maps are by default area specific and can be used only for case studies.

In order to save time and obtain generic results, area models are often used. A common approach is to use geometric models that make use of the average properties of the road and network topologies. There exists a wide range of geometric area models that were shown [30] to unpredictably under- and overestimate the required fiber and duct lengths by up to 30%. This results in unpredictable TCO under- and overestimations and cannot be used for making data-driven business decisions. In Chapter 3, we investigate the applicability of two graph-based area models for strategic network planning. The rest of the dissertation used the Open Street Maps [135] that were prepared for strategic network planning, i.e., the unneeded information was removed or cleaned-up. Here, we do not describe the cleaning-up. An interested reader can refer to Appendix A for more details.

Figure 2.2 shows an OSM example of the planning area of 4 km^2 in central area of Berlin, Germany. The distortion of the square area is due to the projection to the plane for the correct length calculation.

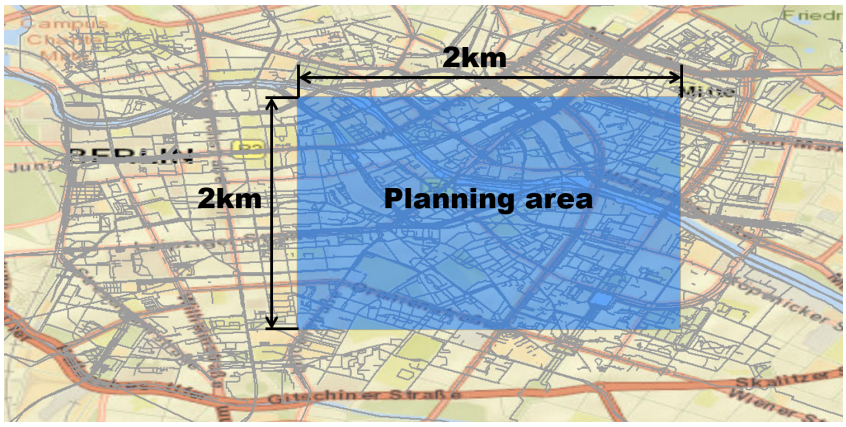

Figure 2.2.: Example ofan OSM planning area on central area of Berlin: 4 km^2 with the plane projection distortion.

As introduced above, the raw geographic data consists of points, lines, and polygons. These data classes include all the available information (for example, lines data class includes rivers, public transport lines, districts boarders, temporary and cycle ways, etc.) about the area and has to be pre-processed, i.e., cleaned-up, to include only the roads and road intersections. Figure 2.3 illustrates the raw data for the selected

planned area of Figure 2.2.

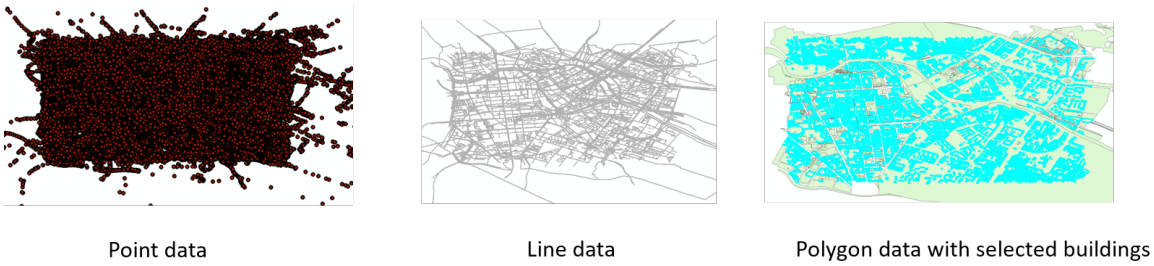

Figure 2.3.: OSM raw data example (central area of Berlin): all the line data, all the point data and all the polygon data with highlighted buildings.

For the strategic network planning we need two data types to model the area: lines consisting only of road segments and points consisting of the the road intersections. In this case, we designate the intersections as the possible aggregation node locations to reduce the problem size. Further, there will be another point class with the demands. The planning results that are obtained on these geographical maps are case study specific and not generalizable. Figure 2.4 illustrates the OSM data that can be used as an input to a strategic network planning case study.

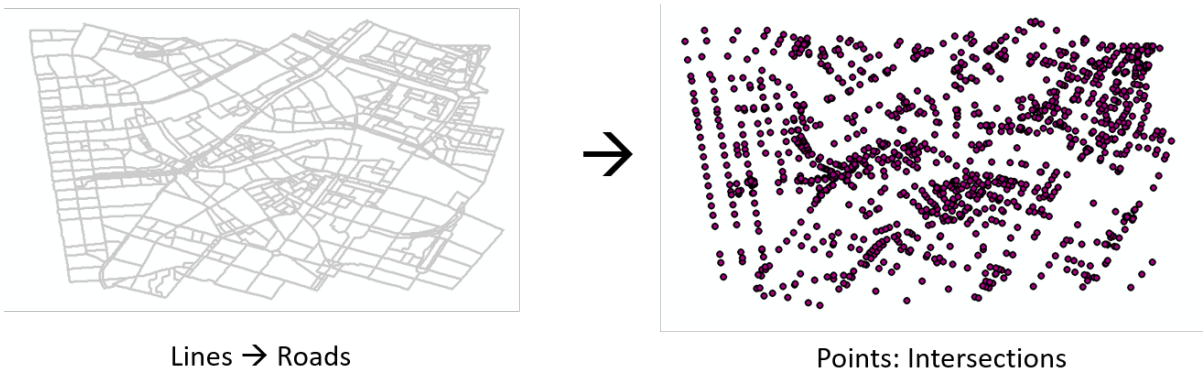

Figure 2.4.: Ready for planning OSM data example (central area of Berlin): the line data includes only the roads and the point data includes the road intersections.

Demands Modeling

By demands here we mean the end points that have to be connected to a fixed network and have specific requirements for this connection, for example on bandwidth or reliability level. Demands for the optical access networks are fixed customers, e.g., buildings or flats. The demands for the optical backhaul networks are Base Stations (BSs)

of the RAN, e.g., MBSs or Small Cells (SCs). In general, demands modeling consists of two parts: demand capacity and demand location models. In this dissertation, we focus on the demands location models as they are crucial for fixed network planning.

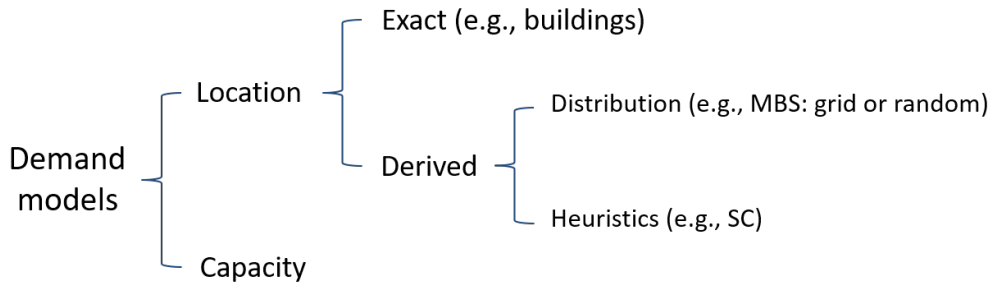

Figure 2.5.: The overview of the demands modeling in the dissertation.

Figure 2.5 summarizes the demands modeling in this dissertation. The location demands can be exact or derived. Below we explain and illustrate the location models options.

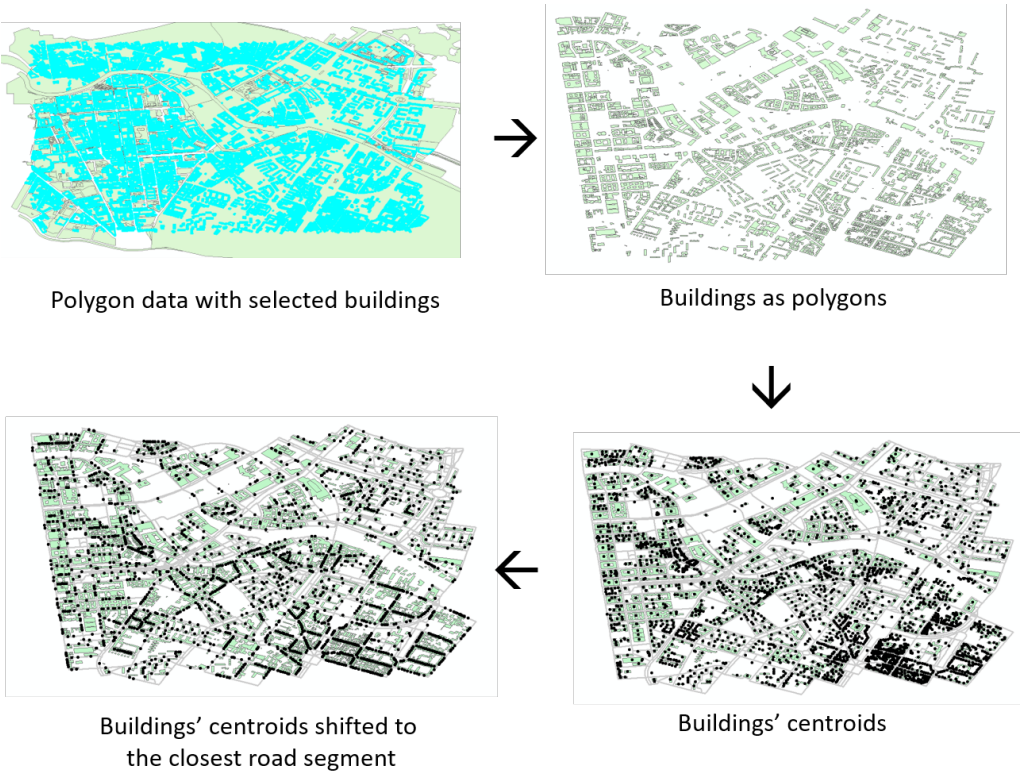

Figure 2.6.: Exact demand location example: buildings locations extracted from the the OSM data.

Exact locations are the demands locations that can be extracted from the map. For example, OSM map normally contains the locations of the buildings. Figure 2.6 shows an example of buildings locations as demands for an optical access network. In this example, we extract the buildings locations from the initial polygon data, find their centroids and shift them to the closest road segment. This shifted points are then used as the planning demands. Other fixed demands as number of households can be obtained from the buildings locations.

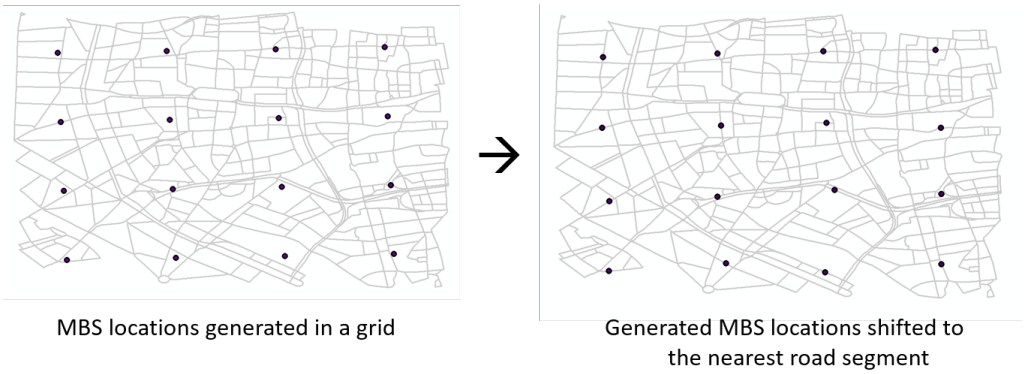

Figure 2.7.: Derived demand location example: BSs locations distributed in a grid.

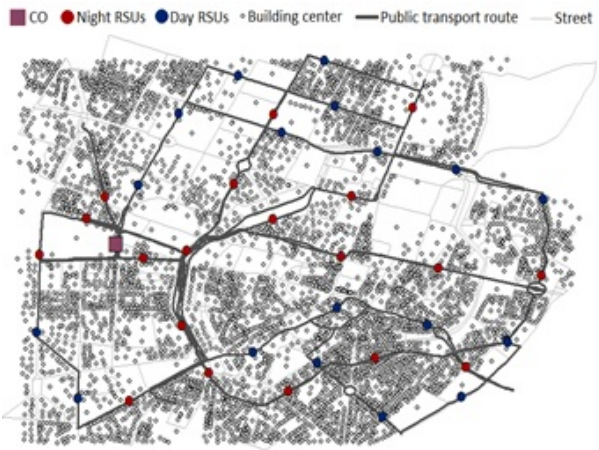

Figure 2.8.: Derived demand location example: SCs are placed according to a heuristic so that they cover the on-ground public transport routes and there is not more than 500 m between them.

The locations of the demands that cannot be found in a map, e.g., BSs or SCs, have to be **derived**: either **distributed** (in a grid or randomly) or placed with **heuristic** (based on chosen criteria). Figure 2.7 illustrates the locations BSs distribution in a grid. For example, for the SCs there could be a heuristic used that for every building with the area bigger than a threshold a SC is placed. Another approach can be to place the SCs based on the public transport routes and activity patterns, as illustrated in Figure 2.8.

In this figure, Road Side Units (RSUs) are the IoT SCs. The information about the public transport routes is extracted from the map. Additionally, the SCs can be placed at the places of interest as stadiums, malls, or other attractions. This information is also available in the map.

2.1.2. Network architectures and technologies

In general, strategic network planning work-flow presented in Figure 2.1 can be used for any type of networks. Figure 2.9 illustrates a high level network structure, where the dashed frame highlights the focus of the dissertation.

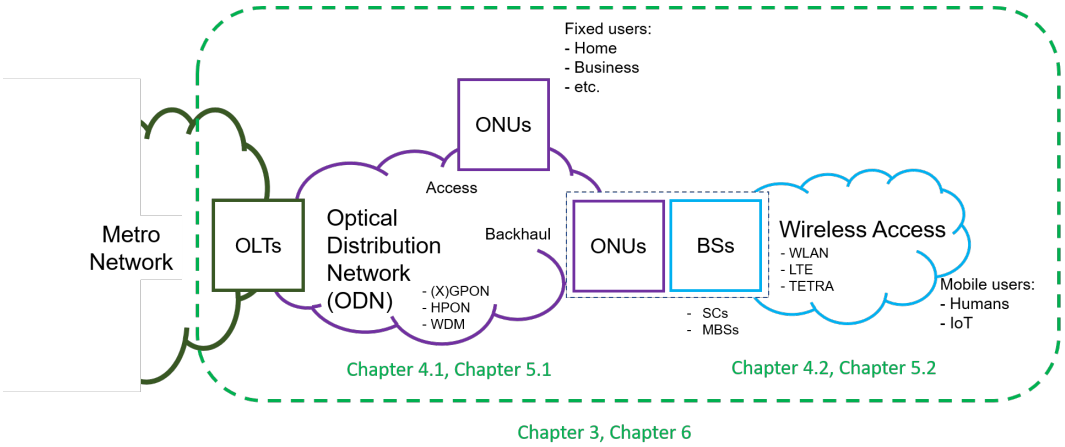

Figure 2.9.: High level network structure considered in the dissertation. ODN as an optical access network for the fixed users (homes, businesses, etc.) or as an optical backhaul network for the BSs (depending on technology, MBSs or SCs) with the collocated ONUs. Wireless access network for the mobile users, e.g., humans or IoT modems. The focus of the dissertation is on the planning of different purpose and converged ODNs (Chapters 4.1 and 5.1) and exploring the existing possibilities of the wireless access networks (Chapter 4.2 and 5.2). The methodologies that can be used for any strategic network planning are presented in Chapters 3 and 6.

By metro network, we refer to the network that interconnects the users of the metropolitan area to the core network (the network that provides connectivity between the different metro networks). The peripheral or "last mile" connections of the fixed end users to the metro network are implemented with an ODN. ODN spans a part of the city. It provides its customers an optical connection to an aggregation point, i.e., a Central Office (CO) with located there Optical Line Terminal (OLT). The CO is connected to the metro network and through a metro node to the core network. If the demands of the ODN are the fixed users as homes or businesses, we refer to an ODN as optical access network. If the demands of the ODN are the BSs, we refer to an ODN

as optical backhaul network. As illustrated in Figure 2.9, optical access and optical backhaul networks can span the same area, and be connected to the same metro and core networks. The optical backhaul connects the wireless access and the metro network.

In this dissertation, we look into ODN as optical access and backhaul networks for wireless access, as well as some aspects of wireless access network themselves. The details on the wireless access networks are presented in the respective chapters, i.e., Chapter 4.2 and Chapter 5.2. We do not focus on the wireless access planning, rather on reusing the existing technologies as in Chapter 4.2 and adapting the existing network services as in Chapter 5.2 depending on the user requirements.

Here, we present the ODN background as it provides the base for the discussion in Chapters 4.1, 5.2 and 6. We consider only passive technologies for the ODN, i.e., **Passive Optical Networks (PONs)**. Passive in this context means that the only active elements (equipment that consumes energy) are located at the end points of the network. For the ODN from Figure 2.9, the active equipment would be located at CO (OLT) and at the fiber termination point (ONU).

ODNs are commonly referred to as Fiber-To-The-X (FTTx). The "X" stands for the point, where the optical fiber is terminated: it can be on the street (in a street cabinet), in the building, in the home or flat of the subscriber, or at the antenna location. The fiber end point in these case is different as illustrated in Figure 2.10 and described below.

- Fiber-To-The-Cabinet (FTTCab): fiber termination point (end point) is a street cabinet. The street cabinet includes an ONU and a multiplexer or a modem for another technology that provides access to the subscribers from the street cabinet to their home or flat. We commonly assume that the rest of connectivity is provided by copper or Digital Subscriber Line (DSL), this is why in Figure 2.10 at the street cabinet a Digital Subscriber Line Access Multiplexer (DSLAM) is shown.

- Fiber-To-The-Building (FTTB): the fiber termination point is in the building. If nothing else is stated, it is our standard architectures with buildings as residential access fiber demands. In this case, the ONU is normally placed in the basement of the building and in the building the connectivity is provided with the existing copper.

- Fiber-To-The-Home (FTTH): is an end-to-end fiber connection, with the ONU at the subscribers home or flat. In the rural cases, as the buildings there are single dwelling units, i.e., only with one subscriber per building, FTTB and FTTH are the same.

- Fiber-To-The-Antenna (FTTA) is a ODNs as an optical backhaul network for wireless access networks. The optical termination point (ONU) here is collo-

cated with a BS of any wireless technology, e.g., LTE or TETRA. In this dissertation, we look into the optical backhaul network as the primary option to satisfy the delay, reliability and capacity requirements of the emerging wireless access networks [18]. There are other technologies available for backhaul network, e.g., microwave [21]. They are used when optical networks are too expensive or impossible to deploy (e.g., high mountains). These other technologies are out of the scope of the dissertation.

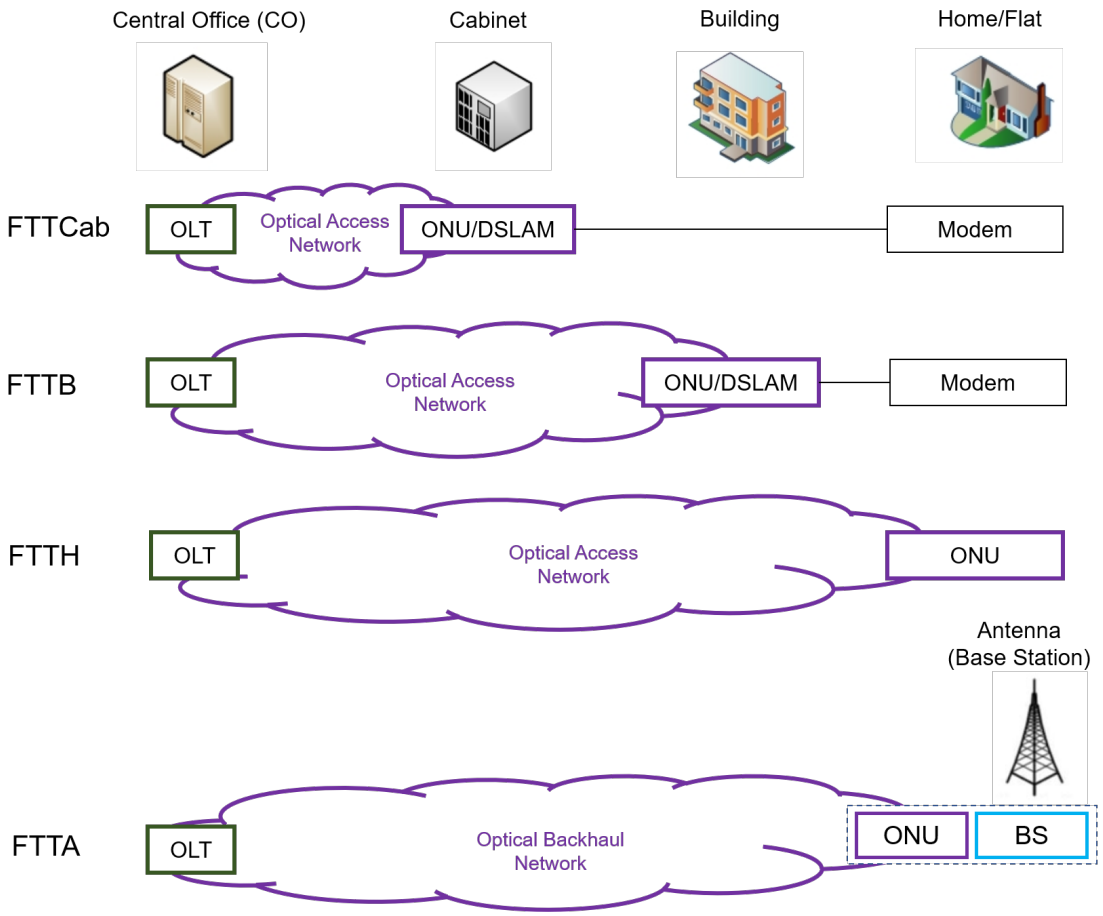

Figure 2.10.: FTTx is defined by the point, where the optical fiber is terminated. FTTCab: the fiber goes from the CO to the street cabinet, where the ONU is placed. The connection from the cabinet to the building or flat is with another technology. In the illustration it is shown for copper connection, this is why there is a DSLAM at the cabinet. FTTB has the ONU and DSLAM per building. FTTH features all optical connection to the very subscriber home. Every subscriber then owns an ONU. In the rural case, FTTB and FTTH are the same as there is one subscriber per building. FTTA defines the case, when a BS is connected with a fiber from the collocated ONU, i.e., the case of optical backhaul.

Normally, a separate ODN is deployed as an optical backhaul for a wireless access

network even for the NPs that also provide residential connectivity [86]. This results in high costs and would be a cost-prohibitive practice for wireless access networks with very dense BSs placement, e.g., as in [18].

To solve the problem of costly coexistence of multiple ODNs with different purposes, we look into optical access and backhaul network convergence as defined in [23]. **Network (structural) convergence** is sharing the physical network as cable plants, cabinets, buildings, sites, equipment, and technologies for several network types (fixed or mobile).

If there is no existing network infrastructure, we deal with the **greenfield** network planning. If there is existing network infrastructure that can be reused, we have a **brownfield** planning case.

Passive ODN Technologies

In this thesis, we look into the following technologies: P2P, GPON, 10-Gigabit Passive Optical Network (XGPON), and Next Generation Optical Access (NGOA): Wavelength Division Multiplexing (WDM)-PON and Hybrid Passive Optical Network (HPON). Figure 2.11 shows an example of the FTTA (see Figure 2.10) or optical backhaul realized with the P2P technology, but in principle it could be any technology that satisfies the wireless access requirements.

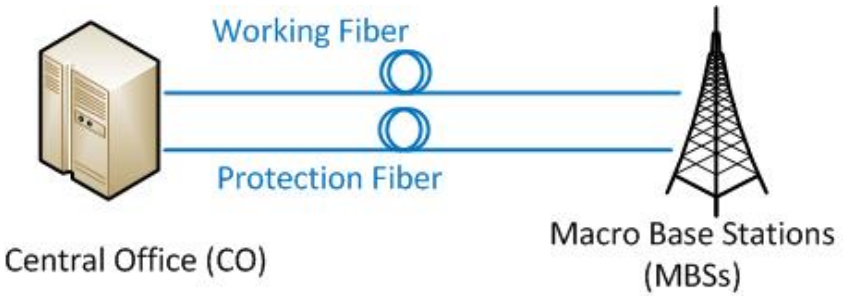

Figure 2.11.: Example of FTTA (optical backhaul network) realization with Point-to-Point (P2P) technology.

Gigabit Passive Optical Network (GPON) is a Time Division Multiplexing (TDM) technology and can provide up to 2.5 Gbps of asymmetrical data rate [56]. The subscriber gets the entire wavelength and filters out the assigned time slots. The data rate (single wavelength) is split between the subscribers at the Remote Node (RN) with a Power Splitter (PS). The number of subscribers is defined by the Splitting Ratio (SR), the higher the SR the less data rate gets the subscriber. The number of RNs defines the number of stages. For example, Figure 2.12 shows a one stage GPON architecture applied to FTTB (FTTH).

10-Gigabit Passive Optical Network (XGPON) is an extension to GPON that provides a symmetrical 10 Gbps data rate per OLT card [37].

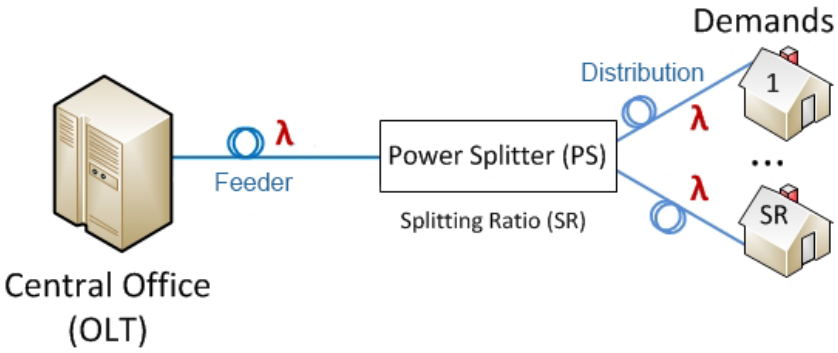

Figure 2.12.: Example of FTTB or FTTH (optical access network) realization with one stage GPON technology.

Wavelength Division Multiplexing (WDM) PON allows sending up to 500 Mbps of data rate on up to 80 separate wavelengths, per OLT card. The wavelengths are sent together on a Feeder Fiber (FF) and then they are demultiplexed at the RN. Each subscriber is provided with an entire wavelength and the users are decoupled from each other already on the physical layer [37]. A full wavelength can be needed for example for the MBSs.

Hybrid Passive Optical Network (HPON) is a two stage technology combining TDM and WDM. Figure 2.13 summarizes the architecture [37]. The first level demands, get a full wavelength through Array WaveGuide (AWG). This is the WDM part of the network. The second level demands (residential access demands) are a typical TDM PON with a PS as RN. In this way, the two types of demands are combined: first level that demands full wavelengths and second level that can share a wavelength in TDM. The first and second level demands are physically decoupled as use different wavelength and potentially even ports. Such decoupling allows safe coexistence of residential and mobile backhaul demands and is a facilitator for the network convergence as introduced later.

We summarize the main HPON particularities as follows [6]:

- Similar to GPON with Dynamic Bandwidth Allocation (DBA) but coping with a higher bandwidth range (full wavelengths available for the first level demands), HPON supports terminals with different bandwidth requirements, whereby demands with lower bandwidth requirements, e.g., residential users, are connected to the PS whereas terminals with higher bandwidth requirements, e.g., BSs, are connected directly to the AWGs.
- It can reuse any existing ODN that has been already deployed by the operator. For example, the HPON can reuse the ODN and the PSs of a deployed GPON.
- It allows greater maximum reach and hence, supports **node consolidation** with a reduced number of central offices. Node consolidation offers cost reductions

through a lower number of active components, lower power consumption, less floor space, etc. [84].

- HPON can support a large number of clients, which in turn depends on the splitting ratio of the AWG and the PS. Some possible examples as outlined in [85] combine AWGs of 40 and 80 wavelengths with 1:32 power splitters which results in more than 1200 and 2500 terminals, respectively.

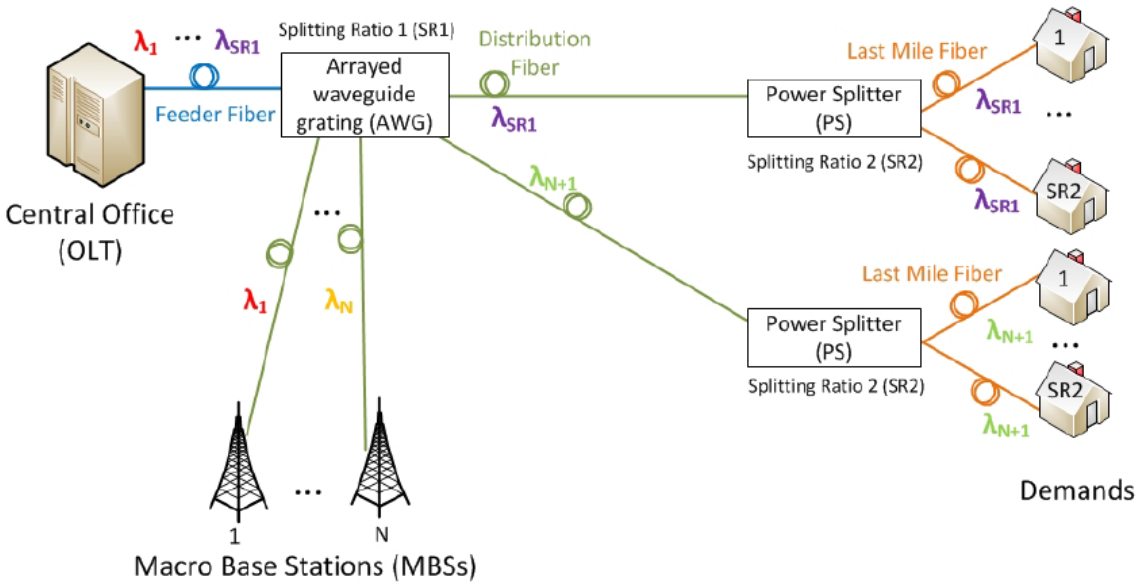

Figure 2.13.: HPON application for mobile backhaul and optical access convergence.

We describe a PON fully, when we provide the following information: technology, FTTx, number of splitting stages. Table 2.1 summarizes the combinations that were considered in the dissertation.

Table 2.1.: PON architectures ans technologies combination summary.

Technology	**FTTx**	**Number of splitting stages**	Illustration
P2P	FTTA	0	Figure 2.11
GPON	FTTCab	1	-
GPON	FTTB, FTTH	1	Figure 2.12
HPON	FTTA + FTTB, FTTH	2	Figure 2.13

2.1.3. Planning objectives

In general, strategic network planning can have different objectives. In this dissertation, we look into the following objectives:

- Ultra-reliable communications, i.e., achieving the desired connection availability as in Chapter 4. Below, we define the main reliability concepts that are used in our studies.
- Network energy efficiency, i.e., reducing the increased energy consumption due to dense demands and network redundancy as in Chapter 5. Due to high variability of energy consumption components, we provide the definitions directly in Chapter 5.
- Network migrations, i.e., maximizing the overall profitability of converged networks over their life-time as in Chapter 6. We conclude this part with the network migration definition.

The planning objectives are defined in the scenario stage of the strategic network planning, as illustrated in Figure 2.1, and have direct influence on the planning, results of the techno-economic analysis and thus the business decision. For example, if the objective is achieving the connection availability, then the planning will include protection schemes. Protection schemes include node redundancy and link protection, resulting in higher TCO due to increased CapEx and OpEx. Reducing the energy consumption could be possible with taking into account the activity patterns of the users by planning so that the active equipment can be put to sleep or dooze mode. Planning migrations means that strategic network planning is evaluated over time, adding an additional level of complexity. Depending on the migration planning algorithm the network planning step of Figure 2.1 is repeated for the individual time stamps of planning time horizon. The techno-economic analysis could be done for every planning problem or for the overall migration. The planning objectives can be also combined.

Network Reliability Concepts

The reliability objectives come from the customer requirements and the need for NPs provide the guarantees for the network performance under the Service Level Agreement (SLA). Apart from the guaranteed bandwidth and delay, the SLA regulates the maximum out time of the network. To model and quantify the ability of a network to function under failures or network survivability, we define the following terms: network reliability, failure, availability, and RBDs.

Network reliability is the ability of a network to perform the required functions, under environmental and operational conditions and for a stated period of time [22].

Failure is the termination of an item's ability to perform a required function [22].

Availability is the probability that an item is able to function at a given time [97]. In this thesis we use the term availability to express the asymptotic availability, i.e., a reliability performance metric which is referring to the probability that the system is up (or available) at any time.

Connection availability is defined as the probability that a connection is in an operable state at a given time. In this thesis we use the term connection availability to express the asymptotic connection availability, i.e., a reliability performance metric which is referring to the probability that the connection is up (or available) at any time.

RBD is a diagram showing how systems' components contribute to the system availability [97]. It is used for the reliability analysis.

This definitions are used to verify that the planned network satisfies the customers' reliability requirements.

Energy efficiency

The energy saving methods for PONs rely on putting the active equipment to sleep and doze mode. One could use the known activity patterns of the customers, group the users by the activity patterns to be able to put more equipment to sleep. We look into it in detail in Chapter 5.

Migration

Network migration or upgrade is the process of updating the network towards new technologies or standards. It is a complex multi-dimensional problem that is spanned over a long period of time and can also have multiple objectives. We look into it in detail in Chapter 6.

2.2. Network Planning

As already mentioned in Chapter 1, strategic network planning requires scalable and reproducible planning algorithm. This is why we look into heuristic algorithm from [43]. Table 2.2 summarizes the high-level heuristic steps.
The ODN demands (e.g., buildings, BSs, or cabinets depending on the FTTx) are first clustered (aggregated). Each cluster has a limit of the demands that can be aggregated to it, i.e., the RN's splitting ratio. This step is repeated for every RN and the fiber layout is done for every fiber type. Finally, the duct is calculated as a post-processing step.

Network planning is labor and cost intensive procedure, on the results of which depends the future of the entire NP. Manual planning is sometimes inevitable, but also it is prone to errors, biases and is not reproducible or comparable. These downsides

Table 2.2.: Planning heuristic summary [43].

Clustering		**Fiber Layout**		**Post-processing**
Demands are clustered to minimize the fiber, the RNs are placed as cluster heads	⇒	Fiber cables layout between the demands and the RNs	⇒	Calculating the duct
For each stage		For each fiber type		Once

are especially critical for large-scale strategic network planning projects. To address this issue, we introduce the Automated Map-Based Strategic Fixed Network Planning Tool (AMS) tool below, in which we have implemented the heuristic planning algorithm from [43]. AMS was used for the planning in this dissertation.

Automated Map-Based Strategic Fixed Network Planning Tool

There are quite a few automated network planning tools, for example myWorld Fiber Planning [130], ESRI fiber planning extensions [131] or 3-GIS [132]. To the best knowledge of the authors, only the network planning consultancies and the following two network planning tools offer the automated strategic network planning solutions: i.e., Comsof [133] and Vetrofibermap [134]. All the introduced tools are commercial and thus not available for academic research, comparison of new planning methods and independent custom extensions. To overcome these limitations, we have implemented a strategic network planning tool - AMS. The code, the used input data and individual video instructions for every implemented architecture are publicly available at [1].

Our proposed AMS [1] is a custom Python-based ArcGIS [129] tool with a friendly graphical user interface, especially developed for the dissertation. Below, we briefly introduce the implemented planning methodology (including planning input, planing algorithm and planning output) as well as the implemented network architectures and their options. The code, the used input data and individual video instructions for every implemented architecture are publicly available at [1].

Planning input is multi-part. First, the planning road topology in ArcGIS format is needed. In most of our studies, we have used geographical maps as the area models, specifically Open Street Maps (OSM) [135]. However, the tool can be used with any other ArcGIS compatible models. For example, we have used AMS with the graph-based road topology models as in Chapter 3. Second, we input the locations of the demands (e.g., buildings' centroids as in Figure 2.6) and the location of the COs. To limit the run time, we limit the allowed RN locations, normally to the road intersec-

tions. Finally, if there is an existing network, which resources can be reused then the brownfield planning is done. That is the existing network becomes also an input to the tool.

The basic **planning algorithm** was introduced in Table 2.2 and consists of clustering, fiber layout and post-processing. Clustering or assigning (aggregating) the demands to RNs is performed either with an in-built ArcGIS location-allocation clustering algorithm [128] or with an upgraded clustering algorithm from [43]. The cluster head locations are where the RNs are placed. It is performed for every stage of the architecture, see Table 2.1.

The fiber layout can be performed only after the RNs have been placed. We use Dijkstra [128] shortest path routing in road metric. The road metric means that the fiber follows the roads and does not use Euclidean distances. We also provide an option of fiber layout that encourages duct reuse. This is a heuristic that sets the costs for already used paths much lower compared to the new paths.

Post-processing gives the duct layout based on the fiber layout obtained in the previous step. At this step also the fiber and duct lengths are calculated. The **planning output** consists of RNs locations, fiber and duct lengths. The lengths can be saved in any format (at this stage a Python dictionary in a .txt file) and in the proprietary ArcGIS form.

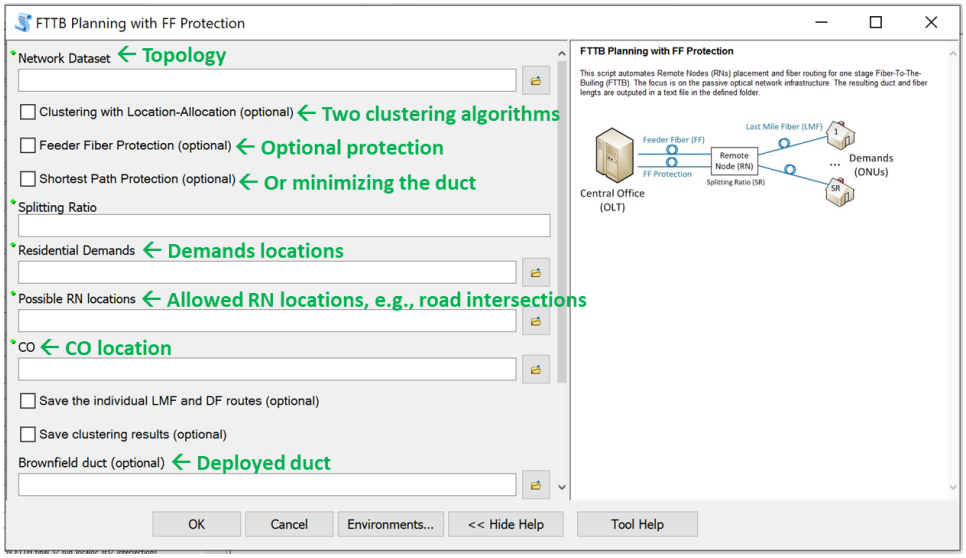

Figure 2.14.: Example of the AMS tool graphical user interface for one stage FTTB with optional protection and brownfield planning.

Implemented architectures and technologies

The full descriptions of the implemented architectures and technologies are available at [1]. The combinations of the implemented in AMS architectures and technologies were summarized in Table 2.1. For each of the implemented architectures and technologies combination, the additional planning parameters can be taken into account:

- Protection: unprotected or link-disjoint protected (shortest path or encouraging duct sharing),
- Greenfield or brownfield. Brownfield is either given as input or calculated.

For each of the implemented infrastructures and technologies there is a separate graphical user interface with the description of the architecture and all the needed inputs. Figure 2.14 shows an example of AMS input parameters for a one stage FTTB architecture. To speed-up the network planning, one can choose not to save the actual locations of the calculated clusters and fiber routes. The planning output is then a part of the input for the techno-economic analysis. The main metrics of the techno-economic analysis are defined below.

2.3. Techno-economic Analysis

Telecommunication networks are costly in deployment and operation. The end users do not have technology preference as long as their requirements are satisfied. In order for NPs to stay profitable, a careful techno-economic analysis has to be done. The main techno-economic parameters are CapEx, OpEx, TCO and NPV. These parameters are defined below.

Capital Expenditures (CapEx) [63] are depreciated over time one-time investments. The set of CapEx cost components includes, but not limited to, the cost of physical infrastructure such as buildings and land, network infrastructure such as ducts, fiber, equipment and supporting software and research and planning costs.

Operational Expenditures (OpEx) [17] are not depreciated over time reoccurring operational costs. Operational Expenditures (OpEx) do not contribute to the infrastructure. The set of OpEx cost components includes all the costs to keep the company operational. For example, it could be energy costs, rent or lease costs for the equipment sites, maintenance costs, salaries and marketing costs, etc. OpEx is calculated per time period, for example per year or network life time.

Total Cost of Ownership (TCO), for our thesis, is defined as a sum of CapEx and OpEx. For an accurate TCO estimation, an accurate evaluation of both TCO components is needed. Based on the TCO comparison of potential technologies, the most suitable technology can be chosen

Present Value (PV) [48] is a "discounted cashflow" or the current value of the sum of money in the future. Eq. (2.1) formalizes the definition of the PV for the current time period t, revenue at time t (cash inflow) R_t, discount rate of the project d and investment made in time t (cash outflow) I_t. This investment could be initial (for t_0 or project start) or additional (required in order to migrate to a newer technology) CapEx as well as the related OpEx costs for the deployed technology. We assume the discount rate to be fixed to 10% [36, 52].

$$PV_t = \frac{R_t - I_t}{(1+d)^t} \tag{2.1}$$

Net Present Value (NPV) [48] allows evaluating the time value of money and is used to derive long-term projects profitability. Eq. (2.2) defines the NPV difference between the present value of cash inflows and the present values of cash outflows, where t is the time iterator, T_{NW} is the project (e.g., network) life-cycle and PV_t is the Present Value (PV) of the net cash flows at the time t.

$$NPV = \sum_{t=1}^{T_{NW}} PV_t \tag{2.2}$$

If the NPV is positive, then the project is profitable. If the NPV is negative, then the project is not profitable. Based on the NPV comparison, the long-term business decisions can be made.

2.4. Summary and Discussion

In this Chapter, we have introduced the necessary background concepts based on strategic network work-flow (depicted in Figure 2.1): scenario definition, network planning and techno-economic analysis that lead to an informed data-based business decision. This work-flow, we follow in the dissertation.

The network planning in the dissertation is performed with a Python-based custom network planning tool for ArcGIS [129] - AMS [1]. It allows flexible, reproducible, and comparable planning open to the industry and academia for use and extension. In the next Chapter, we investigate the possibilities of modeling the area/topology, on which the network planning is performed, with the graph-based models.

3. Graph-Based Road Topology Models for Strategic Network Planning

Physical networks (for example telecommunication, power or water distribution networks) are complex systems that are expensive in both deployment and operation. The success of initial network deployment or later upgrade depends on the results of initial strategic network planning. Strategic network planning concentrates on identifying the most suitable technology and architecture, evaluating the planning methods and defining the major cost factors [26] (see Figure 2.1 in Chapter 2 for work-flow and definitions). The result of strategic network planning significantly depends on the road topology for an accurate estimation of the TCO. The physical infrastructure of a network, e.g., fiber, copper or pipes, has to follow the available for construction roads and cannot cross buildings. The methodology and evaluation presented at this study can be applied to any network planning case.

The most precise network planning results are obtained based on real maps or geographic road topologies, e.g., OSM [135]. In this dissertation, we have used cleaned-up OSM road topologies. The cleaning-up process is complex and time consuming, see Appendix A for details. Moreover, the planning results are area specific and thus cannot be generalized. Often the maps themselves are either expensive (proprietary maps) or inconsistent (open access maps). The question that has to be answered during the strategic network planning stage is not always about a particular area, but about an area type of deployment, e.g., rural or urban; generic feasibility or planning algorithm validation. Thus, the road topologies have to be abstracted and generalized.

In this chapter, we holistically evaluate graph-based road topology models for the strategic network planning of the fixed networks, i.e., ODN as fixed optical access network and optical backhaul for MBSs. A geographical road topology or a graph model are the input to the planning case study. In particular, we look into two graph-based road topology models: Gabriel Graph (GG) [28] and Procedural Generated Topology (PGT) [25]. PGT is used for synthetic cities generation in the game industry. To the best knowledge of the authors, we are the first to look into applicability of the PGT to strategic network planning. The performance of GG and PGT is compared against the real geographical topology (map). We look into the graph properties of the generated topologies. The network planning is done for the ODN and results are evaluated in terms of fiber and duct lengths as they are the topology dependent parameters. We consider two technologies and architectures: one stage GPON FTTB for dense residential users (see Figure 2.12) and protected P2P for the sparse MBS (see Figure 2.11). The comparison is done for three urban cities in Germany: Munich, Cologne, and Berlin.

Our contributions are summarized as follows. We investigate the applicability and limitations of the graph road topology models for strategic network planning. We provide the guidelines for the use of graph road topology models in strategic network planning and identify their limitations. Finally, we provide all the used reference geographical topologies as well as the evaluation and modeling tool in the open access [2]. In this way, our work is reproducible and expendable[1].

The rest of the chapter is organized as follows. First, we introduce the state-of-the-art analysis on the road topology models in Section 3.1. Then, Section 3.2 describes the graph-based topology models, i.e., GG and PGT. Section 3.3 defines the simulation inputs, and the methodology. Section 3.4 presents the topology models evaluation based on ODN planning case study results and gives the recommendations on the models use. The chapter is concluded with the summary and discussion section.

3.1. State-of-the-art Analysis

One way of abstracting the geographic road topologies is creating a geometrical model based on the average topology characteristics and reusing regular structures, e.g., a triangular model [31]. However, it was shown that neglecting the graph structure of road topology results in unpredictable over- or underestimation of the costs by as much as 30% [64]. In this case, the results of strategic network planning cannot be used for decision making and the analysis is not reliable.

Another way of abstracting the road topology is creating a graph-based abstraction. Maniadakis and Varoutas [30] applied GG [28] to network planning and illustrated it with a small FTTB case study. The authors have compared the FTTB planning results bases on the GG topology and some popular geometric models, e.g., Simplified Street Length model [52] or triangular model [31]. The baseline for comparison was the FTTB results for the geographical topology. The study showed that GG model provides a better estimation of the FTTB duct (trenching) lengths compared to geometric models. The duct was shown to be the major cost driver for the optical access network deployments. The comparison was carried out for the three types of topologies based on the demand (house holds density): semi-urban, urban and dense urban.

Although this study was very insightful, it is not reproducible and the methodology of the comparison could impact the result. The authors stated that they used the 1 km$\times$1 km topologies, uniformly distributed demands and a CO located in the middle. The area selection and averaging process could not be extensively described due the space limitations and thus cannot be reproduced. Moreover, the small topologies and centrally located CO might have influenced the results of the network planning.

[1]The code, all the materials and input data will be published after acceptance of the respective study. The materials can be provided upon request.

3.2. Graph-Based Road Topology Models

This section introduces the main principles of the two road topology models considered in this study: the GG and the PGT models.

Gabriel Graph

The GG was introduced for geographical variation research analysis by Gabriel and Sokal in [28]. As presented in [28], V denotes a finite non-void set of nodes on a plane. The distances between two nodes (i, j) in V are Euclidean and denoted as d_{ij}. An edge between (i, j) is formed if $i \neq j$ and they are least square adjacent, i.e.,

$$d_{ij}^2 < d_{ki}^2 + d_{kj}^2, \quad \forall k \in V, k \neq i, k \neq j. \tag{3.1}$$

Figure 3.1 graphically explains the connectivity condition. If there is no other node k within the circle of diameter d_{ij}, the nodes (i, j) are least square adjacent and the edge between them is formed.

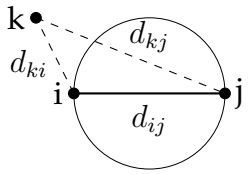

Figure 3.1.: Two points (i, j) in a point set are connected if and only if there is no other point k within the circle of diameter d_{ij} [28].

The least square adjacency graph $G(V)$ is a GG. When applying GG to planning, the input to the model are the potential graph nodes, which may vary according the purpose of the graph; e.g., the road intersections or randomly placed nodes. An interested reader can refer to [29] for more details on GG properties and their use in geographic analyses.

Procedurally Generated Topologies

PGT [25] is a method of creating topologies algorithmically in two steps: “Tensor Field Generation" and “Street Graph Generation" as depicted in Figure 3.2.

Tensor Field Generation As the first step in procedurally generated graphs, a mathematical representation of the graph in a two-dimensional space needs to be generated, i.e., *tensor field* T.
A tensor field T is a continuous collection of *tensors*, one for every point in the area [25]. A tensor t is defined as a 2×2 symmetric and traceless matrix of the form:

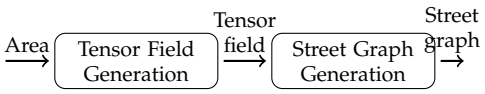

Figure 3.2.: Procedurally Generated Topologies steps [25]

$$R \begin{pmatrix} cos2\theta & sin2\theta \\ sin2\theta & -cos2\theta \end{pmatrix}, \; R \leq 0, \; \theta \in [0, 2\pi].$$

where R and θ are the polar co-ordinates of a two dimensional space, in which the tensor field is generated. Each of these tensors have a major and minor eigenvectors that are perpendicular to each other.

The tensor field T associates every point $\mathbf{p} = (\mathbf{x}, \mathbf{y}) \in \mathbb{R}^2$ in a two-dimensional point space with a tensor given by $T(\mathbf{p})$. Using tensor fields, one defines *hyperstreamlines*, which are a set of vectors of a curve that is tangent to an eigenvector field everywhere along its path [25]. Hyperstreamlines are used to generate the nodes and edges for the visualization of the street graphs.

Different tensor fields, each having their own“basis" can be combined together in order to form a mixed tensor field having a unique set of hyperstreamlines. In this work, we use a mixed field consisting of grid and radial fields combination.

- Grid tensor field models Manhattan grids.
- Radial tensor field models create radial structures, in the form of concentric circles, with a predefined central point.
- Mixed tensor field combines the above two using a exponential decay constant. The grid or radial characteristics can be tuned by tuning an exponential coefficient which reduces the magnitude of the tensor field.

The generic input variables for the mixed field generation are summarized in Table 3.1. Further details and detailed derivation of tensor fields is presented in [27].
Street Graph Generation The visualization of a street network from tensor field T is computed by tracing the hyperstreamlines [32] of the generated tensor field. The tracing begins with populating an arbitrary two dimensional generation area with a set of *seed points*. These seed points are the starting or ending points for the hyperstreamline tracing.

As described in [25], given a point with an eigenvector and the direction of the hyperstreamline movement (positive or negative along either x or y axes of the generation area), hyperstreamlines can be traced using an adaptive Runge-Kutta scheme. When a hyperstreamline approaches the minimum allowable distance from another seed or another hyperstreamline, the process is stopped and the same procedure is

Table 3.1.: Tensor field generation input parameters for Munich.

Parameter	Description	Value
Extent	Size of the generated topology in points	$(0, 0)\ to\ (100, 100)$
Radial center	Location of center of the graph inpoint coordinates.	(x, y)
Exponential co-efficient	Influence of radial curve. Higher values lead to lower influence.	$[0; 1]$
Tensor influence	1-D array to dampen effect of grid and radial tensor fields	$[0.5\ 1\ 0.1\ ...]$

started from the next seed. In many cases, the current hyperstreamline may not encounter any seed or an already generated (traced) hyperstreamline node. For this, we add an additional stopping condition called the “maximum number of tracing steps", which is the maximum number of iterations allowed for every hyperstreamline, before moving to the next seed. The tracing process continues till all the seeds have been processed, which results in a vector of points in the x and y direction, for each hyperstreamline. These points are the nodes of the resultant graph. Due to its complexity, the generation of hyperstreamlines also generates unwanted nodes and edges that are too close to each other. The generated topology is post-processed to remove irregularities.

Figure 3.3 shows how hyperstreamlines are traced from the initial uniform seed placement while varying the maximum number of steps for each of the hyperstreamlines. Each of the sub-figures are assigned an increasing number of maximum steps (10, 30, 60 and 95), which shows that this parameter is directly proportional to the density of the topology. However, the combination of initial seed density and the maximum number of tracing steps has to be stated based on parameter investigation so that the generated topology is neither disconnected, nor too noisy. The top left sub-figure shows the start of the hyperstreamlines tracing with every hyperstreamline allowed to be traced only 10 times. With the increase in maximum number of tracing steps, the tracing continues in the top right and bottom left sub-figures. The final set of the traced hyperstremlines is depicted in the bottom right sub-figure, shows the tracing after each of the hyperstreamline is allowed to be traced either 95 times, or till it encounters a seed. We see that with increasing the maximum number of tracing steps, the generated topology becomes denser, i.e., with more nodes and edges. The noise, i.e., dangles and free standing edges, is removed with post-processing.

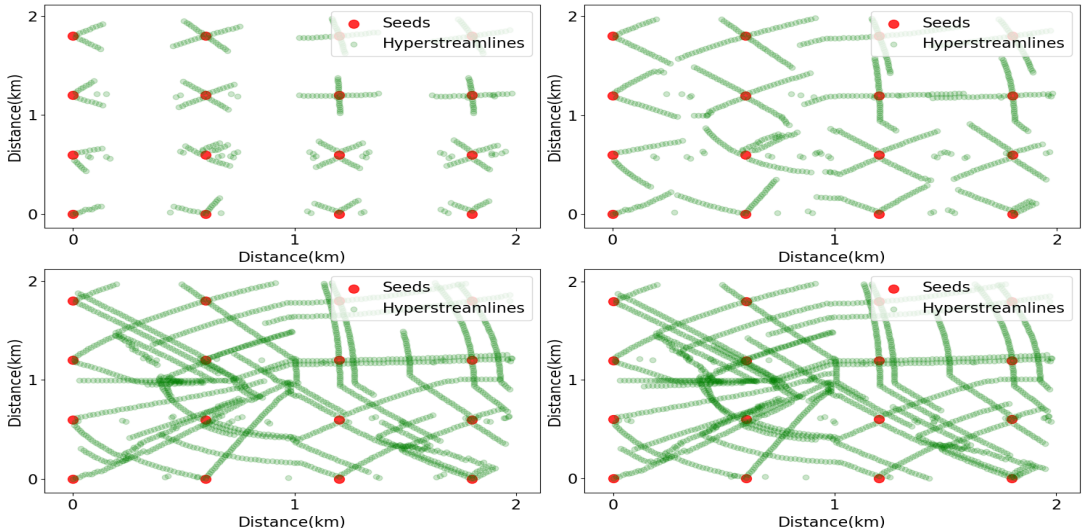

Figure 3.3.: Example of a fixed uniformly distributed seed placement and hyperstreamline tracing in a $4km^2$ generation area with maximum number of tracing steps 10 (top left), 30 (top right), 60 (bottom left) and 95 (bottom right). Hyperstreamline nodes are placed near the seeds or already generated nodes and continue in a particular direction till another seed or hyperstreamline is encountered or maximum number of tracing steps is achieved.

3.3. Evaluation Methodology

The two graph topology models, GG and PGT, have been implemented in a topology generation tool, which is publicly available at [2]. Both models have been implemented in Python for ArcGIS [129] for reproducibility, ease of use, and visualization. These models have been evaluated for different strategic planning case studies with respect real geographic street networks, following the methodology proposed in this section.

Figure 3.4 summarizes the evaluation methodology steps. This section introduces the individual parts in the logical sequence from topology generation to planning analysis.

Topology Generation

Both models (GG and PGT) need some input parameters to generate the topologies. These parameters are related to the area where the strategic planning should be performed. The basic parameters required for both models are the area size in km^2 and the geographical extent (position on the globe) of the original geographical topology. These parameters are used for correct length interpretation. We generate a series of 15 graph-based road topologies and evaluate the errors in the resulting graph properties

and planning results using the geo-topologies as the reference.

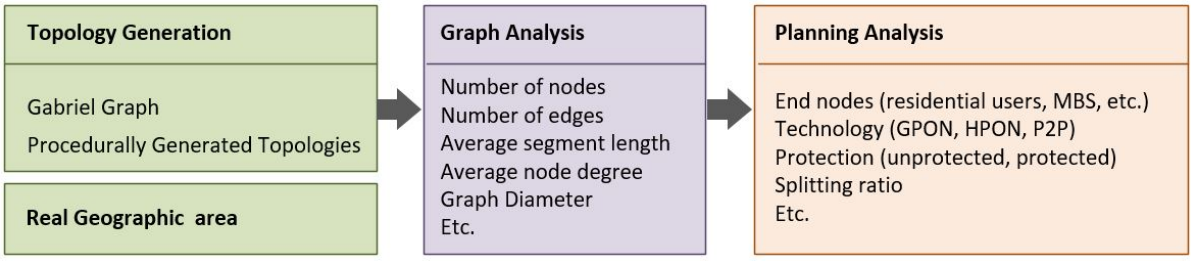

Figure 3.4.: Proposed Topology Evaluation Methodology

GG model requires the number of nodes V of the area, which may get connected following the model of Section 3.2. In our case, these nodes are the possible street intersection nodes. Two GG alternatives that we have considered:

- *GG-real* places the nodes at the real road intersections of the geographic area.
- *GG-orig* places the nodes randomly in the area.

PGT Model as discussed in Section 3.2 requires a number of parameters: generation extent, radial center, exponential co-efficient, tensor influence, seed points density, and the maximum number of tracing steps. All of these parameters have some influence on the generation results.

Graph Analysis

The generated graphs using GG-orig, GG-real and PGT are compared with the original geographic area with respect to the graph properties. In this study, the following graph properties are compared: number of nodes, number of edges, average segment length in meters, maximum segment length in meters, average node degree (average number of incident edges per node) and graph diameter (i.e., longest shortest path between two nodes). If the graph is disconnected, the graph diameter is infinite.

Planning Analysis

As our main goal is the accurate strategic network planning of a fixed access network, the generated graphs must also be compared with respect to the resulting planning for different network architectures. In this study, we look into the ODNs planning of PON. The ODN infrastructure consists of fiber cables, which transmit the optical signal; and ducts, which shield the fiber cables. Enforced by regulators and city regulations, most of urban areas require underground infrastructure, which prompts costly civil labor due to the trenching along the streets. We consider the following two ODN scenarios:

- Unprotected passive optical network (referred in this study as UPON) with on one splitting node such as (X)GPON and WDM PONs, as shown in Figure 2.12. This architecture is suitable for areas with high density of end points requiring up to 10Gbps (e.g., residential users in a FTTB as considered in this study). This architecture distinguishes between the FF interconnecting the central office and the remote node; and the Distribution Fiber (DF) interconnecting the remote node with the end point. The remote node can host different components depending the architecture (e.g., PS if (X)GPON as shown in Figure 2.12), AWG if WDM PON). The ducts containing FFs are referred as Feeder Duct (FD), whereas the ducts containing DF are referred as Distribution Duct (DD). The number of remote nodes and the length of the required fibers and ducts depend on the number and locations of the end points, the splitting ratio of the remote nodes as well as the location of the central office.
- Protected point-to-point architecture (referred in this study as PP2P), which is suitable for areas with sparse density of end points requiring high bandwidth of at least 10Gbps (e.g., MBS as in Figure 2.11).

The network planning methodology proposed by Shahid et al. [43] has been considered in this study. The result gives, among other parameters, the length of the required fiber and duct in meters, which can be converted to cost (e.g., using the cost units as in [56]). We look into two CO placement options: in the corner of the topology and in the center. We expect the planning results of the CO in the corner to accumulate the topology modeling errors. However, it is commonly used for planning results extrapolation on the larger areas. The CO in the center was used in [30] and we use it as a benchmark.

3.4. Evaluation Results

This Section presents selected results of our evaluation of the models' performance for strategic network planning case studies for three German cities: Munich, Cologne, and Berlin. First, we introduce the case studies and then describe the topology generation for GG and PGT models. We show visualization examples of the topology generation results, graph properties analysis as well as the respective planning results and analysis for two ODN scenarios: dense residential demands with no protection (UPON) and sparse MBS demands with protection (PP2P) as introduced in Section 3.3. The planning analysis subsection is concluded with the recommendations on the use of the graph-based road topology models.

Case Studies

Three German cities have been considered: Munich, Cologne, and Berlin. For each city, an area of 4km^2 has been selected and retrieved using OSM [135]. These maps provide accurate information, which includes streets, intersections and buildings. Buildings are given as polygons. The fiber and duct planning along the streets is

based on a routing tool that works with points. In this case, the building's point location is found by pushing the center of each polygon to the closest street segment.

Table 3.2.: Density properties of the selected areas

Topology	Buildings/km^2	Intersections/km^2
Munich	2238,1	104,5
Berlin	1870,9	160,25
Cologne	1285,7	152,5

As discussed in Chapter 2, OSMs do not provide the locations of the MBSs required by the PP2P ODN case. Hence, we apply the commonly used grid distribution of MBSs, which is characterized by the inter-MBS distance [24] (see Figure 2.7). In this work, we consider an inter-MBS distance of 500 m typical for urban areas [33].

Table 3.2 summarizes the building density and road intersection density of the selected areas. Cologne and Berlin have similar number of intersections per km^2 (difference within 10%), while Munich has significantly less intersections.

Topology Generation

After an extensive PGT parameter investigation and manual comparison of the graph properties to geographical topologies, we fix the limits of generation from $(0, 0)$ to $(100, 100)$ in the x and y direction respectively. We also place the center of the radial tensor at the center of the topology, i.e., at $(50, 50)$, exponential co-efficient for the radial tensors is 0.001, and the tensor influence array is set to $[0.5 \quad 1 \quad 0.1 \quad 0.1 \quad 0.1]$ for the combined tensor field and the two grid and two radial tensor fields respectively. However, this can vary based on the amount of radial and straight lines in the desired area. The number of generated intersections with the fixed tensor parameters depends on the initial seed density, and the maximal number of tracing steps.

In our implementation, we have fixed the initial seed point density to 18 while varying the maximum number of tracing steps between 30 and 100. In the case of combination of low initial seed density and low maximum number of steps, the topology is not connected. In case if both initial seed density and maximum number of steps are too high, the topology becomes extremely noisy. Hence, a balance between these numbers is sought. Since an adaptive Runge-Kutta method is used to trace hyperstreamline nodes (shown in green in Figure 3.3), the numerical solution obtained is approximate. In our case, an approximate solution is acceptable as we are interested in the statistical properties and not in a concrete realization. For a given geographical topology, the maximum number of steps with the best fit is found by binary search and included in the naming convention: "PGT-95", where 95 is the maximum number

of tracing steps.

This a limiting factor for the PGT model use, it requires an extensive parameter investigation before it can be used. In this study, we have done the investigation for the urban area. The applicability of the parameters to the other areas is out of the scope of the study and has to be done prior to the modeling.

For each area, three different topologies have been generated: GG-orig, GG-real and PGT. We focus on a particular case of the 4km^2 Munich area as an example, which real geographical topology has been obtained from Open Street Map and depicted in Figure 3.5 a).

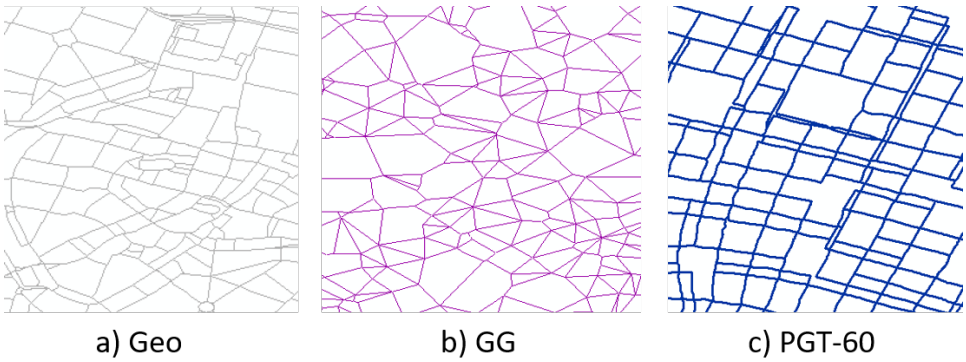

Figure 3.5.: Road topologies examples: a) "Geo" or cleaned-up Open Street Map b) "GG" or Gabriel Graph and c) "PGT-60" or Procedurally Generated Topology with $max\_number\_of\_tracing\_steps = 60$ and seed points density fixed to 18.

- GG-real: the real location of all the intersection nodes of Figure 3.5 a) are given as input. Then, based on their distance and the GG approach presented in Section 3.2, they are connected. The resulting graph looks similar to the Figure 3.5 b), but the intersection locations are extracted from the map.
- GG-orig: the number of nodes in this area are 418, which are randomly distributed. Then, based on their distance and the GG approach presented in Section 3.2, they are connected. The resulting graph is shown in Figure 3.5 b).
- PGT: the seed density is 18 and the maximal step number is 60. The resulting graph is shown in Figure 3.5 c).

3.4.1. Graph Analysis

The evaluated graph parameters are: number of nodes ($\#nodes$), number of edges ($\#edges$), average segment length (av_len), average node degree (av_degree), and average graph

diameter ($av\_diameter$).

Figures 3.6-3.8 show the averaged graph properties of the 15 topologies generated with GG-orig, GG-real and PGT-nmax modeling Munich, Cologne and Berlin geo-topologies respectively. The results are normalized with the graph properties of the geographical topologies and are shown in %.

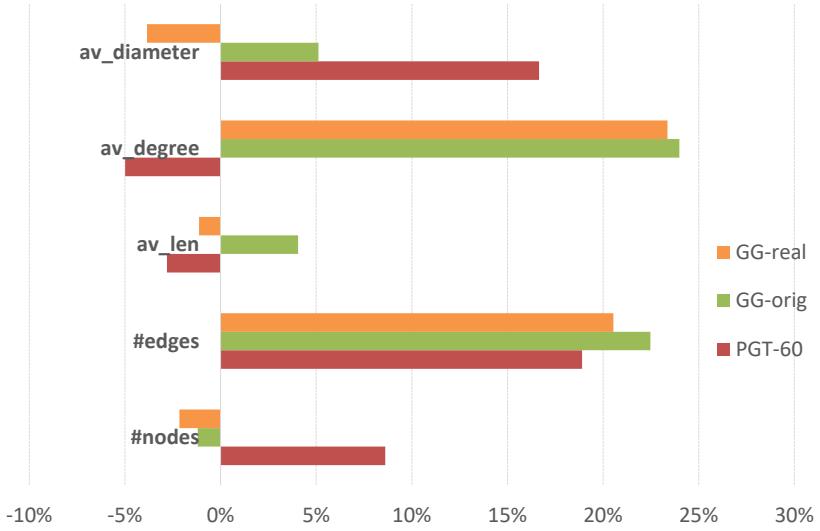

Figure 3.6.: Munich: GG and PGT road topologies graph properties normalized to the geographical topology, in %.

The main comparison is conducted between the Gabriel Graph as in [28] denoted as GG-orig and Procedural Generated Topology as in [25]. GG-real is an unrealistic scenario, where we know the exact locations of the geographical road intersections and use them as the input to the GG model. This case is listed for completeness.

The graph properties do not show any consistent trends other than the $\#edges$ is overestimated by every model for every geographical topology within the $20 - 30\%$ interval. The $av\_diameter$ is overestimated by the PGT and tens to be underestimated by the GG, except for GG-orig for Munich. GG consistently overestimates the av_degree, and PGT tends to estimate the av_degree within the $\pm 10\%$ interval. The av_len is an inconclusive property with a significant variation depending on the geo-topology. The $\#nodes$ is underestimated by the GG due to the generation method: not all the input nodes get connected (see Section 3.2). There are cases, when GG-real has slightly more nodes than the geo due to the topology processing (see Figure 3.8).
The graph properties do not have a particular meaning for strategic network planning without the planning analysis results as planning results are the metric. We could not observe any trends in the graph structure of the used urban geo-topologies, except for the average node degree close to 3.2. We further note that we have investigated the influence of models' inputs resulting in the graph properties closer in some pa-

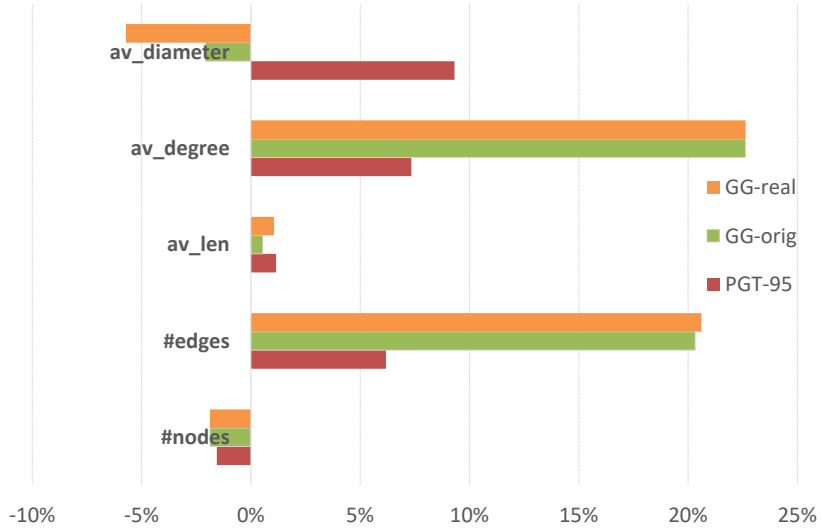

Figure 3.7.: Cologne: GG and PGT road topologies graph properties normalized to the geographical topology, in %.

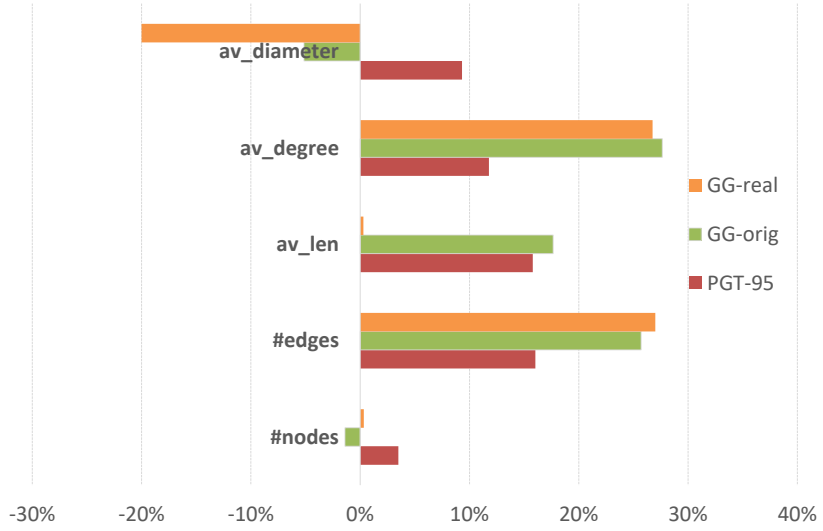

Figure 3.8.: Berlin: GG and PGT road topologies graph properties normalized to the geographical topology, in %.

rameters to the geo-topology. For the GG-orig, we have given as input more random points (i.e., 10%) than in the geo-topology. Although the number of nodes became closer to the geo-topology, the planning results did not improve. Similar observation was made for the PGT model: the planning results did not improve with achieving the number of nodes closer to the geo-topology. The interpretation of the model's performance in terms of modeling the geographic topology can only be done based on the planning results.

3.4.2. Planning Analysis

This Subsection evaluates the suitability of the generated graphs in order to perform strategic planning analysis. For this purpose, the planning analysis for the two previously defined ODN scenarios on the different generated graphs are compared with respect to the planning results on the geo-topology. The analysis focuses on the error in estimation of the duct lengths as they are the major cost driver. The results for the fiber lengths can be found at [2].

The graph and planning analyses are done for the road graphs, where the nodes are the road intersections and the edges are the street segments. Below, we illustrate the network planning on the graph for both architectures: UPON in Figure 3.9 and PP2P in Figure 3.10. The main goal of these illustrations is to provide an intuition to the fact that the road topologies directly influence the planning results.

Unprotected passive optical network (UPON)
The scenario for one stage (X)GPON applied to dense residential demands without protection was presented in Chapter 2, Figure 2.12. There are two types of fiber and duct: DF and DD and FF and FD. Buildings are clustered according to the remote node splitting ratio and the centroid of each cluster is considered as the remote node location. The CO location influences only the FF and FD (between CO and RN) as the DF and DD depend on the remote node and building locations [43].

Figure 3.9.: UPON planning on the PGT-60 graph of Munich. CO is shown as green circle, remote nodes as pink circles and buildings as gray dots. The FD is shown as purple lines and the DD as orange lines.

Figure 3.9 depicts a UPON planning example for Munich. The underlying road topology is generated with PGT model. It is the same topology as in Figure 3.5. The CO location is shown in the center as a green circle, the remote nodes are represented with small pink circles and the buildings as gray dots. The FD interconnecting CO with remote nodes is shown in purple lines, whereas the DD interconnecting remote nodes with buildings are shown in orange lines. All the planning results of the Munich graphs are summarized in Table 3.3.

We observe that the error in the total duct estimation with central CO is insignificant (less than 0.5%) for both GG-orig and PGT. However, the GG-real based on real street intersections results in $\geq 7\%$ error in the total duct length estimation. On the other hand, placing the CO in the corner implies larger duct differences for the GG graphs, but almost accurate for the PGT graph. This means that PGT was able to generate a graph resulting in duct lengths similar to the real planning. The observations are valid for the Munich geo-topology. The same studies have been performed in Cologne and Berlin, as summarized in Tables 3.4 and 3.5 respectively. The full set of results, including all the absolute values and generated topologies, is available at [2].

Table 3.3.: UPON, Munich, central and corner CO: Length different of FD and DD with respect the geo-topology

		GG-real	**GG-orig**	**PGT-60**
FD	CO central	1,3%	-2,6%	3,3%
	CO corner	12,2%	14,8%	25,7%
DD		8,9%	1,4%	-1,7%
Total duct	CO central	7,1%	0,4%	-0,5%
	CO corner	9,6%	-4,7%	0,1%

Table 3.4.: UPON, Cologne, central and corner CO: error in FD and DD estimation with respect the geo-topology

		GG-real	**GG-orig**	**PGT-95**
FD	CO central	-3,5%	2,1%	4,7%
	CO corner	-11,2%	0.3%	4,9%
DD		12,8%	4,3%	-4,5%
Total duct	CO central	8,3%	3,7%	-2,0%
	CO corner	5,5%	3,1%	-1,6%

From the results presented in Tables 3.3-3.5, we cannot conclude, which of the models (GG and PGT) universally results in a smaller error in total duct length estimation. The conclusion here is that based on results, both of the models can be used for the total duct length estimation. The planning results for dense demands seem to be robust as there are many demands (see Figure 3.9) and the possible inconsistencies in

topologies are leveraged out.

For central CO, the GG-orig and PGT-95 perform similar with not more than 3.7% error for the total duct estimation. The GG-real in this case performs worse with the errors up to 8.3% in the total duct length estimation. The CO placed in the corner of the topology results in total duct length overestimations, mostly due to the errors in the FD length up to 21% for GG and 31% for PGT-95. However, the DD does not depend on the CO location [43] and overweights the FD in the total duct lengths, thus the total error does not exceed 10% for GG-real, 5% for 7% for PGT.

Table 3.5.: UPON, Berlin, central and corner CO: Length different of FD and DD with respect the geo-topology

		GG-real	**GG-orig**	**PGT-95**
FD	CO central	-1,7%	6,2%	11,6%
	CO corner	-4,9%	21,7%	31,0%
DD		0,8%	-0,3%	0,7%
Total duct	CO central	0,4%	0,7%	2,4%
	CO corner	-0,3%	3,8%	6,4%

Sparse MBS demands with protection (PP2P)
Figure 3.10 shows the planning results visualization for the P2P MBSs planning with link-disjoint protection (see Figure 2.11). The distance between the MBS is approximately the inter-MBS distance from [33], i.e., 500m. The small changes come from pushing the MBSs to the closest road segment in every topology. The thick dark green lines represent the working paths and the thick orange lines represent the protection paths. These planning results are summarized in Tables 3.6-3.8.

In the PP2P scenario, the demands are MBSs and compared to the previous UPON scenario they are sparse demands. Hence, we expect more variability of the planning results. Further, both of the total duct components (working and additional protection) depend on the CO placement, unlike the DD in the UPON scenario [43].

Tables 3.6-3.8 summarize the errors the estimation of the working, additional protection and total ducts with CO location in the center or in the corner. The first observation that we make is that the placement of the CO in the corner of the topologies results in unpredictable over- and underestimations for the working and protection duct length up to 33% (consistent with the dense demands scenario). This is expected as the corners of the topologies accumulate all the discrepancies with the geo-topology, thus placing the CO corner would be equivalent to accumulating the error on every

path. In this scenario, both of the total duct components depend on the CO location and are approximately of equal total length. Thus, the error propagates to the total duct with up to 17%. For a more sensitive scenario with sparse demands, we do not recommend putting the CO in the corner due to the unpredictability of the results.

Figure 3.10.: PP2P planning on the PGT-60 graph of Munich. CO is shown as green circle, MBS as small dark circles. The working duct is shown as green lines and protection duct as orange.

Table 3.6.: PP2P, Munich, central and corner CO: summary of difference in duct lengths of the working and protection paths for the MBSs demands with respect the geo-topology

		GG-real	**GG-orig**	**PGT-60**
Working	CO central	0,3%	-5,3%	0,7%
	CO corner	5,7%	12,4%	22,9%
Protection	CO central	1,6%	4,9%	12,9%
	CO corner	-16,4%	-20,0%	-8,7%
Total duct	CO central	0,9%	-0,4%	6,5%
	CO corner	-6,2%	-5,0%	5,9%

For the CO placed in the center, we observe that for the working duct the PGT tends to overestimate from 0.7% for Munich to 8.4% for Berlin. GG-orig tends to underestimate the working path duct from -5.3% to -1.7% for Cologne. The GG-real graph with the real intersections shows the best results with not more than 0.5%. The additional protection duct is more over- and underestimated as it has to take longer paths (link-disjoint to working) and the differences in node degrees and diameter have more

influences. The total duct evaluation on the graph street topologies results in maximal difference of 6.5% for PGT and -9.9% for "GG-orig". In general, for the urban type of topologies and central CO the difference in total duct is about 10%. As we have expected, PP2P is a more sensitive scenario as UPON and this results in higher duct estimation error. From the planning results presented here, we cannot choose a uniformly better performing topology model.

Table 3.7.: PP2P, Cologne, central and corner CO: summary of difference in duct lengths of the working and protection paths for the MBSs demands with respect the geo-topology

		GG-real	**GG-orig**	**PGT-95**
Working	CO central	0,5%	-1,7%	4,1%
	CO corner	9,8%	14,2%	20,0%
Protection	CO central	-18,0%	-16,7%	-10,9%
	CO corner	-32,7%	-23,0%	-13,9%
Total duct	CO central	-9,6%	-9,9%	-4,1%
	CO corner	-13,5%	-6,2%	1,4%

Table 3.8.: PP2P, Berlin, central and corner CO: summary of difference in duct lengths of the working and protection paths for the MBSs demands with respect the geo-topology

		GG-real	**GG-orig**	**PGT-95**
Working	CO central	0,1%	2,4%	8,4%
	CO corner	16,1%	19,4%	27,8%
Protection	CO central	-5,6%	-12,2%	-2,8%
	CO corner	-28,4%	-6,9%	6,1%
Total duct	CO central	-3,0%	-5,4%	2,4%
	CO corner	-6,9%	5,8%	16,5%

Recommendations on Graph-Based Models Use

The demonstrated analysis showed that the generated graph-based road topologies can be used as reliable modeling of the road topology. It showed for the urban case and CO placed in the center, the error in total duct lengths estimation for the sparse

demands (MBSs) under 10% for GG-orig and under 6.5% for PGT. For the dense demands (residential) the graph street topologies perform even more stable and show the differences in total duct of not more than 3.1% for "GG-orig" and 2.4% for PGT. We recommend verifying the performance for other types of areas with the available implementation of both models and analyses [2].

Using graph street topologies can be a good benchmark for comparing the network planning methods to obtain general results. The results do not show any statistically significant advantage of one graph-based model over another. Due to the initial parameter tuning overhead for PGT, we recommend using the GG-orig due to its simplicity as it requires only the number of random points to interconnect.

3.5. Summary and Discussion

In this chapter, we looked into application of graph-based road topology models for strategic (fixed) network planning and algorithms validation. We carried out a holistic evaluation: topology generation, graph and planning analyses. The planning analysis consisted of two parts: optical access network planning for dense residential demands and optical backhaul network for sparse MBS. We showed that for the sparse demands the graph-based models result in difference with geographic planning of not more than 10% and for dense - 5%. We provide recommendations for graph-based road topology models use and provide access to our implementations, results and input data [2].

4. Reliable Converged Access Network Planning

Emerging and extending ultra-reliable communications and applications require the connection availabilities of at least five nines (0.99999) [126] not only in the core and metro networks, but also in the access. The access networks that we consider in this dissertation, as defined in Chapters 1 and 2, are optical and wireless (see Figure 2.9 for the relations between optical backhaul, optical and wireless access networks). Although the requirements to reliability are the same, the challenges are different.

Optical access networks are commonly unprotected as the SLA does not foresee availability with residential users but with e.g., business and BSs as the business losses are higher. There are special users, e.g., for business customers, for which the connections are protected. For the ultra-reliable services, a certain end-to-end connection availability is required and this includes the optical backhaul, i.e., ODN. Deploying a separate reliable ODN would imply prohibitive costs for an NP. The reusing of existing infrastructure and converged planning could significantly decrease the cost of making the backhaul reliable [65].

Section 4.1 shows the protection schemes and their reliability analysis for ODN as a backhaul for ultra-reliable communication independent of a residential optical access network and making use of convergence with it. The results were first published in [6], where also the energy consumption was analyzed. In this dissertation, for the sake of preserving the logical flow, we first present the reliability results and then, in the next chapter, the respective energy consumption analysis results.

For the wireless access networks, there are the ways of improving the connection reliability, for example, as reliable modulation and coding, but they are normally not reusing the existing technological redundancy. By technological redundancy, we mean multiple simultaneously deployed technologies, e.g., TETRA and LTE. We refer to such case as to "heterogeneous wireless protection", when we use the benefit of having multiple technologies to improve the wireless connection availability.

Section 4.2 is dedicated to the heterogeneous wireless protection case for ultra-reliable communications, including the measurements on an implemented testbed and the reliability analysis. We follow closely our published study [7]. The chapter is concluded with the "Summary and Discussion" section.

4.1. Reliability Performance of Converged Optical Distribution Networks

Facing the challenges of new communication requirements (e.g., five nine availability requirements of the ultra-reliable services) that are costly in addressing, the NPs are considering reusing and upgrading the already deployed ODNs (e.g., implementing some optical fiber and reusing copper, where possible) in order to satisfy these requirements at limited cost to increase their profitability. With this study we address accommodating heterogeneous demands, supporting a wide range of services with different delay sensitivity and bandwidth requirements, and satisfying ultra-reliability requirements.

In a conventional scenario, in the same deployment area multiple ODNs coexist. For example, there is already deployed a GPON residential access ODN (see Figure 2.12 in Chapter 2), and the MBSs are connected to the aggregation network via separate backhaul network (e.g., as in Figure 2.11). However, such separate networks owned by the same NP are inefficient, require complex operation, maintenance and upgrades and thus are unnecessary costly in both deployment and operation.

An HPON network (see Figure 2.13 in Chapter 2) can serve as the underlying architecture to support converged optical networks [60]. In this case, the same architecture can be used to interconnect different types of terminals (residential users, business users, MBSs, etc.) based on their bandwidth and reliability requirements. The number of COs is reduced due to node consolidation as a result of longer passive reach.

As noted earlier, arising ultra-reliable communications require an end-to-end connection availability ≥ 0.99999 [126]. This is a higher connection availability requirement than the currently offered by the existing unprotected ODNs. The tree topology of the ODN (with no redundant links) makes the optical backhaul vulnerable to link cuts. Depending on the particular location of the link cut, this may disconnect some users of ultra-reliable services, which is unacceptable as these are often safety-related applications. In order to ensure the connectivity in the presence of link cuts, a suitable protection scheme must be deployed.

One important concern of NPs is to find a compromise between the investments required to offer protected optical backhaul and the expected increase of revenues from the customers (i.e., how much are the customers willing to pay for an increased network reliability performance). Different solutions have been proposed for HPON architectures, aiming at reducing the required investments [86], energy consumption and failure detection time [87].

This study aims at comparing connection availability and failure detection times of three different protection schemes for GPON and HPON architectures, applied to a optical backhaul for ultra-reliable communications. In Subsection 4.1.2, the consid-

ered ultra-reliable communication scenario is described. The details of the three protection schemes are presented in Subsection 4.1.3. Reliability analysis results are then presented in Subsection 4.1.4. The energy consumption part of this study is presented later in Chapter 5.

4.1.1. State-of-the-art Analysis

In the traditional single purpose optical access networks, most of the links stay unprotected due to high implementation costs and do not require a high level of connection availability. Moreover, in the case of a connection failure, a low number of users is disconnected. Such a failure has a low impact on NP's reputation and finances, if any. Even for the traditional optical backhaul networks, the impact of a connection failure is limited. If a BS gets disconnected it impacts only the attached subscribers, which depending on technology could be tens to hundreds and is not comparable in volume to core or metro network failures. Thus even the optical backhaul network is commonly unprotected.

With the introduction of the ultra-reliable communications, the connection availability requirements to the backhaul networks of five nines result in a necessity of protecting not only the core and metro networks, but also the backhaul network. In order to reduce the implementation costs, the existing infrastructure could be reused (brownfield planning) or hybrid multi-purpose networks could be introduced (converged planning). This would reduce the Capital Expenditures (CapEx). To reduce Operational Expenditures (OpEx), the power consumption of the access segment has to be reduced as it was shown to be the main contributor for optical networks [108]. The power saving methods include putting the equipment that is not used to dooze/sleep mode, i.e., exploiting the activity patterns of the users [109].

The state-of-the-art protection architectures for TDM/WDM as [102], [103], [104], [105] and HPON [106][107] use the Loss of Signal (LOS) of the uplink transmission to track the failure of the ONUs. This could be unsuitable for networks that put equipment to dooze/sleep modes to save energy.

The optically looped back protection scheme for protection of ultra-reliable demands in energy-efficient HPON was introduced in [88]. We discuss the details of the protection schemes in Section 4.1.3. In [87], authors looked into the application of the scheme to a generic hybrid optical backhaul network. A similar analysis has to be provided for the ultra-reliable communication scenario.

4.1.2. Ultra-Reliable Communication Scenario

Ultra-reliable communications require an end-to-end connection availability of more than 0.99999 [126]. In this study, we consider a particular example of ultra-reliable communications, i.e., Intelligent Transportation System (ITS).

ITS is not bound to a specific technology neither in RAN [89], nor in backhaul implementation. The most prospective technologies for ITS RAN are LTE (and later 5G) and IEEE 802.11p or Dedicated Short Range Communication (DSRC) [90]. To date, only some of the ITS services are realized with most of them yet to be implemented, especially those relating to safety applications. For the intended implementations in some countries like in USA [91], DSRC was already chosen as the main technology for ITS realization.

In this study, we look into a realistic starting ITS deployment scenario - on-ground public transport: bus, tram and trolleybus lines. We focus on a DSRC-based public ITS RAN with a GPON backhaul as depicted in Figure 4.1. The maximal data rate supported by DSRC RSUs is only up to 54Mbps [92], thus GPON as a backhaul satisfies the bandwidth requirements and the main focus of the study is on reliability requirements. To satisfy the reliability requirements to the ITS backhaul network, we explore the applicability of three protection schemes presented later in Subsection 4.1.3. The protection schemes can be used with the state-of-the-art single purpose or converged optical ODN, e.g., GPON, or as a part of NGOA, e.g., HPON.

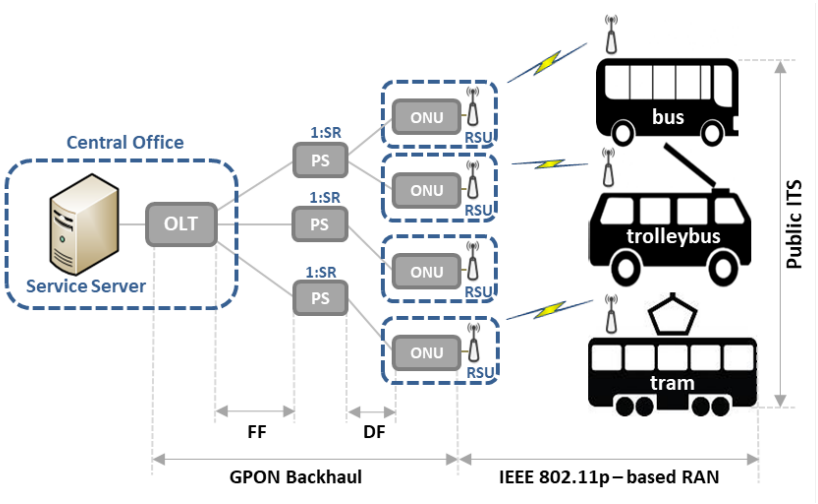

Figure 4.1.: Communication Network Infrastructure for public Intelligent Transportation System (ITS) with DSRC-based RAN and Gigabit Passive Optical Network (GPON) backhaul. ©IEEE/OSA 2017

The ITS base stations or RSUs are connected with the GPON backhaul network to the Service Server (SS) for centralized processing and control. In our setup, SS is collocated with the OLT, at the CO. The fiber between the OLT and Power Splitter (PS) is referred to as FF. The fiber between PS and ONU is DF. All the ONUs are collocated with the respective RSUs.

We further explore two scenarios: greenfield and brownfield. In greenfield scenario, there is no prior infrastructure available. We investigate this setting using PSs with

different SR: 8, 16 and 32 considering an 80% port use (the remaining unused 20% of ports are kept for redundancy or future use [86]). In the brownfield scenario, there is an existing residential GPON infrastructure for FTTB with SR = 32 and 80% port use. This leaves us with seven ports at the PS that are free for ITS implementation.

Road Side Unit Activity Pattern

An advantage of focusing on public ITS is the availability of information regarding the activity times of public transport. The RSUs and thus the ONUs placement is fixed, that is, the placement is based on heuristics, offering coverage along all considered routes of public transport ITS, e.g., day and night buses. In our study, based on DSRC radio access, the inter-station distance between the RSUs is 500m due to communication range limitations of DSRC [96]. This placement heuristic resulted in 38 RSUs and corresponding ONUs.

If an RSU serves only day buses, then it has a natural inactivity time and can be put to sleep during this time. For such RSUs in our study, we predetermine a sleep duration by considering the time slot when all RSUs are inactive, that is, the time when no transport (i.e., no buses, trams nor trolleybus) circulate through the area covered by these RSUs.

Figure 4.2 illustrates the physical meaning of Sleep Slot Duration (SSD). As timetables are different for working days, weekends and holidays, we consider a minimal and a maximal SSD.

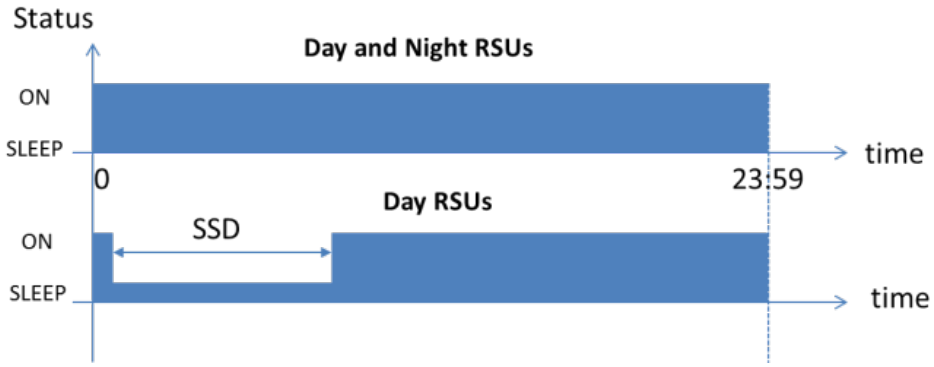

Figure 4.2.: Sleep Slot Duration (SSD) for public ITS. ©IEEE/OSA 2017

Table 4.1 provides details on the two groups of RSUs, day RSUs (with sleep time) and day and night RSUs (always active). The minimal SSD and RSU allocation to day or day and night was obtained from route timetables that are publicly available [139]. The maximal SSD was arbitrarily chosen for comparison purposes. This value can be seen as an upper bound for the sensitivity analysis or a maximum time, representing weekend, holiday, other city and other timetable differences.

Table 4.1.: RSU Activities Based on On-Ground Public Transport Activity [139]. ©IEEE/OSA 2017

Day RSUs, id		**Day and Night RSUs, id**
3,4,12,13,16,17, 19, 20, 25, 26, 27, 28, 29, 30, 31, 33, 35, 36		1, 2, 5, 6, 7, 8, 9, 10, 11, 14, 15, 18, 21, 22, 23, 24, 32, 37, 38
Min. SSD	*Max. SSD*	Always active
3.1h	12h	

ODN Planning Particularities

The ODN planning is performed with the AMS Tool (see Chapter 2). However, there are clustering particularities due to activity patterns introduced earlier that can be considered for OpEx, i.e., energy consumption cost reduction.

RSU clustering can be done independently from the RSU activity pattern, i.e., based solely on geographic position with the objective to minimize the overall fiber length. This option is referred to as "ind". In this case, there are no guarantees that some OLT ports can be put to sleep during the inactivity time. However, we expect the shortest fiber lengths.

Alternatively, the RSUs can be grouped depending on their activity pattern, i.e., clustering the day RSUs and the day and night RSUs separately. In this case, it is possible to put some OLT ports to sleep if all RSUs (and ONUs) belonging to the PS connected to an OLT port are put to sleep. This approach is referred to as "dep" and it has potential to save more energy. The downside of the dependent clustering could be longer fiber length and the reduced end-to-end connection availability.

4.1.3. Protection Schemes: P-Active, P-AS and RP

In this Subsection, we introduce the three protection schemes for passive ODNs as they were proposed in [87] for two stage HPON. The protection schemes are:

- Disjoint Fiber Protection (P-Active),
- Energy-Efficient Disjoint Fiber Protection (P-AS),
- Reflective Disjoint Fiber Protection (RP).

In the two stage schemes below, RN1 implements the wavelength de/multiplexing function and RN2 implements the power splitting function. In order to achieve protection and survivability, active components are added only to CO and RSUs, leaving the ODN completely passive to allow reuse of legacy TDM-PONs for HPON deployments and for GPON compatibility. All the ONUs and RSUs are collocated as shown in Figure 4.1.

Disjoint Fiber Protection

The P-Active architecture is a protection scheme, where both the FF and DF of every ONU are protected. As illustrated in Figure 4.3, the P-Active architecture provides 1:1 protection, where each RSU is connected to the CO via a disjoint FF and a disjoint DF.

Here, the standard definition of disjointness is considered whereby disjoint fibers are those located in different geographically separated ducts. In contrast to the unprotected HPON architecture, redundant and additional components (or equipment) are deployed at the CO, RN, and ONU to achieve protection. At the CO and ONU, an additional OSW denoted as OSW1 and OSW2 in the figure, respectively, is implemented for protection switching. At RN1, two 1×2 couplers and two $2 \times N$ AWGs are deployed.

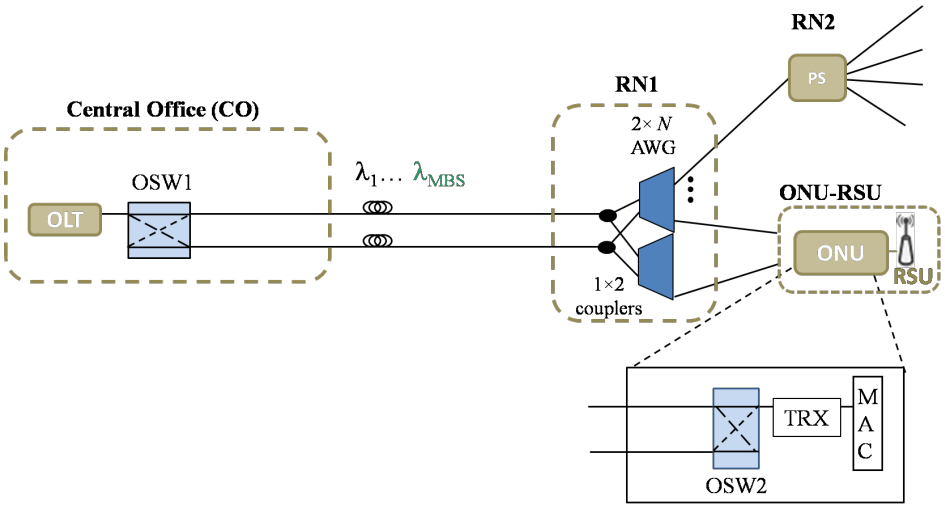

Figure 4.3.: P-Active and P-AS protection schemes. ©IEEE/OSA 2017

Under normal operating conditions, at Optical SWitch (OSW)1 and OSW2 upstream and downstream traffic traverses the primary FF and the primary DF. When a failure (primary FF, primary DF, 1×2 coupler, or AWG) occurs, a LOS is detected at the CO and the RSU, which triggers OSW1 and OSW2 shift the traversing signals onto the disjoint protection paths.

Energy-Efficient Disjoint Fiber Protection

The Energy-efficient Disjoint Fiber Protection scheme (denoted as P-AS) has the same architecture as the P-Active, see Figure 4.3. As alluded to by its name, this protection architecture achieves high energy-efficiency due to the sleep state capability of its ONUs (integrated with the RSUs in this study) [93]. In this architecture, ONUs can transition between an active and a sleep state where the latter supports powering down transceivers to save energy when no data is to be sent/received, i.e., during the inactivity time.

The drawback of this scheme is that the failures that occur during the inactivity time will be detected only when the ONU transitions back to the active state. Hence, the outage duration and, consequently, the penalty on operators will be larger than in P-Active albeit P-AS is more energy-efficient.

Another drawback of the P-AS architecture is that the SS, which relies on the LOS of upstream transmissions to detect failures in the network, may erroneously trigger protection switching of OSW1 when all ONUs are in a sleep state. LOS is commonly used in conventional networks to detect the occurrence of an equipment or fiber failure and to trigger protection switching of the affected traffic onto the backup path. A LOS alarm will be activated at the head-end if an incoming signal has no transitions over a period of 175 ± 75 contiguous pulse intervals (ITU-T G.775 [94]). Using the absence of incoming transmissions to detect failures and trigger LOS alarm is therefore ineffective in P-AS since:

- ONUs in sleep state have zero output power and may erroneously set off the LOS alarm at the CO,
- an ONU in sleep state cannot continuously monitor the network until it transitions out of the sleep state to reinstate LOS monitoring.

Reflective Disjoint Fiber Protection

The Reflective Disjoint Fiber Protection (denoted as RP) addresses the limitations of the P-AS by employing an out-of-band continuous wave monitoring signal, λ_M [87]. Here, λ_M is spaced an integer multiple of the AWG's free spectral range away from the ONU's downstream and upstream wavelength channels. Such wavelength assignment allows λ_M to be detected at and reflected from the ONU.
The RP architecture, depicted in Figure 4.4, achieves the energy efficiency of the P-AS scheme by allowing sleep state during the inactivity time, while enabling fast failure detection. Compared to an unprotected scenario, this architecture requires additional equipment to facilitate protection. This includes an OSW1, two WDM filters, and a monitoring module (Monitoring Transmitter (TxMon) and Monitoring Receiver (RxMon)) at the CO; two 1×3 couplers and two $2 \times N$ AWGs at RN1; and two WDM filters, an OSW2, and a monitoring receiver RxMon at each ONU.

Under normal working conditions, λ_M is launched into the ODN and a fraction of the optical power of λ_M is reflected at the AWG. The reflected λ_M is then detected back at the monitoring module at the CO. In the event of a working path failure, the reflected λ_M is absent at the OLT thereby triggering the OSW1 to switch to protection. Also, the absence of λ_M at the ONU triggers the transition of OSW2 to protection.

RP architecture does not rely on upstream transmissions to trigger LOS alarm. Consequently, failures can be continuously monitored during the inactivity time, when the ONUs are in the sleep state as there is no traffic.

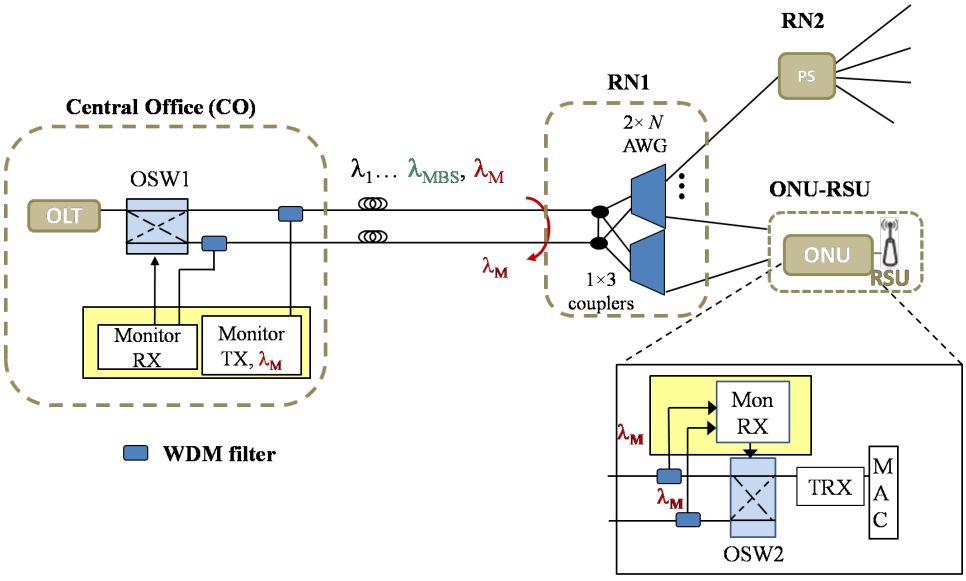

Figure 4.4.: RP protection scheme. ©IEEE/OSA 2017

4.1.4. Reliability Analysis: P-Active, P-AS and RP

In this study, we compare P-Active, P-AS and RP protection schemes (see Subsection 4.1.3) to the UnProtected (UP) architecture in terms of connection availability and failure detection time. The first comparative study for the protection schemes was presented in [95]. It has considered residential users and LTE MBSs for different areas given average traffic models available in the literature.

In this study, we consider a case of a specific ultra-reliable communication deployment, i.e., DSRC-based ITS. Unlike conventional optical residential access or even mobile bakchaul, traffic safety applications of ITS require high reliability and low failure detection time. Therefore, here we study the survivability performance of GPON-based optical bakhaul network with HPON reliability schemes as a candidate deployment for ITS.

We define the connection availability for each case based on the definitions in Chapter 2 and component i availability as shown in Table 5.1 and denoted by a_i. The calculation of connection availability takes into account the average fiber length. The RBD in Figure 4.5 shows that a link of length l_{FF} can be seen as a serial connection of 1 km links.

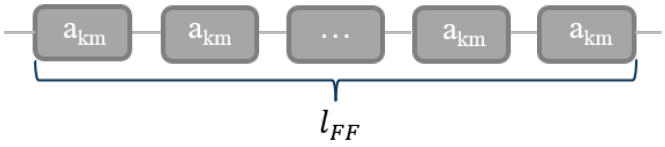

Figure 4.5.: RBD of the average FF availability.

In order for a link of length l_{FF} to be available, all the individual serially connected a_{km} have to be available. Thus, we define average FF availability as:

$$a_{FF} = \prod_{i=0}^{l_{FF}} a_{km} = a_{km}^{l_{FF}}, \tag{4.1}$$

where l_{FF} is the average FF length in km.

We define DF availability, a_{DF}, in the same way. Protection elements are labeled following the working path notation, but with a dash, e.g., $a_{FF'}$.

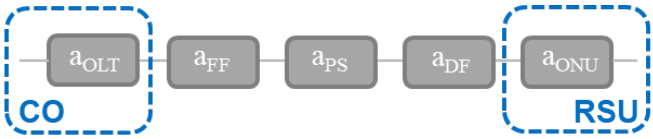

Figure 4.6.: RBD of the UP architecture. ©IEEE/OSA 2017

The RBD for the UP architecture is shown in Figure 4.6. The RBD consists of the blocks representing the OLT, FF, PS, DF and ONU connected in series (every element has to be functioning so that the connection is available) and hence, the availability, denoted by a_{con}^{UP}, is computed as the product of their availabilities:

$$a_{con}^{UP} = a_{OLT} \cdot a_{FF} \cdot a_{PS} \cdot a_{LMF} \cdot a_{ONU}. \tag{4.2}$$

Having the same network components, P-Active and P-AS feature the same RBDs, shown in Figure 4.7. Thus, they have the same availability as in Eqs. (4.3)-(4.5).

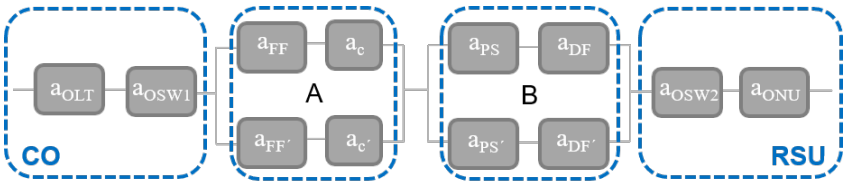

Figure 4.7.: RBD of the P-Active and P-AS architectures. ©IEEE/OSA 2017

$$a_{con}^{UP} = a_{OLT} \cdot a_{OSW1} \cdot a_A \cdot a_B \cdot a_{OSW2} \cdot a_{ONU} \tag{4.3}$$

$$a_A = 1 - (1 - a_{FF} \cdot a_c)(1 - a_{FF'} \cdot a_{c'}) \tag{4.4}$$

$$a_B = 1 - (1 - a_{PS} \cdot a_{LMF})(1 - a_{PS'} \cdot a_{LMF'}) \tag{4.5}$$

For the RP architecture, we have additional filter components (a_f) that influence connection availability model, as shown in Figure 4.8.

Table 4.2.: GPON Component Availability [100]. ©IEEE/OSA 2017

Element	Availability	Notation
OLT per port	0.9999638	a_{OLT}
ONU	0.999961	a_{ONU}
OSW	0.999994	a_{OSW}
TxMon	(0.9999994)[1]	-
RxMon	(0.9999994)[1]	-
PS	0.999999	a_{PS}
Coupler	0.9999993	a_c
WDM filter	0.999994	a_f
Fiber per km	0.9999857	a_{km}

[1] The value is stated for completeness. See Eqs. (5.1)-(5.3) .

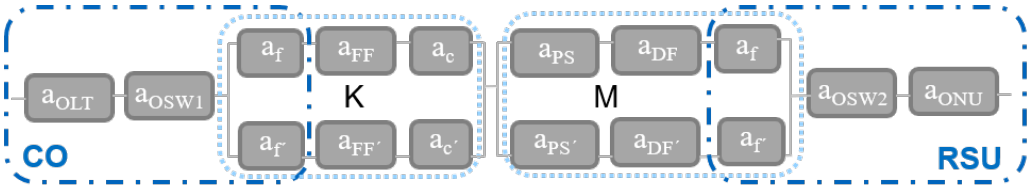

Figure 4.8.: Reliability Block Diagram (RBD) of the Reflective Disjoint Fiber Protection (RP) architecture. ©IEEE/OSA 2017

The RP connection availability is calculated as follows:

$$a_{con}^{UP} = a_{OLT} \cdot a_{OSW1} \cdot a_K \cdot a_M \cdot a_{OSW2} \cdot a_{ONU} \tag{4.6}$$

$$a_K = 1 - (1 - a_f \cdot a_{FF} \cdot a_c)(1 - a_{f'} \cdot a_{FF'} \cdot a_{c'}) \tag{4.7}$$

$$a_M = 1 - (1 - a_{PS} \cdot a_{LMF} \cdot a_f)(1 - a_{PS'} \cdot a_{LMF'} \cdot a_{f'}) \tag{4.8}$$

These RBDs and equations are the basis of the following reliability analysis results for the greenfield and the brownfield scenarios.

Greenfield Results

The average connection dependability depends on the average fiber length. Figure 4.9 shows an example of working and protection fiber lengths for SR=16. Here, we compare the fiber lengths as a result of independent and dependent clustering, normalized to the number of PSs for FF and ONUs for DF. How much additional fiber is required in the dependent clustering over the independent clustering depends on the topology connectivity and ONU (RSU) density. In our case, the topology is well connected, but the ONU density is low (compared to a typical FTTB scenario). The total additional fiber length is only about 11%.

Figure 4.10 illustrates the average end-to-end greenfield connection availability. From the UP results, we can clearly see the impact of clustering and respective average fiber lengths changes. That is the average end-to-end connection availability for the UP for the dependent clustering is always lower than that for an independent one. As expected, all protection schemes improve connection availability, leveraging the difference between clustering and SRs. The results indicate the similar reliability performance of the protection schemes of four nines. In the current configuration, even with the protection schemes the five nines are not achieved.

Figure 4.9.: Fiber length with independent and dependent clustering, normalized to the number of PSs for FF and ONUs for DF, SR=16. ©IEEE/OSA 2017

When we observe the RBDs of the protection schemes as in Figure 4.7 and Figure 4.8, we see that two serial components, i.e., OLT port and ONU, feature low availability of only 0.9999638 and 0.999961 respectively. Both of the components feature only four nines availability. Our results show, that this is unacceptable for the ultra-reliable communications. Further, the OSWs feature five nines availability and are also serial components. In order to evaluate the protection schemes, we remove the unreliable serial components from the analysis, i.e., OLT port, ONU, and OSWs. The resulting availability we call the ODN connection availability as it does not include the end points. Already for the UP case, the average connection availability becomes four nines instead of three for the end-to-end average connection availability as was shown

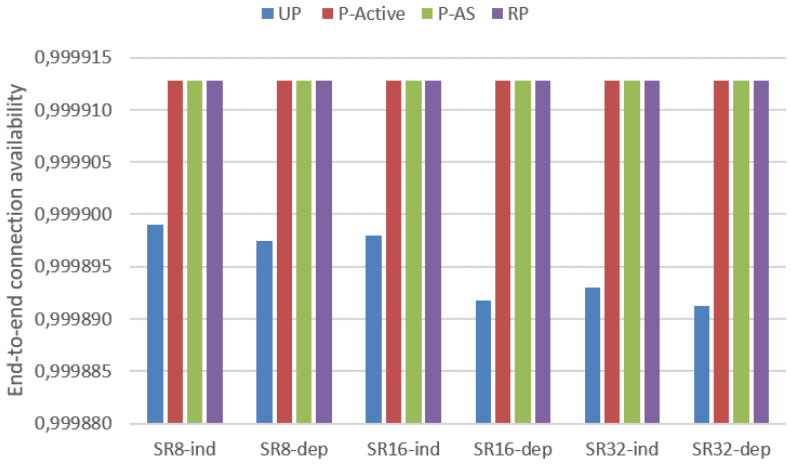

Figure 4.10.: Average end-to-end connection availability for the greenfield scenario. ©IEEE/OSA 2017

in Figure 4.10. Figure 4.11 summarizes the average ODN connection availability for the three protection schemes. We do not show the availability of the UP case in the figure due to a dramatic difference in scale between four nines and nine nines.

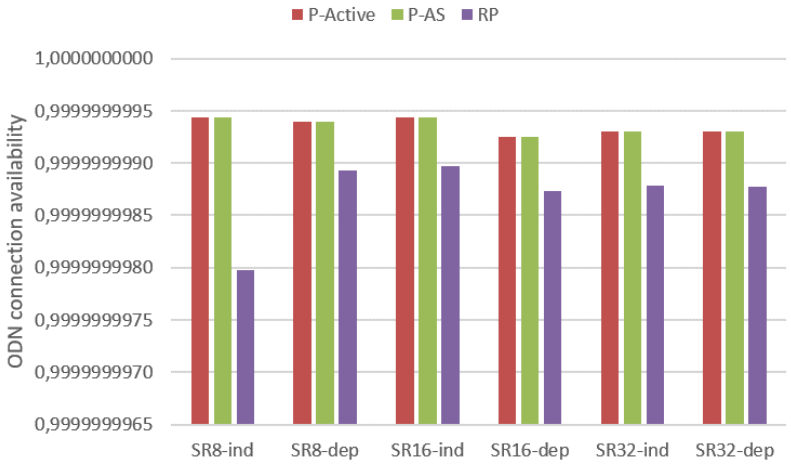

Figure 4.11.: Average ODN connection availability for the greenfield scenario of the protection schemes. The UP ODN connection availability is slightly more than four nines, while the protection schemes result in at least eight nines availability.

From the results in Figures 4.10 and 4.11, we conclude that the reliable ODN is not enough and the availability of the bottlenecks, i.e., of the serial components, have to be improved. There could be two approaches to it: purchasing more reliable components or duplicating the components.

Further, for the ITS safety applications as an example of typical ultra-reliable com-

Table 4.3.: Failure Detection and Restoration Times. ©IEEE/OSA 2017

	UP	P-Active	P-AS	RP
Detection, ms	3.5	3.5	3.5	0.000524
Restoration, ms	14400000[1]	10.5[2]	10.5[2]	10.5[2]

[1] This value represents a four hour reparation time [101], including the traveling time to the failure site, testing and independent of the number of required technicians.
[2] Switching time to the protection path.

munication, low failure detection time is a crucial metric. A standard safety application (that relies on SS) end-to-end latency is bounded by 100 ms [99]. In the case of a failure, the detection and restoration time of the backhaul network shall be as low as possible. Table 4.3 summarizes the failure detection and restoration times for all the protection architectures and compares their values to the UP [98], [100]. So the RP architecture is able to provide the lowest failure detection time, thus minimizing the delay due to a failure.

Brownfield Results

Figure 4.12 summarizes the FF lengths per PS and DF lengths per ONU for working and protection paths in the brownfield case. As in the brownfield case maximal number of clustered ONUs per PS is defined by the free ports that are not used by the residential users. The FF in this case is reused from the FTTB dark fiber and is presented for completeness. The difference in total fiber length between the results of independent and dependent clustering is only in DF and is 19%.

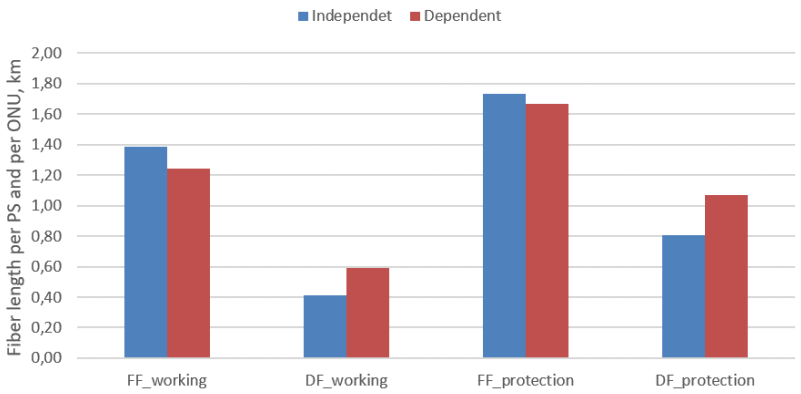

Figure 4.12.: Fiber lengths for working and protection FF per PS and DF per ONU (optical ITS backhaul). ©IEEE/OSA 2017

The average connection availability of the optical ITS backhaul for the brownfield

scenario is illustrated by Figure 4.13. We observe that, as in the greenfield scenario, protection increases the average end-to-end connection availability to four nines independent of clustering. We see that the five nines are not achieved. The reasons here are the same as in the greenfield scenario: low availability of the serial components. Figure 4.14 summarizes the average ODN connection availability.

The average ODN connection availability is consistent with the average fiber length in the Figure 4.12. This means that the dependent clustering features longer fiber length due to the additional constraint of clustering with respect to the activity pattern and thus lower average ODN connection availability. Further, the RP scheme features slightly lower average ODN connection availability due to an additional filter component. However, with the availability of nine nines the impact is measured in seconds per year. In order to improve the average end-to-end connection availability, an NP shall improve the availability of the serial components as in the greenfield case.

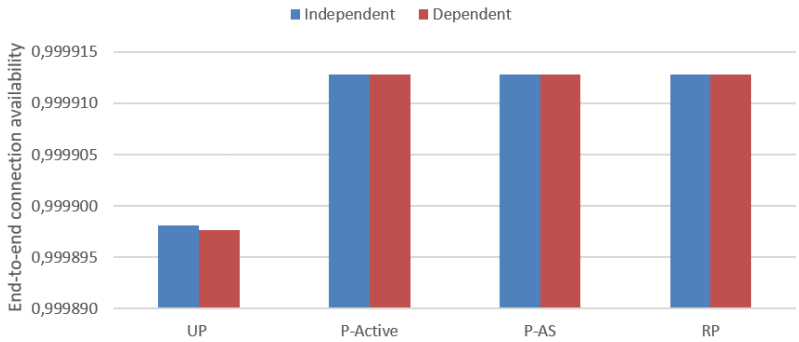

Figure 4.13.: Average end-to-end connection availability of the brownfield scenario. ©IEEE/OSA 2017

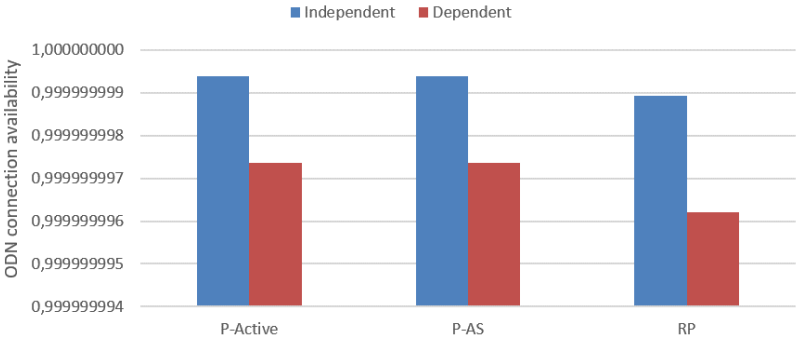

Figure 4.14.: Average ODN connection availability of the brownfield scenario of the protection schemes. The UP ODN connection availability is slightly more than four nines, while the protection schemes result in at least eight nines availability.

4.2. Reliability Performance of Converged Wireless Access Networks

In this section, we look into a particular challenging case of wireless ultra-reliable communications, i.e., emergency networks. Emergency networks are used by the public safety organizations like police, fire-fighters and armed forces. For these networks, communication reliability provision is crucial for every end-to-end connection, including the naturally unreliable wireless connection.

So far the most common safety application in emergency networks are voice calls. Voice calls can tolerate up to 3% packet loss and require a data rate in the range of kbps [110]. Conventional reliable wireless access networks such as TETRA use robust coding and modulation to guarantee communication availability, but sacrificing the data rate [111]. Reliable wireless technologies as TETRA can satisfy the data rate requirements of the voice and messaging, but not the multimedia services [111]. Thus, a wide range of multimedia applications that could be beneficial in the emergency surroundings as video transmissions and self-updating maps, cannot be supported.

Here, we present a feasibility study on facilitating heterogeneous network interconnection by a radio-to-router protocol (DLEP) without adding extra complex network elements. The feasibility study includes implementation, measurements, and availability analysis. We implement DLEP-based router to switch between the three technologies: WLAN, narrowband LTE and TETRA [140]. In a laboratory testbed of WLAN and narrowband LTE, we have measured reliability-relevant metrics: packet loss and inter-technology switching time. These measurements are further used in the availability analysis for the average wireless link availability calculation for the individual technologies. TETRA characteristics were obtained in previously conducted field trials. To conclude on the proposed architecture suitability for the ultra-reliable communications, we conduct availability analysis. We analyze the impact of the joint use of the heterogeneous communication technologies on the average end-to-end connection availability and verify that ultra-reliable requirements on average system's availability of five nines are satisfied. Thus, the contribution of this study is twofold: (1) feasibility study and (2) reliability analysis.

This section is organized as follows. In Subsection 4.2.2, we describe our testbed and introduce the most important implementation details. subsection 4.2.3 shows the results of packet loss and switching time measurements for WLAN and narrowband LTE. These packet loss measurements are then used to define the empirical average wireless link availability for the reliability analysis. Subsection 4.2.4 presents the reliability analysis.

4.2.1. State-of-the-art Analysis

Existing wireless broadband communication technologies, such as LTE or WLAN, enable high data rates. The challenge for these technologies is to ensure the required average connection reliability levels, i.e., five nines [126]. One possible option to increase the reliability is to use multi-path TCP [124], which relies on existing connection diversity. Connection diversity can be achieved by using different wireless links from one technology, e.g., WLAN as in [112]. However, this approach has a number of drawbacks. For example, using the same frequency band and thus sensitivity to the weather conditions.

A prospective way to minimize the influence of the individual technology's drawbacks is to take advantage of heterogeneous networks. Authors in [113] propose integrating LTE and TETRA based on seamless handover between them using Media Independent Handover IEEE 802.21 standard. There are further options to integrate WLAN and TETRA [112], satellite communications and TETRA [114]. A more radical approach would be to design a heterogeneous network, for example through use of a service platform [115] or a multi-tier hierarchal network architecture based on cognitive radio [116]. While all of these approaches have their advantages, they as well share some drawbacks. One of the major drawbacks is the lack of availability analysis. As emergency and safety networks are a part of ultra-reliable communications, meeting the reliability requirements is of high importance. Finally, a common drawback is a need in adding new network elements to the existing architectures.

4.2.2. Scenario and Proposed System Architecture

Emergency networks differ in technology and application, e.g., dedicated to police or fire fighters. However, they feature common reliability and data rate requirements. For this study, we assume a scenario, where three communication networks exist in parallel, but do not allow direct traffic routing from one network to another. It can be safely assumed that TETRA network is already deployed; WLAN and LTE are either deployed in parallel to TETRA or used, where available.

In particular, we consider an emergency vehicle convoy scenario. The emergency vehicle convoy consists of several vehicles carrying staff members and network infrastructure to maintain communication between vehicles and back to the command post. Each vehicle carries a full narrowband LTE Infrastructure (Enhanced Packet Core (EPC) and evolved Node B (eNB)), TETRA Infrastructure (Digital Switch (DXT) and TETRA Base Station (TBS)), and finally WLAN Access Pointss (APs). This configuration makes it possible for all the vehicles to send data to the command post. Staff members carry Hybrid Terminals (HTs), which support all the wireless access technologies. We upgrade this system architecture with a DLEP-enabled router [140] for an automatic change of the wireless access networks. The resulting architecture is summarized in Figure 4.15.

Dynamic Link Exchange Protocol (DLEP) is a radio-to-router protocol designed to provide standardized communication between a router and a radio modem. Link layer information from remote radio devices can be used by the router to make decisions on selecting different radio links and to make network convergence faster in the case of mesh networks. DLEP works between the radio and locally connected router only, there is no overhead transported over the radio links.

In our laboratory setup, in the dashed frame in Figure 4.15, we implemented the DLEP specification draft using the open source implementation of Optimized Link State Routing Protocol [142]. The laboratory setup consists of the narrowband LTE infrastructure, WLAN Access Point, High Power LTE Modem and DLEP routers. We performed the measurements on the WLAN and LTE networks.

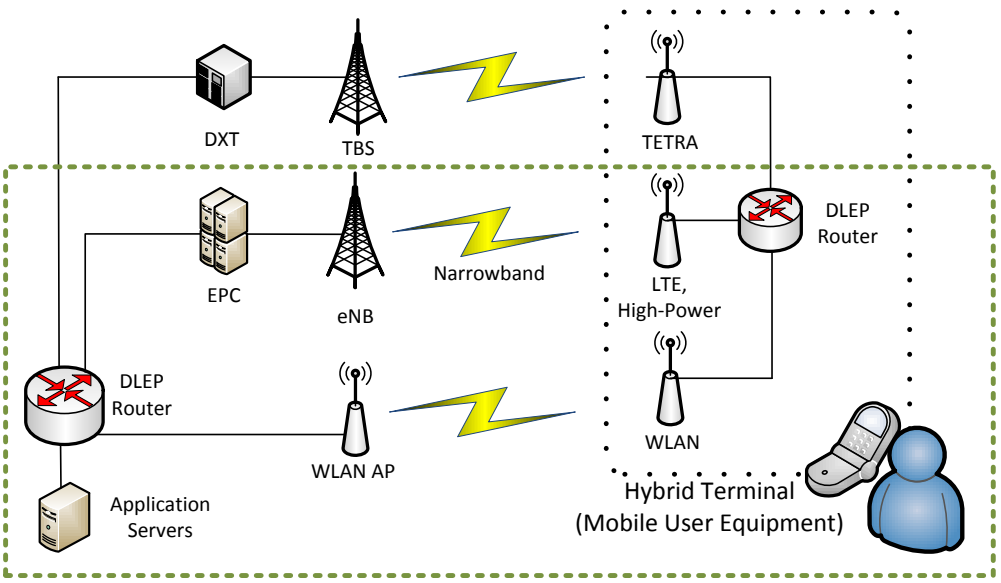

Figure 4.15.: Proposed system architecture and laboratory prototype (in the dashed frame) for interconnection of the heterogeneous wireless access networks though DLEP. Narrowband LTE Infrastructure: EPC, eNB. TETRA Infrastructure: DXT, TBS. WLAN AP. ©IEEE 2017

Table 4.4 summarizes the used technology parameters. We list the TETRA parameters as we used in our coverage calculations. Our coverage calculations are based on path loss models. For TETRA and LTE networks, we used the path loss models from [117] and [118], respectively. In order to obtain comparable coverage of LTE and TETRA, we use high power receiver modem [145]. The path loss model to determine coverage of WLAN in the outdoor open area is given in [123].

Note that although we use narrowband LTE to achieve similar coverage as with TETRA,

the available data rate with the narrowband LTE is still more than 26 times higher than with TETRA and is sufficient for the chosen services.

Table 4.4.: System Specifications. ©IEEE 2017

Parameters	**Value**
Height of Base Station	30 m [117]
Height of User Equipment	1.5 m [117]
TETRA	
Frequency band	380 MHz
TBS Transmit Power	40 dBm [122]
User Equipment Transmit Power	35 dBm [119]
Receiver Sensitivity	-103 dBm [119]
Data Rate	28.8 Kbps
Coverage (from path loss calculation [117])	18.78 km
Narrowband LTE	
Frequency band	400 MHz
eNB Transmit Power	46 dBm [121]
High Power Modem Transmit Power	37 dBm [145]
Receiver Sensitivity	-101.7 dBm [120]
Data Rate	(767.4 ± 9.84) Kbps
Coverage (from path loss calculation [118])	18.34 km
WLAN	
Frequency band	2.4 GHz
Access Point Transmit Power	26 dBm [144]
Receiver Sensitivity	-71 dBm [120]
Data Rate	(19.6 ± 0.06) Mbps
Coverage (from path loss calculation [123])	1.44 km

4.2.3. Measurements: LTE and WLAN

In this Subsection, we show the results of the measurements on the laboratory prototype for LTE and WLAN. The results for TETRA have been obtained in the field tests. First, we describe the measurement set-up: we state the traffic model and the tools that were used. Then we show the results for the average packet loss measurements. Based on the instantaneous packet loss values and service requirements, we define an empirical wireless link availability. The empirical wireless link availability is later used in our availability analysis.

Table 4.5 summarizes the three User Datagram Protocol (UDP) traffic cases that have been used in our measurements to cover all the data rate requirements of the emergency services. We assume cyclic traffic of 5ms, 10ms or 20ms sending cycles. Sending different packet sizes (32, 64, 128, 256, 512 and 1024 Bytes) at these cycles results in different data rates [125]. We use iPerf [143] to generate the traffic between the transmitter and receiver. To perform the measurements of packet loss using the prototype in the laboratory, Wireshark [141] is used. Note that in our laboratory prototype, we cannot change the distance between the transmitter and receiver up to the coverage limits due to the space limitations.

Table 4.5.: Measurement Traffic Characteristics and Data Rates. ©IEEE 2017

Packet Size	**Generated Data Rate**		
	5ms Cycle	**10ms Cycle**	**20ms Cycle**
32 Bytes	0.0512 Mbps	0.0256 Mbps	0.0128 Mbps
64 Bytes	0.1024 Mbps	0.0512 Mbps	0.0256 Mbps
128 Bytes	0.2048 Mbps	0.1024 Mbps	0.0512 Mbps
256 Bytes	0.4096 Mbps	0.2048 Mbps	0.1024 Mbps
512 Bytes	0.8192 Mbps	0.4096 Mbps	0.2048 Mbps
1024 Bytes	1.6384 Mbps	0.8192 Mbps	0.4096 Mbps

Figures 4.16, 4.17 and 4.18 show the measurement results of the average packet loss for narrowband LTE and WLAN for 5ms, 10ms and 20ms cycles respectively. From Tables 4.4 and 4.5, we observe that narrowband LTE supports data rates up to 800 kbps or respectively packet sizes of less than 512 Bytes for 5ms cycle or 1024 Bytes for 10ms. This is confirmed by results of the average packet loss measurements for narrowband LTE, where we observe an abrupt increase in packet loss after the respected packet sizes. In general, for all the guaranteed data rates the average measured packet loss for the narrowband LTE network and WLAN is less than 1%.

Figure 4.19 shows an example of the measured instantaneous packet loss for the

WLAN and LTE networks for the packet size of 32 Bytes, and the cycle time of 20ms over a period of 300ms. For the same example, the average packet loss as shown in Figure 4.18 is always lower than 1%. However, in Figure 4.19 we observe that there are packet loss bursts.

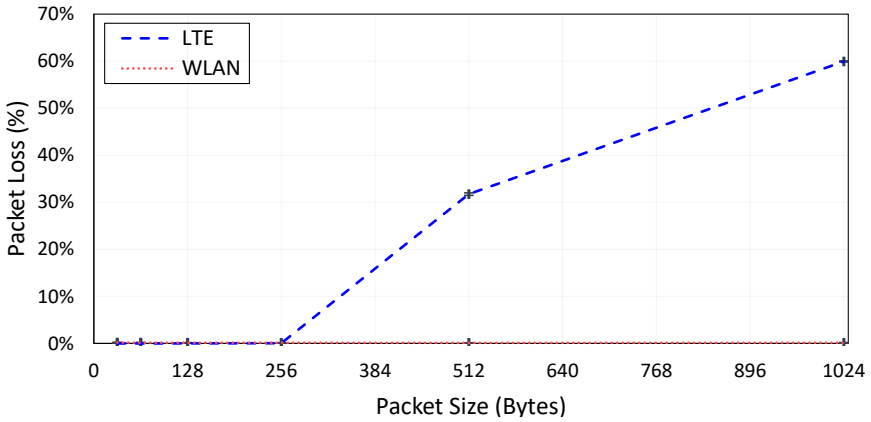

Figure 4.16.: Average packet loss dependency on the packet size, with 5ms generation cycle. ©IEEE 2017

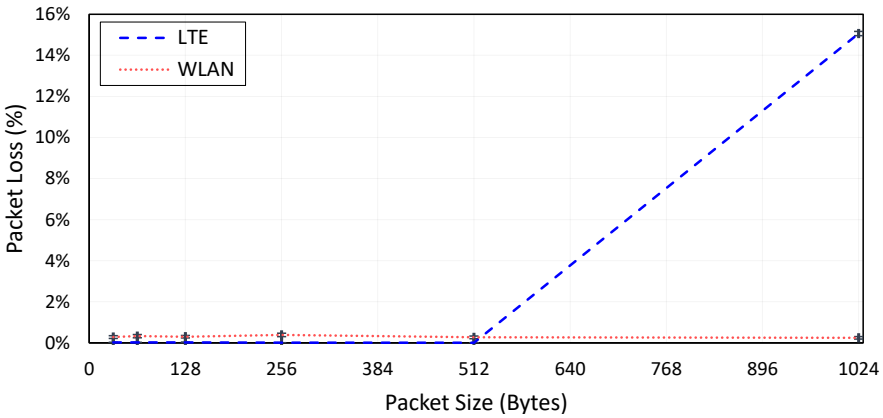

Figure 4.17.: Average packet loss dependency on the packet size, with 10ms generation cycle. ©IEEE 2017

To quantify the wireless channel reliability through packet loss, we define the tolerable packet loss thresholds based on the requirements of the emergency applications. We consider two applications: Critical Safety Messaging (CSM) and Voice over IP (VoIP).

For VoIP, we can tolerate packet losses up to 3% [110], but for the CSM, we can tolerate only up to 1%. With this threshold definition and the measurements example in Figure 4.19, we conclude that the average packet loss is a metric that is not enough to quantify the wireless link availability.

We define the average wireless channel availability as:

$$Availability\ (a) = \frac{T_{\text{Measured}} - \sum_{i=1}^{N} \Delta t_i^{\text{Violated}}}{T_{\text{Measured}}}, \tag{4.9}$$

where T_{Measured} is the measurement period, which is 3600 seconds (1 hour); $\Delta t_i^{\text{Violated}}$ is the time when the packet loss violates the given threshold (1% and 3%).

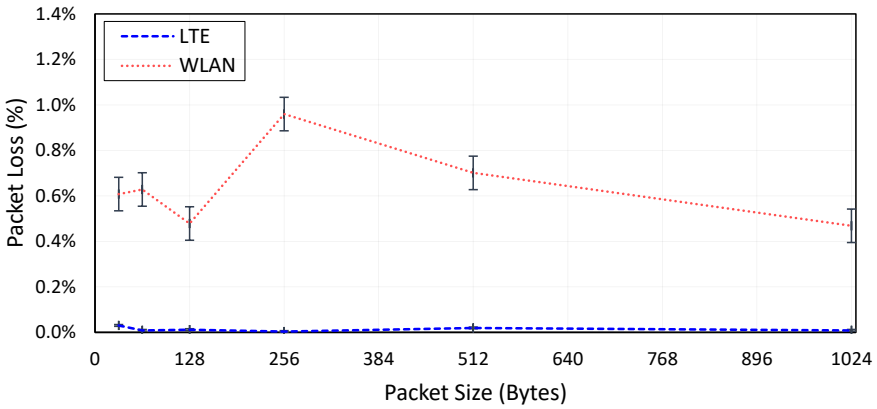

Figure 4.18.: Average packet loss dependency on the packet size, with 20ms generation cycle. ©IEEE 2017

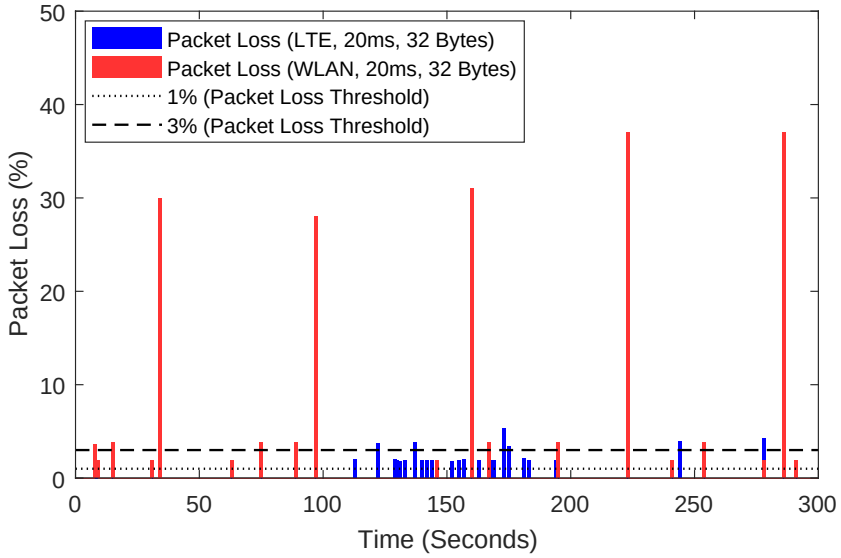

Figure 4.19.: Example of instantaneous packet loss measurements over 300s, with 20ms cycle and 32 Bytes packet size. ©IEEE 2017

In our measurements, we used different packet sizes and cycle times, see Table 4.5, to cover different types of traffic observed in a packet data network. In order to generalize the measurement results, we average the wireless link availabilities calculated

with Eq. (4.9) of the individual runs for the availability (7200 runs) and for the switching time (64 runs). Table 4.6, summarizes the resulting average availability of the wireless links of LTE and WLAN.

Table 4.6.: Average Wireless Link Availability. ©IEEE 2017

Packet Loss	**Application**	**Average availability, %**	
		WLAN	Narrowband LTE
1%	CSM	94.000000	98.861111
3%	VoIP	97.111111	99.555556

Table 4.6 shows that both LTE and WLAN individually violate the required availability threshold (five nines) already at the wireless link level. Thus there is a need in wireless link protection. In this study, we consider a heterogeneous protection scheme that would allow automated switching from one technology to another in the case of a failure in mobile RAN. Here, we define a wireless link failure as violation of the tolerable packet loss level.

If a wireless link failure occurs while data transmission, the transmission shall be switched to the available technology. The time between the failure recognition and data transmission set-up over a functioning wireless access technology, we refer to as "switching time". Table 4.7, shows the switching time between the LTE and WLAN. To measure the switching time we sent a ping continuously while switching off the working path (LTE or WLAN) so that it switches to the backup path (WLAN or LTE). We observe that the switching times are symmetrical and within 1.5s for both directions, when taking the 95% confidence intervals into account.

Table 4.7.: Average Switching Time. ©IEEE 2017

Technology	**Average Switching Time, s**
LTE $\rightarrow$ WLAN	1.42 ± 0.27
WLAN $\rightarrow$ LTE	1.06 ± 0.15

Knowing the switching time is important for wireless link failure definition. A wireless link failure can be defined as an insufficient wireless channel quality over a critical period of time. It is not reasonable to switch to another wireless access technology if the failure time is significantly less than the switching time. Wireless links are influenced by the factors, as weather conditions or interference, which presence is usually limited in time. It makes the wireless link failure definition a challenging and requirement-dependent task. This task, however, is out of the scope of this study.

4.2.4. Reliability Analysis: LTE, WLAN and TETRA

In this Subsection, we analyze the average wireless connection availability for our scenario. Unlike fixed networks, where the user location is known at any time, we deal with mobile users, thus we have to consider the user's mobility. We assume that a user has a uniform probability of being anywhere within the system's coverage. The overall average wireless connection availability is then calculated as:

$$a_{\text{connection}} = \sum_{i=1}^{N} a_i p\{d_{i-1} \leq x < d_i\}, \tag{4.10}$$

where N is a number of logical regions, a_i is the average connection availability in the region i, and $p\{d_{i-1} \leq x < d_i\}$ is the probability of finding the user in this region.

We have rounded the coverage for TETRA and narrowband LTE to 18.3 km (see Section 4.2.2, Table 4.4). So, in this scenario, there are $N = 2$ analysis regions as visualized in Figure 4.20.

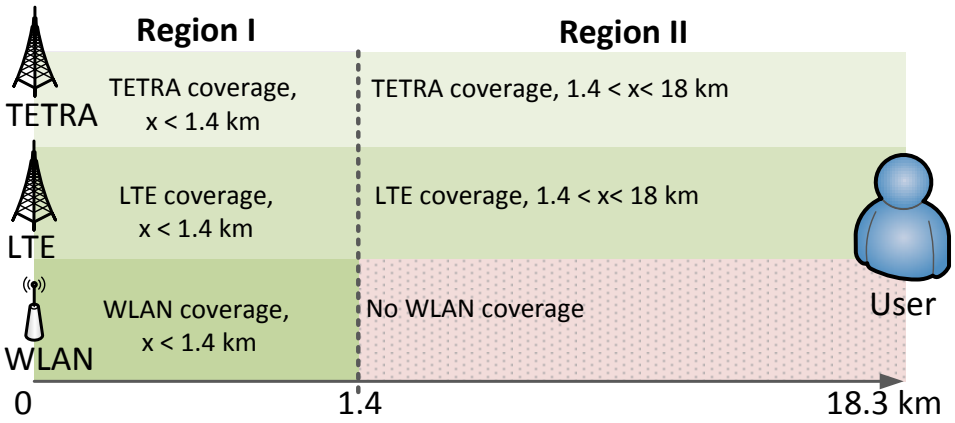

Figure 4.20.: Two reliability analysis regions: $N = 2$, where x denotes user position. Region I: all three technologies WLAN, narrowband LTE and TETRA are available. Region II: only TETRA and narrowband LTE are available. ©IEEE 2017

In region I, all the three technologies (WLAN, LTE and TETRA) are available. This region is defined by the smallest coverage range, i.e., of WLAN or $d_1 = 1.4$ km as shown in Table 4.4. In region II, both, LTE and TETRA, are available. In this case, the region has radius of $d_2 = 18.3 - 1.4 = 16,9$ km. In this case, there is also a possibility of multi-hop WLAN connection. That is mobile WLAN-capable terminals in an ad-hoc mode, interconnect so that the entire coverage span can also be covered with WLAN. However, due to low wireless connection availability of WLAN and serial concatenation of the links, this protection option is out of the scope of the study.

Our average connection availability analysis is based on the Reliability Block Diagrams (RBDs). The average wireless link availabilities for WLAN and LTE are defined by the measured packet loss, see Eq. (4.9) and Table 4.6. The average wireless link availability for TETRA has been obtained in the previous field trials. The average availabilities for the LTE and TETRA core and access network elements as well as for WLAN Access Points (AP) have been obtained from the documentation.

As the DLEP router is a new element, we derive the needed level of availability from the connection availability requirement of five nines. Another new element in our study, is a Hybrid Terminal (HT). A HT is a user equipment that supports WLAN, LTE and TETRA and has DLEP capabilities. We assume for it the same average availability as for the DLEP router. Table 4.8 summarizes the individual average availabilities of all system's components.

Table 4.8.: Individual Average Availabilities for WLAN, LTE and TETRA. ©IEEE 2017

Component	**Symbol**	**Average Availability**
DLEP Router or HT: derived	a_{DLEP} or a_{HT}	$\geq$0.999996
TETRA		
Total: DXT, TBS and Wireless Link	a_{TETRA}	0.99998
Narrowband LTE		
EPC	a_{EPC}	0.9999616012
eNB	a_{eNB}	0.9999448717
WLAN		
AP	a_{AP}	0.9999948718

In this Subsection, we show the analysis for the individual protection regions. The Section is concluded by showing the analysis results for the average connection availability over the entire system's coverage.

Region I: WLAN, LTE, and TETRA

Within the coverage radius d_1 of 1.4 km, WLAN, LTE and TETRA networks work in parallel. Communication traffic can be sent using any technology based on the traffic requirements, e.g., priority, required bandwidth, and network availability. Figure 4.21 depicts the RBD and Eq. (4.11) formalizes the average availability for this region.

$$a_{d_1} = a_{\text{DLEP}}(1 - (1 - a_{\text{TETRA}})(1 - a_{\text{LTE}})(1 - a_{\text{WLAN}}))a_{\text{HT}}, \tag{4.11}$$

where a_{DLEP} and a_{HT} are obtained through average system availability calculation with a target value of five nines, a_{TETRA} has been obtained through field trials (see Table 4.8),

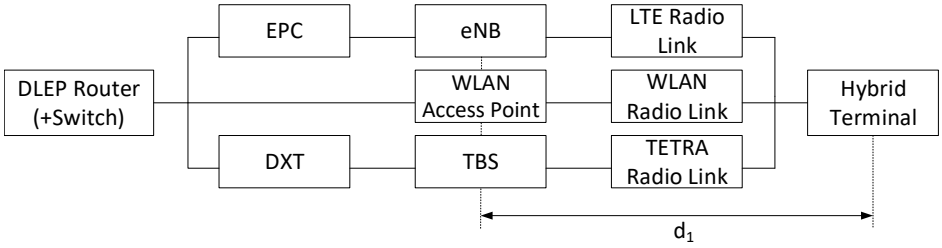

Figure 4.21.: Reliability Block Diagram of the Region I or $d_1 = 1.4$ km, where WLAN, LTE and TETRA are present. ©IEEE 2017

$a_{\text{LTE}} = a_{\text{EPC}} \cdot a_{\text{eNB}} \cdot a^{\text{LTE}}_{\text{WirelessLink}}$ and $a_{\text{WLAN}} = a_{\text{AP}} \cdot a^{\text{WLAN}}_{\text{WirelessLink}}$.

Wireless link availabilities for WLAN and LTE for both reliability critical services, i.e., Critical Safety Messaging (CSM) and VoIP, were presented in Table 4.6 in the previous Subsection. The rest of the available bandwidth is assumed to be used by the supplementary multimedia traffic, e.g., video. Table 4.9 summarizes the average end-to-end connection availability analysis results for the first region, i.e., for CSM and VoIP.

Table 4.9.: Region I: Average Wireless Connection Availabilities for WLAN, LTE and TETRA individually and for heterogeneous protection case. ©IEEE 2017

Technology	**Average Connection Availability**	
	CSM	VoIP
WLAN	0.93998766	0.97109836
LTE	0.98851074	0.99545448
Protection		
WLAN + LTE	0.99930307	0.999860894
WLAN + TETRA	0.99999080	0.999991422
LTE + TETRA	0.99999177	0.999991909
WLAN + LTE + TETRA	0.99999199	0.999991997

From Table 4.9, we conclude that the individual WLAN, LTE and TETRA wireless connections cannot guarantee the required average connection availability of five nines.

Using TETRA allows achieving four nines level of availability, however, only for 28.8 Kbps of traffic. Using LTE and WLAN allows expanding the possible set of services to multimedia. If LTE and WLAN are used with TETRA, both or individually, the required availability of five nines for CSM and VoIP can be achieved. Using LTE and WLAN without TETRA does not achieve even the level of availability of TETRA.

Region II: LTE and TETRA

In this region, LTE and TETRA operate in parallel providing voice and data services. Only LTE can be utilized for the video traffic in the remaining bandwidth. In this case, we consider the distance $d_2 = 18.3$ km as the wireless link has to be available on all the distance to the base station. The RBD of the network for this case is shown in Figure 4.22 and the average connection availability is given by Eq. (4.12).

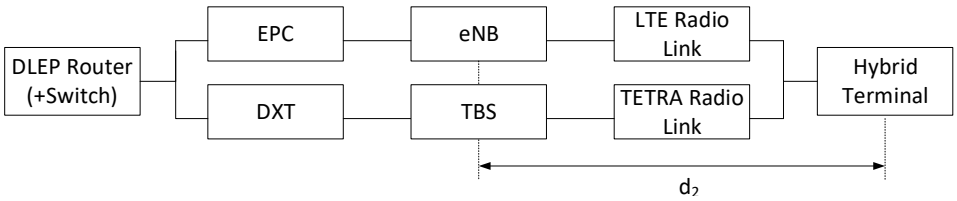

Figure 4.22.: Reliability Block Diagram of the Region II or $d_2 = 16.6$ km, where LTE and TETRA are present. ©IEEE 2017

$$a_{d_2} = a_{\text{DLEP}}(1 - (1 - a_{\text{TETRA}})(1 - a_{\text{LTE}}))a_{\text{HT}} \tag{4.12}$$

Table 4.10.: Region II: Average Connection Availabilities for LTE and TETRA individually and for heterogeneous protection case. ©IEEE 2017

Technology	**Average Connection Availability**	
	CSM	VoIP
LTE	0.98851074	0.99545448
Protection		
LTE + TETRA	0.99999177	0.999991909

Table 4.10 summarizes the values of the average availabilities for the CSM and VoIP. We observe, that LTE can compliment TETRA on the entire coverage range providing the required five nines availability and significantly increasing the data rate.

Average End-to-End Connection Availability

Applying Eq. (4.10), we obtain the average connection availability over the entire coverage range. Table 4.11 summarizes the obtained values with the minimal DLEP router availability of 0.999996, so that the requirement holds.

We further observe, that using WLAN does not significantly influence the availability values. However, WLAN offers high bandwidth and features low cost, thus it can

be used as a complimenting technology for providing connection for the applications with lower reliability requirements. Critical VoIP and CSM data shall be transfered over the protection pair of LTE and TETRA.

Table 4.11.: Average Connection Availability over Entire Coverage Range. ©IEEE 2017

Traffic	**Average system availability**	
	WLAN+LTE+TETRA	LTE+TETRA
CSM	0.99999192	0.99999177
VoIP	0.99999179	0.99999191

The overall connection availability results are influenced by the user distribution, which is not limited to uniform. Therefore, we have included the individual values for both regions in Tables 4.9 and 4.10. There are other factors that shall be considered in the future work, for example detecting wireless link failures and deciding, when to switch to a protection technology depending on the switching time as discussed in Section 4.2.3.

This proof-of-concept study shows that for the ultra reliable communications, as emergency vehicle convoy, using heterogeneous wireless networks as protection allows achieving five nines availability, while increasing the available data rate.

4.3. Summary and Discussion

In this chapter, we have looked into reliable converged access network planning for two types of ultra-reliable communications: safety applications of the DSRC-based ITS and emergency networks. The ultra-reliable requirements on the end-to-end availability (five nines) are hard to satisfy and sets very strict limits on the backhaul. These limitations are normally neglected in the state-of-the-art. Moreover, redundant and extra monitoring equipment add to the overall network consumption and thus also the OpEx. Finally, the equipment that was put to sleep has to be woken-up either by a timer or by network triggering. These energy consumption aspects are investigated in the next chapter.

5. Energy-Efficient Converged Access Network Planning

As presented in Figure 2.1, energy efficiency can be one of the objectives of the strategic network planning. For the NPs, there could be different motivation for having this objective. For example, to comply with the green initiatives and reduce the CO2 emissions [108] and reducing the network TCO by reducing the OpEx.

In this chapter, we look into the energy-efficient converged access planning. Section 5.1, introduces our analysis of energy consumption of survivable access networks (see Chapter 4, Section 4.1 for scenario and state-of-the-art analysis). With the growing network density and equipment redundancy due to reliability requirements, the energy consumption and thus OpEx also grows. therefore, we aim at reducing the energy consumption with putting the inactive equipment to sleep and adopting network planning to the equipment activity patterns. The results were first published in [6] and we follow closely the description in it.

After the equipment was put to sleep it has to be woken-up either by the timer or with a network trigger. An industry state-of-the-art network wake-up approach in circuit switched networks, e.g., Global System for Mobile communications (GSM), was sending a Short Message Service (SMS). In fully packet switched networks, as LTE, LTE-A and 5G; the SMS in its previous form does not exist. In [5], we have presented the results of on network measurements on waking-up with SMS and proposed Session Initiation Protocol (SIP) message. Section 5.2 follows closely our publication.

5.1. Energy Consumption of Converged Optical Distribution Networks

In this section, we look into energy consumption of survivable passive optical converged networks that were introduced in Chapter 4, Section 4.1. The energy consumption analysis was done for the scenario as described in Subsection 4.1.2 and P-Active, P-AS and RP protection schemes as introduced in 4.1.3. Here, we present the scenario for energy evaluation (Subsection 5.1.1) and its results (Subsection 5.1.2).

5.1.1. Annual Energy Consumption: Survivable Optical Converged Networks

In this Subsection, we describe the methodology used in evaluating the annual energy consumption of the UP and the three protection schemes: P-Active, P-AS and RP. We present the annual energy consumption for the active components of the GPON backhaul network.

Table 5.1 summarizes the GPON component power parameters. Although GPON is a passive network, the transceivers in the CO and ONU are active and thus consume energy. At the CO, each OLT port can transition to sleep mode if all connected ONUs are in the sleep mode. A port in sleep mode consumes only 30% of the power consumed in the active state [98].

Table 5.1.: GPON Active Component Power Parameters [100]. ©IEEE/OSA 2017

Element		Power, W	
OLT per port[1]	active	13	$P^{active}_{OLT_{port}}$
	sleep[2]	3.9	$P^{sleep}_{OLT_{port}}$
ONU	active	5	P^{active}_{ONU}
	sleep	0.75	P^{sleep}_{ONU}
OSW	1		P_{OSW}
TxMon	1		P_{TxMon}
RxMon	1		P_{RxMon}

[1] Derived from [95] for SR=32.
[2] Based on [87].

Here the Layer 2 optical equipment, i.e., switching, is excluded from power consumption calculations. It is important to point out that the values were obtained by only considering the physical layer OLT power consumption. For the protection case, further active elements are added, for example OSW, TxMons and RxMons.

First, we define the annual energy consumption equations for the UP and P-Active protection architectures. The active elements in this case are never put to sleep. The total energy consumption per year is calculated as:

$$E^{UP} = (P^{active}_{OLT_{port}} \cdot N_{PS} + P^{active}_{ONU} \cdot N_{ONU}) \cdot 24 \cdot \frac{365}{1000} \tag{5.1}$$

$$E^{P-Active} = (P^{UP} + P_{OSW} \cdot (N_{PS} + N_{ONU})) \cdot 24 \cdot \frac{365}{1000}, \tag{5.2}$$

where N_{PS} and N_{ONU} are the numbers of PSs and ONUs, respectively. We adopt the notation of $N_{element}$ to denote the number of any network elements.

In the UP case, the active elements are the OLT ports and ONUs, as represented by Eq. (5.1). For the P-Active protection case, Eq. (5.2), we add one OSW for the OLT and an OSW per ONU to provide protection. Thus, consumed power is determined by the number of PSs and ONUs.

In P-AS and RP, equipment can be put to sleep to save power. An ONU can transition to sleep outside its activity hours. In our case, the RSUs and their corresponding ONUs that are active during the day can be put to sleep during SSD (see Figure 4.2).

However, an OLT port can be put to sleep only if all the ONUs connected to the same PS are in sleep mode. If during assignment of ONUs to PSs, we do not take into account user activity patterns (independent clustering indicated as "ind"), the OLT ports cannot, in most of the cases, be transitioned to the sleep mode. The annual energy consumption for P-AS is described as follows:

$$E^{ind(P-AS)} = E^{ind(P-AS)}_{24-T_{SSD}} + E^{ind(P-AS)}_{T_{SSD}} + E^{ind(P-AS)}_{24}, \tag{5.3}$$

whereby the three terms on the Right Hand Side (RHS) represent the annual energy consumption components of the network elements that are active during the various intervals of the day. The first term represents the annual energy consumption component due to the time interval $(24 - T_{SSD})$, in which all ONUs are active (day):

$$E^{ind(P-AS)}_{24-T_{SSD}} = P^{active}_{ONU} \cdot N_{ONU} \cdot (24 - T_{SSD}) \cdot \frac{365}{1000}. \tag{5.4}$$

The second term represents the annual energy consumption component due to the T_{SSD}, i.e., sleep time (SSD) or night, in which the day ONUs are in a sleep mode and only the night ONUs are active:

$$E^{ind(P-AS)}_{T_{SSD}} = (P^{sleep}_{ONU} \cdot N^{day}_{ONU} + P^{active}_{ONU} \cdot N^{night}_{ONU}) \cdot T_{SSD} \cdot \frac{365}{1000}. \tag{5.5}$$

Finally, the last term of the RHS represents annual energy consumption of the OSW and OLT ports that are always active:

$$E^{ind(P-AS)}_{24} = (P_{OSW} \cdot (N_{PS} + N_{ONU}) + P^{active}_{OLT_{port}} \cdot N_{PS}) \cdot 24 \cdot \frac{365}{1000}. \tag{5.6}$$

For RP, the general equation of its annual energy consumption is the same as Eq. (5.3) but with the additional contributions from the active monitoring components:

$$E_{24}^{ind(RP)} = (P_{OSW} \cdot (N_{PS} + N_{ONU}) + (P_{TX_mon} + P_{RX_mon}) \cdot N_{PS}^{day} + \\ + P_{RX_mon} \cdot N_{ONU}^{day} + P_{OLT_{port}}^{active} \cdot N_{PS}) \cdot 24 \cdot \frac{365}{1000} \quad (5.7)$$

As introduced in Subsection 4.1.2, RSUs can be grouped depending ("dep") on the activity pattern. In this case, some OLT ports can be transitioned to sleep mode during the T_{SSD}. The number of such ports corresponds to the number of PSs, for which all connected ONUs can be simultaneously transferred to the sleep mode. In our case, all day ONUs can be put to sleep during T_{SSD}.

Annual energy consumption in the T_{SSD} interval component is then composed of active and sleep parts. The active part is due to active (always-on) ONUs and their corresponding OLT ports. The sleep part, respectively, is due to day ONUs and their corresponding OLT ports:

$$E_{T_{SSD}}^{dep(P-AS)} = (P_{ONU}^{active} \cdot N_{ONU}^{night} + P_{OLT_{port}}^{active} \cdot N_{PS}^{night}) + \\ + P_{ONU}^{sleep} \cdot N_{ONU}^{day} + P_{OLT_{port}}^{sleep} \cdot N_{PS}^{day}) \cdot T_{SSD} \cdot \frac{365}{1000}. \quad (5.8)$$

During the time $(24 - T_{SSD})$, all the ONUs and thus OLT-ports are active. The annual energy consumption component from the time intervals $(24 - T_{SSD})$ is calculated as:

$$E_{24-T_{SSD}}^{dep(P-AS)} = (P_{ONU}^{active} \cdot N_{ONU} + P_{OLT_{port}}^{active} \cdot N_{PS}) \cdot (24 - T_{SSD}) \cdot \frac{365}{1000}. \quad (5.9)$$

Finally, OSWs are active 24h:

$$E_{24}^{dep(P-AS)} = P_{OSW} \cdot (N_{PS} + N_{ONU}) \cdot 24 \cdot \frac{365}{1000}. \quad (5.10)$$

RP annual energy consumption differs from the P-AS only in the 24h component due to the presence of the monitoring system and is given by:

$$E_{24}^{ind(RP)} = (P_{OSW} \cdot (N_{PS} + N_{ONU}^{day}) + (P_{TX_mon} + P_{RX_mon}) \cdot N_{PS}^{day} + \\ + P_{RX_mon} \cdot N_{ONU}^{day}) \cdot 24 \cdot \frac{365}{1000}. \quad (5.11)$$

5.1.2. Energy Consumption Analysis Results

In this Subsection, we present the annual energy consumption results for the greenfield and brownfield cases. We also show a sensitivity analysis of the energy consumption to the proportion of the day and night ONUs.

Power consumption figures in this subsection show independent and dependent clustering with minimum and maximum SSD. For example, notation "ind_ssd3.1" would stand for the results for independent clustering with SSD= 3.1h. For the brownfield scenario, additional notation of "+b" is used, it means that in this case residential users were taken into account, i.e., existing FTTB network.

Greenfield

Figure 5.1 depicts the annual energy consumption for the SR = 8. It shows the outcomes arising from the independent and dependent ONU (or equivalently RSU) clustering for two different sleep slot duration values. Generally, protection always mean redundancy and trade-offs with other characteristics. In Figure 5.1, P-Active results in significant increase in yearly power consumption compared to the UP.

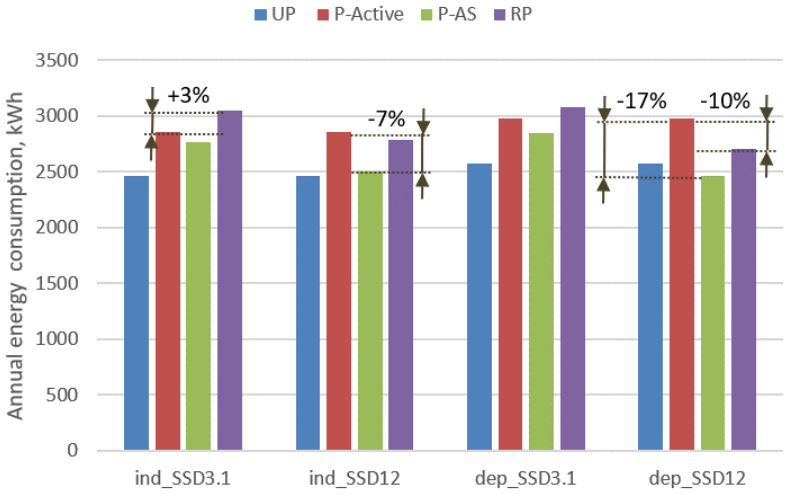

Figure 5.1.: The annual energy network consumption, SR=8. ©IEEE/OSA 2017

The power consumption is the lowest for the UP as it has the lowest number of active elements, i.e., only OLT ports and ONUs. In the case of independent RSU clustering, there are in total seven PSs with SR = 8. For the activity pattern dependent clustering, there are four clusters for day ONUs and four clusters for day and night ONUs. This leads to a total of eight PSs, one more than the independent clustering. We observe that the annual energy consumed by the additional active equipment due to an extra cluster, and thus by the extra OLT port, is compensated by the energy saving of the P-AS and RP schemes.

For P-Active there are several additional active components such as OSWs that are always active. Consequently, changing SSD does not impact the power consumption. As for P-AS, activity information of the public ITS is exploited to place some of the active components into sleep mode during SSD. Unsurprisingly, power consumption of P-AS is reduced by up to 7% compared to P-Active, where savings are higher for

longer SSD. The number of PSs derives the number of additional active elements, and the SSD has to be long enough to compensate for the increase in the power consumption. For example, with SR = 8 dependent clustering results in more clusters, i.e., PSs, and SSD = 3.1 hours results in more power consumption than in the independent case, while SSD = 12 hours, in lower power consumption of the dependent clustering.

Finally, the power consumption of the RP architecture fluctuates around the P-Active values. Specifically, with SSD_{min} it is 3% higher and with SSD_{max} it is 10% lower. This small additional power consumption is attributed to the additional monitoring components but this is in exchange for significantly improved failure detection times, see Table 4.3.

Figure 5.2 depicts power consumption per year for SR = 16 and shows that with the same amount of PSs (number of clusters) the activity pattern dependent ONU clustering results in the same power consumption levels for UP and P-Active as for independent. As for P-AS, the additional components result in up to 12% additional power consumption compared to the unprotected case for the SSD_{min} and dependent clustering. As for the RP architecture, its yearly power consumption shows similar fluctuations as in the previous case.

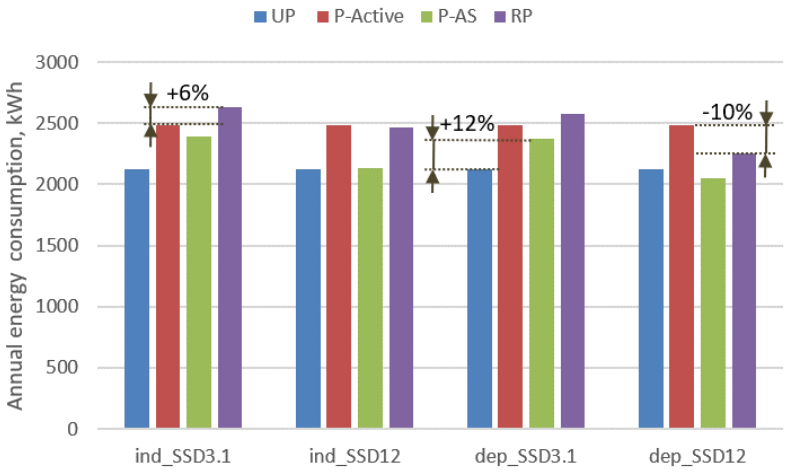

Figure 5.2.: The annual energy network consumption, SR=16. ©IEEE/OSA 2017

Figures 5.3 and 5.4 show the sensitivity analysis of the yearly power consumption for different portions of day-only ONUs (increased or decreased by 25%) with minimal SSD = 3.1 (Figure 5.3) and maximal SSD = 12h (Figure 5.4). P-AS shows the same trends for both values of SSD. Power consumption has an inverse relation with the number of day ONUs. The more day ONUs there are, the more can be put to sleep. As there are no additional active components, compared to the P-Active , this directly results in power consumption decrease.

As for the RP, it can be observed in Figure 5.3 that an increase in the number of day

ONUs results in power increase. This effect is due to the addition of active monitoring components and the gain from the sleep mode being insufficient to compensate for the power consumption increase. Figure 5.4 shows the opposite case, when the chosen SSD is adequate, and hence the reduction in power consumption from sleeping ONUs outweighs the additional power consumption from additional active monitoring components.

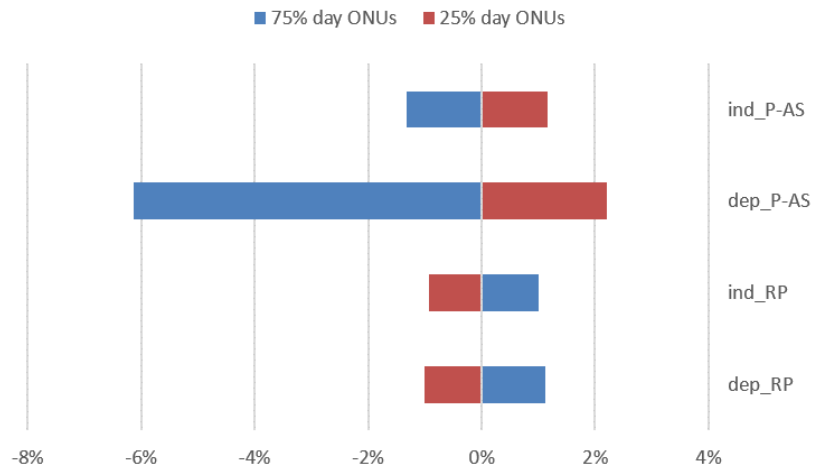

Figure 5.3.: Annual energy consumption sensitivity analysis, SR =16. We compare 50% of day ONU with an increase and decrease by 25% showing the difference between power consumption with min SSD=3.1h. ©IEEE/OSA 2017

Brownfield

For the brownfield, we assume an existing FTTB GPON network for 4877 buildings [135], clustered with SR = 32 and 80% port use. This leaves us with seven free ports per existing PS. The FF in this case is already installed for the FTTB. For the ITS backhaul, we reuse this GPON network and cluster the ONUs to already available PSs. This clustering, as in the greenfield, is done either independently from or dependently on RSU activity patterns. In activity-dependent clustering, we first cluster the RSUs that are active only during the day and connect them to the closest PS, which was already placed according to the FTTB planning. The PSs to which the day ONUs are connected, with no more ports available, are then excluded from the possible PSs for the day and night RSUs in the second stage. In the greenfield scenario, there was no need for PS exclusion as all PSs are newly placed, depending on the network needs.

Figures 5.5 and 5.6 show the yearly power consumption for the two cases: only optical ITS backhaul (Figure 5.5) and the entire GPON with the FTTB (Figure 5.6). These two cases show the difference in the impact of protection on power consumption, depending on the ratio of protected elements to the unprotected.

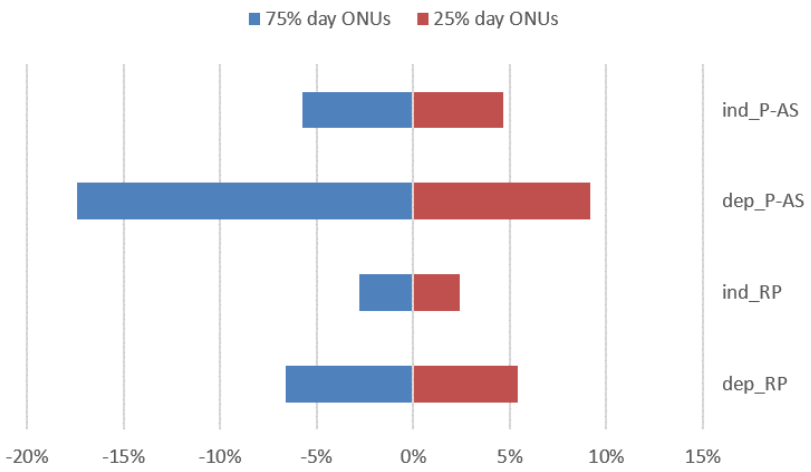

Figure 5.4.: Annual energy consumption sensitivity analysis, SR =16. We compare 50% of day ONU with an increase and decrease by 25% showing the difference between power consumption with max SSD= 12h. ©IEEE/OSA 2017

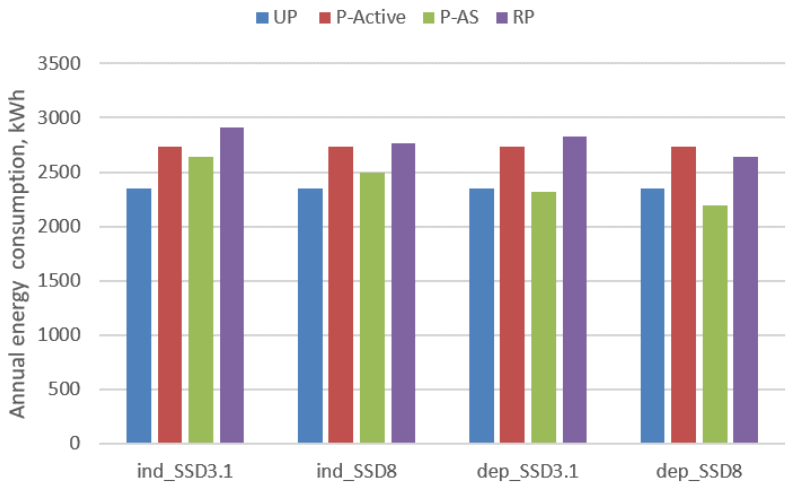

Figure 5.5.: Annual energy consumption of the ITS optical backhaul network. ©IEEE/OSA 2017

In the brownfield case, there can be seven ports used per PS, which results in six PSs in the independent and dependent clustering. For the independent clustering there are in total seven PSs and for dependent - eight. To a great extent, the number of PSs defines the number of active elements, and hence the power consumption of the brownfield scenario is less than that of the greenfield scenario with SR = 8. However, it is higher than that of the greenfield scenario with SR = 16 or 32.

Note that the max SSD in this case is determined not only by the public transport ac-

tivity pattern, but also by the FTTB users. As it was shown in [83], the maximum SSD for residential users (FTTB) is eight hours. For the brownfield scenario the maximal SSD thus is eight hours as the OLT port can be put to sleep only if all the corresponding ONUs are also in sleep mode.

Figure 5.6 depicts the total power consumption by the GPON network, including that of the ITS backhaul and the buildings. We observe that in this case, the trends are similar to the results in [95], where the planning was done for a HPON and only the Macro Base Stations (MBSs) were protected. The majority of the ONUs, i.e., buildings, were unprotected.

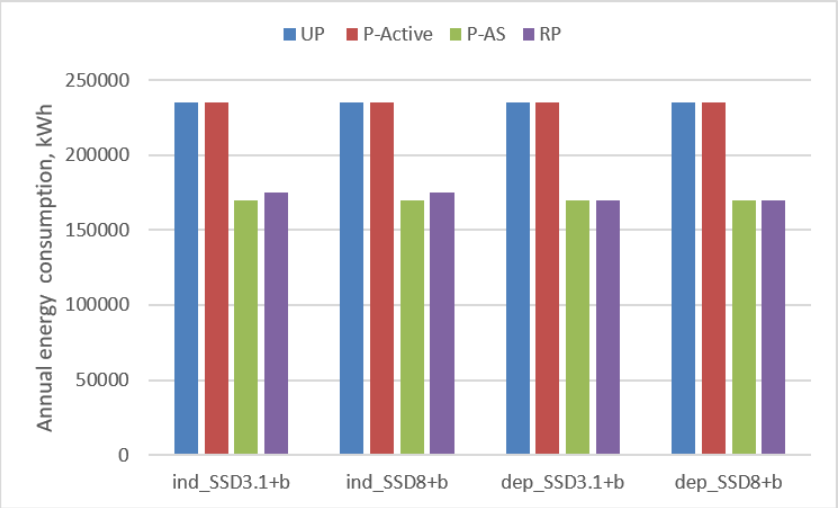

Figure 5.6.: Annual energy consumption of the total GPON network, including ITS optical backhaul and FTTB. ©IEEE/OSA 2017

If we take into account the number of buildings in the total GPON network, i.e., 4877 ONUs, an increase in the power consumption due to protecting ITS ONUs (RSUs), i.e., 38 ONUs, is marginal, with P-Active about 0.2% compared to the unprotected. Thus, the energy savings in Figure 5.6 are mostly driven by putting to sleep the residential ONUs. There is still some small difference between the independent and dependent clustering for P-AS and RP. This difference, however, does not change the overall trend.

5.2. Enabling Energy-Efficient Wireless Access Networks through Network Initiated Wake-ups

The wireless access network also strive the energy-efficiency for the same reasons as ODNs: ecological and economical. Moreover the existing solutions have to be cost-efficiently migrated to the next generation networks, i.e., from circuit switched to packet switched. These migrations have to be planned at the same time with the network in order to make sure that the functions are not lost.

Here, we look into a challenging IoT case, where the modems, e.g., sensors, are often placed in hardly-accessible locations. It is not foreseeable to charge such modems every day as humans charge their phones and its energy-efficiency becomes of primary importance for the entire IoT network. Moreover, keep-alive messages increase network load [82] and bursts of them can lead to network element outages. This is especially critical for the large scale of devices as IoT.

Reducing energy consumption of the modems is possible through putting the modem into idle (sleep) mode and waking it up, when needed. A wake-up is a push-process, i.e., network or specific server initiated, as a result of which the modem establishes network connection. Network-initiated wake-ups also allow avoiding signaling bursts through coordinating the wake-up time of devices.

A critical challenge of the wake-ups is minimizing the additional delay. Delay can be a crucial issue for some of the 5G applications, e.g., opening a car through a smartphone application. Thus the delay has to be minimized. Further challenge in large scale wake-ups over cellular is modem addressing. For the IoT scale, there will not be enough unique telephone numbers, but enough IPv6 addresses. So the preference shall be given to IP addressing.

5.3. State-of-the-art Analysis

In related work, there are a number of approaches to wireless wake-ups. First approach is to add an additional low-power wake-up receiver as in [77] or [78]. Although such an approach is application-optimized, it results in more complex and thus expensive hardware. Moreover, it is often distance restricted. Second approach, is to use built-in modem wireless technologies. For example, authors in [71] suggest using GSM for wake-ups and then running all the applications over Wi-Fi. Authors of [73], instead of using GSM, add a second low-power channel.

[66] and [68] suggest using SMS for wireless wake-ups. SMS over GSM delay evaluation is presented in [75]. This paper shows measurements of SMS delays for single message and bursts, presents analytical analysis of the number of SMS congesting the control channel, it is sent on. However, the measurements were conducted in 2006,

when from 2009 packet-based messengers such as WhatsApp became popular, changing the network load of SMS. Moreover, SMS in its traditional way is not present in LTE and thus requires additional network functions [66].

A natural replacement for SMS could be SIP messaging though an IP Multimedia Subsystem (IMS) [68]. This implies that modems maintain IMS registration, creating heavy load on the IMS. There are suggestions to replace SMS with IP-based wake-ups, e.g., [79]. This solution is dependent on the network functions realized in the underlying network. Moreover, this IP-method is described only conceptually. There are no measurements or discussions on crucial aspects such as delay.

A careful LTE delay evaluation is done in [76]. Among other interesting results, they have measured random access and Radio Resource Control (RRC) connection establishment delay for different radio conditions (good, average, bad). These measurements are well-suited to define, which IoT applications can be LTE-based, but they do not focus specifically on wake-ups. The state-of-the-art on wireless wake-ups misses a packet-switched wake-up solution with validating measurements of crucial parameters as delay; and comparison of different solutions.

In this study, we investigate the case, when the communication infrastructure is already implemented. For instance, there is a set of Mobile Network Operators (MNOs) with infrastructure for Human-to-Human communications. Any changes to the existing network architecture are expensive and time-consuming. Thus, in order to allow choosing from a wider range of MNOs and technologies, a wake-up mechanism shall be network-neutral. For example, wake-up solution shall not depend on the IMS presence in the LTE network. Final note is that energy consumption in active or idle mode primely depends on the underlying technology, network setup and concrete user equipment. For example, SMS-based wake-up over GSM and LTE provides us with different energy consumption figures. We take this into account in our analysis.

At the moment, GSM networks are planned to be dismantled due to rapidly growing data traffic [137]. Thus wake-up solutions based on circuit switched services, e.g., SMS, have to be replaced with some packet-switched solutions. In this study, we introduce Over-The-Top (OTT) SIP messaging for wireless wake-ups over packet-switched networks; in our case, over LTE. The main advantages of the proposed OTT SIP are low delay, independence from underlying physical network (no specific functions required) and ease of implementation. It is treated by the underlying network as normal best effort traffic.

The contribution of this study is twofold. First, we have implemented in a real testbed an OTT SIP wake-up method to measure and to analyze the delay. The measurements have been conducted over 24h for two German MNOs. Moreover, we show measured peak voltage on the modem for LTE idle and connected network states. Second, we benchmark performance of SMS over GSM and SMS over LTE through IMS. Finally, we show peak modem voltage with GSM network. Modem voltage for OTT SIP and

SMS over LTE case is the same as it does not depend on the wake-up method, but on the underlying technology, i.e., LTE. Based on these measurements, we evaluate the prospects of OTT SIP wake-ups compared to the state-of-the-art SMS-based solutions.

This section is organized as follows. In subsection 5.3.1, SMS options over GSM and LTE are discussed. OTT SIP wake-up is introduced in subsection 5.3.2. Subsection 5.3.3 follows with the measurement methodology, results and wake-up methods comparison.

5.3.1. Short Message Service Wake-ups

We investigate SMS wake-ups over two cellular networks: GSM and LTE. In our implementation, we run two SMS clients on a single laptop. Each SMS client has a separate modem and antenna: sender and receiver. The modems are forced to use either GSM or LTE. Addressing in both SMS cases is through telephone numbers.

SMS over GSM

We consider point-to-point SMS [67] over GSM. Simplified, an SMS passes through the GSM access network or Base Transceiver Station (BTS), then GSM core network and SMS Service Center (SMS-SC). Finally, it makes the same way back to the receiver as shown in Figure 5.7.

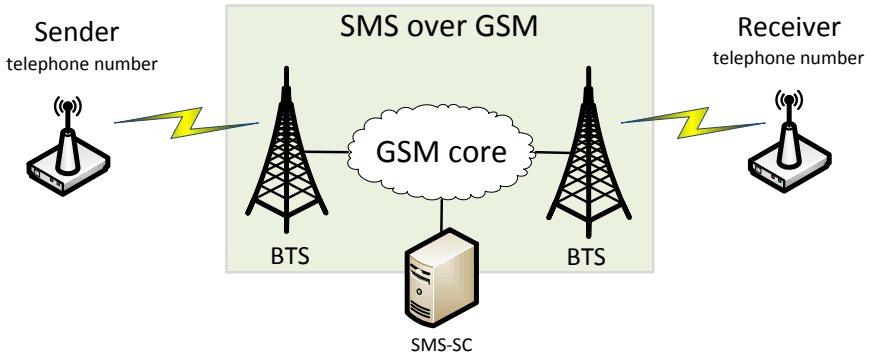

Figure 5.7.: SMS over GSM. ©ACM 2016

SMS is transmitted over a Standalone Dedicated Control CHannel (SDCCH). SDCCH gets congested with about 23 SMS sent simultaneously [75]. GSM network is a circuit switched network, thus an idle state is straight forward and there is no need in accessing BTS information.

Effectively, GSM channel is used as a low power wake-up channel. SMS itself, in this case, is used as a trigger. It is also possible to receive an SMS delivery acknowledgment.

SMS over LTE

LTE is fully packet switched and there is no direct equivalent to SMS. There are two options to transmit an “SMS" over LTE [80]: through legacy circuit switched network, e.g., GSM; or through LTE network, i.e., IMS. These two cases are depicted in Figure 5.8.

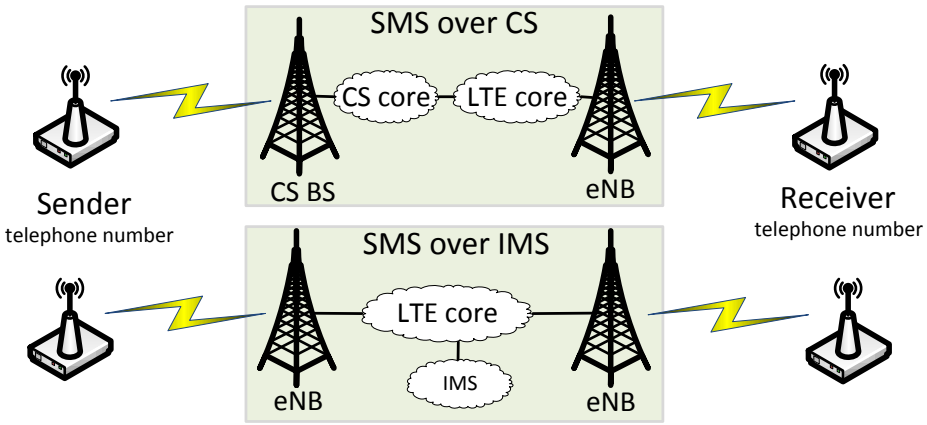

Figure 5.8.: SMS over LTE. ©ACM 2016

If an MNO has no IMS, then an SMS is first transmitted through circuit switched network to Mobility Management Entity (over a special interface from circuit switched to packet switched) in LTE. Then it is encapsulated in a non-access stratum message, i.e., in control messaging as paging, authentication or update.

If an MNO has an IMS, then the SMS is transmitted as a SIP MESSAGE through IMS and connected to it IP Short Message Gateway. Effectively, SMS over IMS can be seen as a SIP-based wake-up solution described in [68].

5.3.2. Over-The-Top Session Initiation Protocol Wake-ups

For wireless wake-ups in packet switched domain of LTE, we use SIP instant messaging and presence leveraging extensions (SIMPLE) [69]. We take advantage of the page mode messaging [70] or instant messaging: no session is established and messages are less than 1300 bytes. Message size restriction allows packing it to a SIP INVITE message, sent at the beginning of each session establishment. Thus, this method is an extension to usual SIP signaling. In this study, we use UDP as the transport protocol. This wake-up solution we call OTT SIP as it does not require any specific network functions and is defined between two generic clients.

Figure 5.9 explains the OTT SIP wake-up over LTE. There are two general user (modem) states in LTE network: idle and active. However, there are more substates. Evolved packet system Mobility Management (EMM) defines if a user (modem) is registered in the network. As soon as the user is attached, EMM state is registered. RRC is active, when any connection to the eNB is established: for both signaling, e.g.,

registration in the network, and user data transmissions. Evolved packet system Connection Management (ECM) is active only for user transmissions. We define modem idle state as:

- Modem is registered in the network: EMM - registered;
- There is no active connection: RRC - idle, ECM - idle.

The state of the modem can be obtained either from the base station, i.e., eNB, which is controlled by MNO, or through instant voltage on the module.

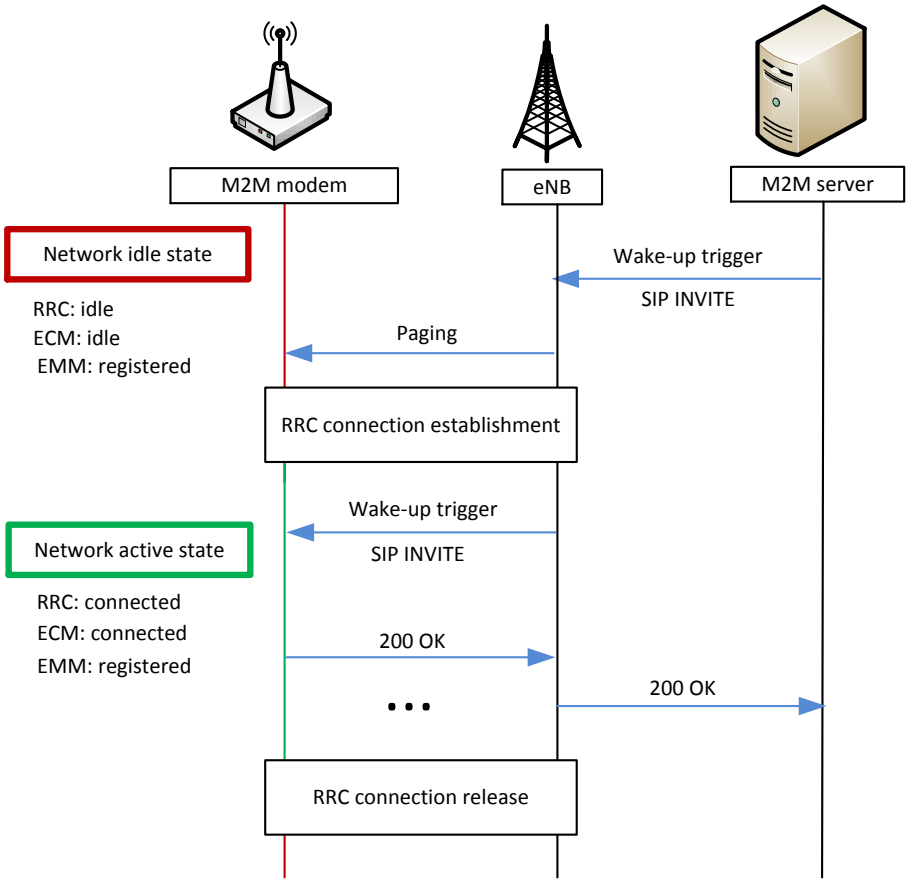

Figure 5.9.: Over-The-Top (OTT) SIP wake-up over LTE network. ©ACM 2016

A server (any generic server) initiates communication with the modem: a wake-up trigger is sent, i.e., a SIP INVITE message. This message passes through LTE network and arrives at the eNB, near which the Machine Type Communication (MTC) modem is located. eNB knows that there are no active connections with the modem and initiates paging procedure to inform the modem about an incoming message. After it an RRC connection to eNB is established, and MTC modem goes to the active state: EMM - registered, RRC - active, ECM - active. The wake-up trigger is delivered. Delivery is confirmed by the 200 OK message, defined in SIP. After communication with

the server is over, RRC connection is terminated by the eNB. The modem goes back to idle.

SIP wake-up measurement setup is shown in Figure 5.10. Two SIP clients run on a single laptop with different sender and receiver modules as in the SMS case. The difference form the SMS case is in the modem addressing.

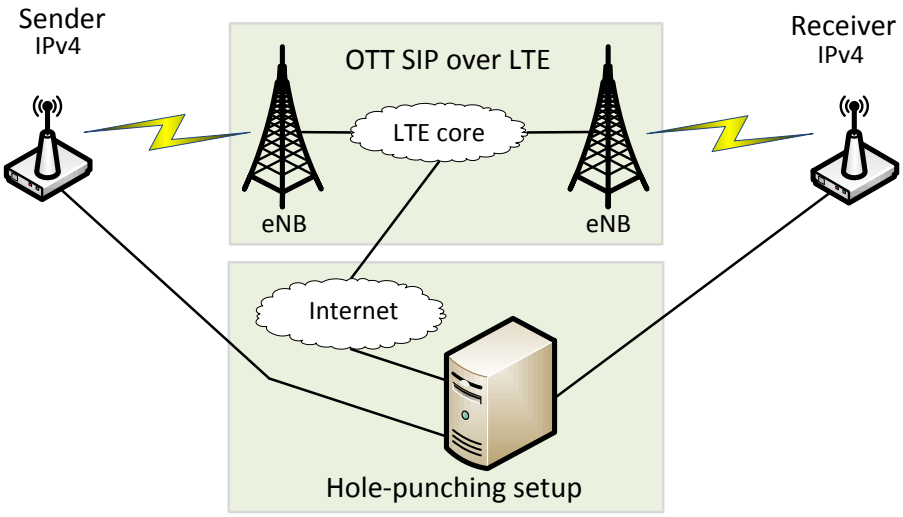

Figure 5.10.: Over-The-Top (OTT) SIP over LTE. ©ACM 2016

Addressing in networks is controlled by the MNO. In our case, two German MNOs, i.e., O2 and Telekom, use IPv4. Already now, before wide IoT deployment, there are not enough IPv4 addresses to provide every user with a unique static IP address [81]. Thus local IPv4 addresses are used inside the MNO networks. These addresses are hidden by the Network Address Translator (NAT) rules to allow global addressing. However, the User Equipment (UE) itself knows only its local address and no NAT rules. This problem is known as NAT-traversal problem. As depicted in Figure 5.10, we use a server with a public IP address and hole-punching to overcome this issue. In IPv6, there are enough IPs to provide each device with a unique address.

5.3.3. Measurements: SMS vs. SIP

This subsection presents and analyzes energy consumption and delay measurements. First, we show the energy measurements. The main focus of our measurements, however, lies on delay of different wake-up solutions and proof-of-concept for the OTT SIP solution. The subsection is concluded by comparison of the OTT SIP over LTE and SMS-based wake-up solution over GSM and LTE, based on the previously introduced criteria.

Measurements Setup

Our testbed consists of two ME909u-521 miniPCIe Modules from Huawei [136] with respective antennas. The modules are connected to a laptop though MiniPCI to USB adapters. Voltage measurement methodology is similar to [71], [72] or [73]. We have connected a resistor ($10Ohm$) in parallel to the modem and measured the voltage on it with a digital oscilloscope.

Delay measurement setups for SMS and OTT SIP are as in Figures 5.7, 5.8 and 5.10 respectively. For OTT SIP experiments, we used four SIM-cards from German Mobile Network Operators (MNOs): two SIM-cards from Deutsche Telekom and two SIM-cards from O2. For SMS-based measurements only Deutsche Telekom SIM-cards were used. The measurements were conducted in a city center location in Munich.

Energy Consumption Measurements Results

Through energy consumption measurements, we can find the most important network parameter for the delay measurements: time-to-idle (or inactivity timer). Time-to-idle defines the time, after which eNB releases the radio resources and the UE goes to the network idle state, see subsection 5.3.2.

We further look into Discontinuous Reception (DRX) cycles. DRX parameters influence UE energy consumption in the idle state, for both GSM and LTE, and energy consumption in connected state, for LTE. LTE-A Releases 12 and 13 already discuss a possibility to increase DRX cycles for IoT applications in order to save more energy. The influence of DRX cycles on energy consumption was shown in [74] and is out of our scope.

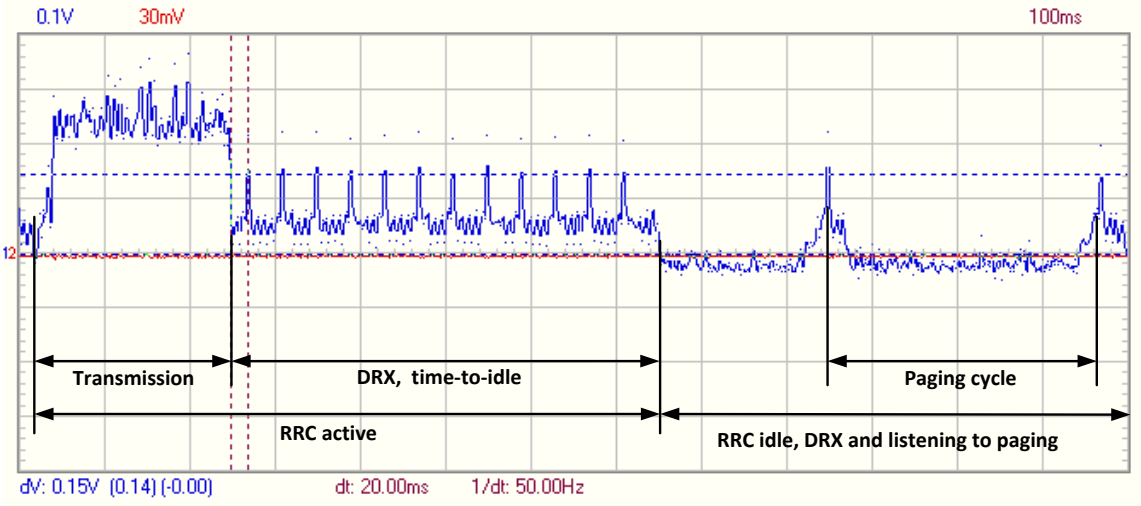

Figure 5.11.: Voltage on the module over time example: transmission, active and idle Discontinuous Reception (DRX). ©ACM 2016

Figure 5.11 is a print-screen of a digital oscilloscope, where we have designated the relevant network states. Instant voltage measurements allow clearly distinguishing LTE idle and active states. First, for approximately $45ms$, there is an active transmission, e.g., receiving a file. It is followed by short DRX cycles, each of $6ms$. This short DRX happens still in connected state. After approximately $72ms$, eNB resources are released and modem goes into idle state with long DRX cycle or paging cycle is $60ms$. For the delay measurements, it means that after time-to-idle has passed (inactivity timer ran out) the modem can be woken up again, as in Figure 5.9.

Table 5.2.: Peak voltage measurements. ©ACM 2016

Technology	**Idle, mV**	**Active, mV**
GSM	43.7 ± 2.2	430 ± 21.5
LTE	170 ± 8.5	250 ± 12.5

Table 5.2 summarizes peak voltage on the module for idle and active states with a 5% inherent measurement error. From the values, we observe that LTE is more energy-efficient in the active state. However, the peak voltage in the idle state is an order of magnitude higher than for GSM. For IoT applications it means that, from the energy conservation prospective, GSM is more efficient, when the modem has to stay in the idle state for long periods of time. Generally, energy consumption is technology dependent and cannot be influenced by wake-up methods in any other way as technology and modem choice.

End-to-end Delay Measurements Results

We show delay distributions for 24h, each hourly measure is an averaged value of the measurements conducted in this hour. We use 95% confidence interval. SMS were sent every 60s summing up to totally 1413 over GSM and 1343 over LTE. OTT SIP messages were sent every 30s resulting in 2736 for O2 and 2867 for Deutsche Telekom. For each case, i.e., SMS over GSM and LTE, we show selected examples of delay measurements.[1] The maximal experienced loss was 5 messages, which is less than 0.4% of 1343, normally the experienced loss was from zero to one message.

In OTT SIP case, IPv4 addresses are used. The NAT-traversal problem [81] is addressed through hole-punching once, before the measurements start. During the measurements the address has not changed. Thus hole-punching does not influence the measured delays.

[1]Full delay measurements are available under:
`https://github.com/tum-lkn/cellular-wakeup-data`

SMS-based wake-ups: GSM and LTE
Figure 5.12 illustrates the SMS wake-up delay distribution over a day for GSM and LTE. In the figure, x-axis is time of the day and y-axis shows the delay in seconds. Average delay per hour for SMS over GSM is shown in blue and over LTE in green. All the measurements are depicted with 95% confidence intervals.

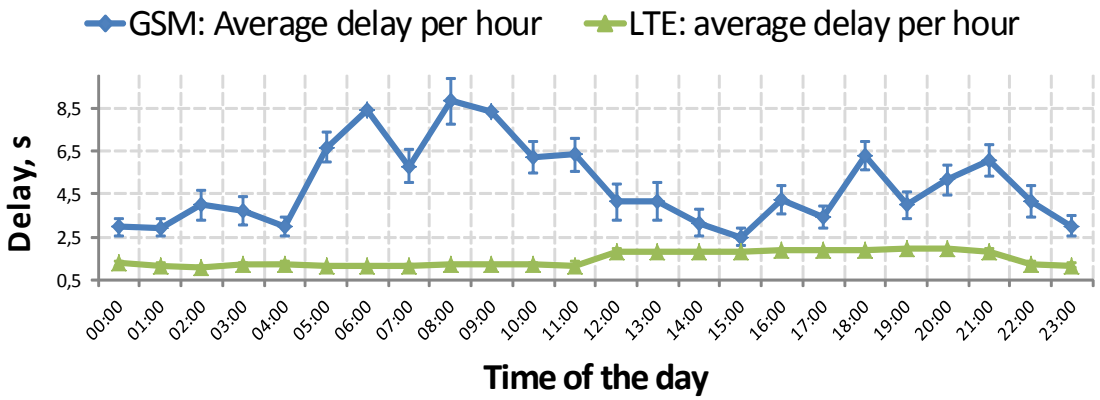

Figure 5.12.: SMS over GSM and LTE delay distribution over the day. ©ACM 2016

SMS over GSM features a highly variable delay distribution from 2.5s to 8.5s, resulting in average delay per day of 4.9s. Empirical delay distribution is presented in Figure 5.13. The x-axis shows delay in seconds, and y-axis frequency of occurrence. The color code is the same as in Figure 5.12. From this distribution, we observe the corresponding peaks at 2.5s and at 8.5s. The two peaks distribution is also observed in the hourly pattern. There is also a tail of outliers up to 40s.

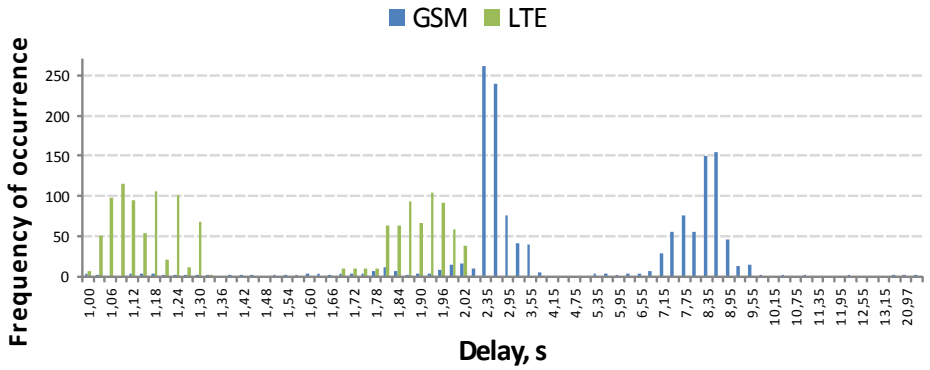

Figure 5.13.: SMS over GSM and LTE delay histogram. ©ACM 2016

Compared to the measurement in [75], the average delay of SMS over GSM is two times lower. The reason is that the measurements in [75] were conducted in 2006, when SMS was a popular mean of text messaging. After 2009 a wide range of packet switched communications started to get used for user messaging, e.g., WhatsApp.

This freed resources at the SDCCH. In our measurements, we have investigated one pair of sender and receiver and cannot draw the conclusions on the influence of number of users on the wake-up delay.

Delay distribution of SMS over LTE shows little variation and an average delay per day of 1.5s. There is a delay peak from 12:00 to 21:00. These delays are also reflected in Figure 5.13. Unlike SMS over GSM, the trend is not based on an hourly distribution. SMS over LTE features a significantly lower delay with lower variation and no outliers compared to SMS over GSM.

From Figure 5.12 we observe that the average delay of SMS sent over GSM is 3.3 times higher than over LTE. Deutsche Telekom launched Voice over Long-Term Evolution (VoLTE) in 2016 [138], i.e., it has IMS. This allows us to conclude that the SMS is sent over IMS, i.e., it is a SIP message.

Over-The-Top Session Initiation Protocol
For OTT SIP measurements, we used two SIM cards and compare wake-up performance over two MNO networks. Figure 5.14 summarizes the delay distribution over a day for the SIM-cards: O2 in blue and Deutsche Telekom in green. Average delays per day for O2 and Deutsche Telekom are similar: $0.59s$ and $0.56s$ respectively. However, the variance over the day is higher by Deutsche Telekom, which is illustrated by wider confidence intervals and overall higher deviations. This variance trend is confirmed in Figure 5.15. O2 delay values are higher and more densely grouped, i.e., with lower variance.

Generally, we observe that there is no big difference in performance of OTT SIP wake-up method over two MNO networks. This empirically shows that the method's performance is not dependent on the network architecture.

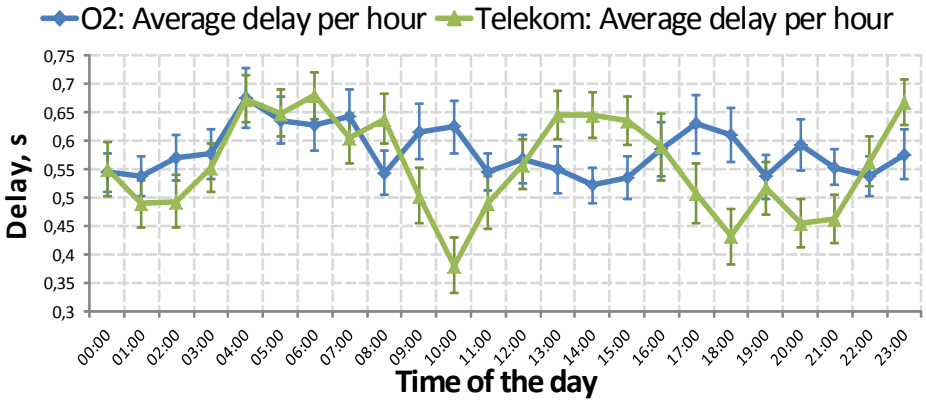

Figure 5.14.: OTT SIP delay distribution over the day. ©ACM 2016

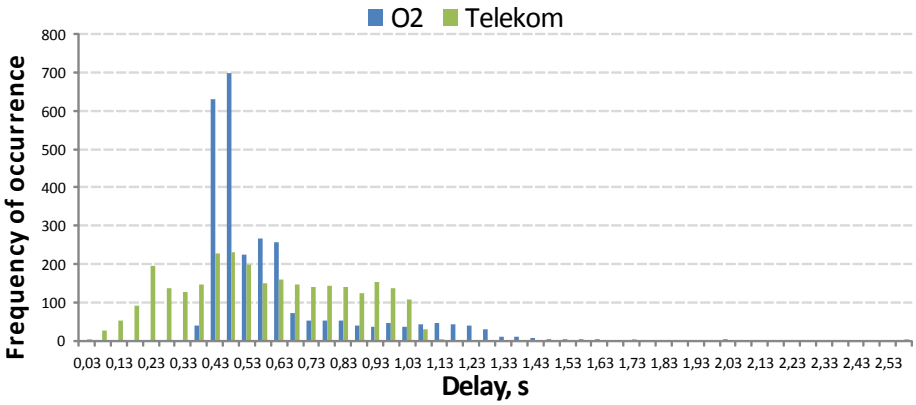

Figure 5.15.: OTT SIP delay histogram. ©ACM 2016

Comparison
Here, we summarize wake-up methods characteristics based on delay and energy measurements, and in accordance with the challenges that were described were described earlier. Based on this analysis, we compare two wake-up solutions: SMS (over GSM and IMS (LTE)) and OTT SIP over LTE.

Delay. Table 5.3 summarizes the average delay per day with respective 95% confidence interval for all the measured cases. From the values, we observe that OTT SIP wake-ups feature the lowest average delay, irrespective of the underlying MNO. SMS over IMS (LTE) has the second lowest delay (approx. 2.7 times higher than OTT SIP), followed by the SMS over GSM (approx. 3.2 times higher than SMS over IMS). Moreover, as we have seen in Figures 5.13 and 5.15, SMS over GSM has the highest variance and number of outliers. Thus for the services with strict delay requirements, OTT SIP is better suited than SMS over any cellular network.

Table 5.3.: Comparison of average delay per day. ©ACM 2016

	SMS		**SIP**	
	GSM	LTE	O2	Deutsche Telekom
Delay, s	4.9	1.5	0.59	0.56
95% c.i.	±0.79	±0.14	±0.02	±0.04

It has to be noticed that for IoT a question of scalability is of crucial importance. For SMS over GSM, [75] analytically shows that the solution does not scale well. SMS over IMS (LTE) or SIP messaging through IMS was discussed in [68], it requires IMS registration. This can be an overload to the network with the IoT scale. OTT SIP solution is sent as normal SIP INVITE message for best effort traffic. It does not require any additional registration anywhere or specific resources of control plane. Thus it has a potential to scale without any network changes.

Addressing. SMS wake-up solutions utilize unique telephone numbers. In this case, direct addressing is possible. As OTT SIP is sent as normal Internet traffic, addressing is through IP. The type of addressing is defined by the MNO. At the moment, both of the networks, O2 and Deutsche Telekom, use IPv4 addressing. It rises NAT-traversal problem [81] that is not present in the SMS case. This problem is solvable through hole punching and a server with a public IP address (see Figure 5.10). It can be seen as a complication over the SMS solutions. However, if we take into account the large scale of IoT devices, there are not enough unique telephone numbers for all the connected devices. This problem is similar to IPv4 address deficiency. The lack of IPv4 numbers is solved through IPv6.

Network independence. SMS wake-ups in the networks before LTE (with circuit switched part) demand SMS-SC. Although, it is a separate network component, it is wide spread and can be considered as a technical state-of-the-art. SMS is sent over a control channel and is a standard MNO service. SMS over LTE can be realized in two ways: through IMS or through special interface to circuit switched network [80]. In MNO's networks, there is no way for user (modem) to know, how exactly the network is constructed. Moreover, it has to be noted that for all VoIP services an IMS is needed. Thus if the MNO offers VoIP, the SMS over LTE is most likely to be over IMS. This, however, cannot be guaranteed. OTT SIP solution is generic Internet traffic, i.e., SIP INVITE. In this case, the underlying network does not have to include an IMS or any other specific network functions. In general, any packet switched network can be used.

Energy consumption. As shown in Table 5.2, GSM is the most energy-efficient in the idle state. This result is consistent with [71]. LTE is more efficient in the active state. SMS solution can be based on both, GSM and LTE. For the applications with rare transmissions and with strict energy consumption requirements, GSM-based solutions are better suited. LTE-based solutions are better suited for more often transmissions. It has to be noted that, these figures and conclusions are technology related. For example, SMS and OTT SIP can be used over 3G network, then energy consumption figures can change significantly. There are initiatives in 3GPP to lower the energy consumption for IoT applications in Releases 12 and 13. This problem cannot be solved with any wake-up solution.

Based on this comparison, for the devices under strict energy constrains, we recommend using GSM-based solutions. For devices under stricter delay constrains OTT SIP is recommended. Note that security considerations are out of the scope of our analysis.

5.4. Summary and Discussion

In this chapter, we have looked into energy efficiency aspects of converged network planning. First, we have investigated how the energy consumption of the backhaul

network can be reduced, when taking the demands steady activity patterns into account during the network planning. We looked into the trade-off between the reliability of the network and additional power consumption and how does it impact the total power consumption of the converged network. In the second part of the chapter, we have looked into network triggered wake-ups to turn on the equipment that was put to sleep to save energy. We proposed and benchmarked an off-the-shelf SIP-based solution for packet switched networks. Finally, we benchmarked its performance against the state-of-the-art circuit switched SMS wake-ups in terms of power consumption and delay.

In the next chapter, we put the time perspective on network planning looking and technology migrations to maximize the project profitability for the network's lifetime.

6. Migration Planning of Converged Access Networks

Bandwidth-hungry services are becoming a daily reality for every household. Online gaming, HD-TV and an overall growth of employees working remotely from their homes challenge NPs with ever growing bandwidth requirements. The NPs are forced to upgrade the network by the competition and governmental initiatives [42], while fighting to maintain a sufficient gap between their costs and revenues. This upgrade, or migration, to the next technology while satisfying user and regulatory requirements calls for careful strategic network planning to fulfill the requirements, while maximizing the benefits of the operator [59]. This is why a migration is classified in Figure 2.1 (Chapter 2) as one of the strategic network planning objectives. The chapter follows closely our published work [9].

As explained in Chapter 2, ODN technologies provide, among other benefits, longer reach and higher sustainable data rates, which makes them an ideal candidate to provide high speed data rates to customers [44]. However, these ODNs come in various configurations, each with their own type of equipment and dimensioning. A simple modeling of costs cannot suffice in finding the best technology to be deployed. Since deployment of optical access networks lasts over a long period of time (between five and ten years), an analysis involving time value of money is required to find out a cost-effective solution.

A migration project (further referred to as "project") consists of a multi-dimensional, multi-period planning problem and its solution involves market penetration forecasting, dimensioning of the network infrastructure and processes, as well as evaluation of their Total Cost of Ownership (TCO) [40]. Due to migration planning complexity and lack of open network TCO models, the state-of-the-art migration models are case study specific, focusing either on a single migration technology or a single migration path. Throughout this work, the term migration path refers to the technology sequence (in time) from the starting technology to the goal of the migration. Migration project thus reuses the methodology of the network planning over multiple periods of time. Hence, the migration study summarizes the contributions of all the network planning presented in this dissertation.

The **contribution** of this study is as follows. First, we propose a generic Rational Agent based algorithm to maximize the migration project profitability while taking into account user uncertainty. The introduced algorithm makes migration decisions (when to migrate to which technology) keeping in mind the migration goal, which in our case is to maximize the project profitability over the network lifetime. This algo-

rithm aims to serve as a strategic analysis tool to help network planners, researchers and industry managers to make business decisions (as defined in chapter 2), compare solutions, estimate time and costs, evaluate impact of new solution, etc. The proposed algorithm is validated with realistic case studies: migrating from copper based networks to Passive Optical Networks (PONs) in different deployment areas (rural, urban and dense urban) and user mixes (residential and converged planning). The validation includes creating a database of PON technologies and architectures [3], calculating their realistic costs based on geographical data (using the network planning tool available at [1]) and finally, performing a comprehensive sensitivity analysis to validate our assumptions.

Our case studies results show that the network operators can achieve higher profitability while providing the required data rates to different subscribers with the flexible migration end state. In this case, the final state is chosen by the migration algorithm to maximize economic value instead of targeting a concrete technology. Furthermore, accounting for user churn allows avoiding overestimating the project profitability. In this study, we present selected results for the urban area, the full set of results can be found in [3]. Last but not least, an important contribution of this study is the full reproducibility of the study, as all the implementations are publicly available [1, 146] as well as a complete database of the techno-economic parameters [3].

The rest of this chapter is organized as follows. First, we introduce the related state-of-the-art analysis. Section 6.2 describes the problem formulation and assumptions for the migration algorithm. It lists and explains all the necessary inputs to conduct a migration study. Section 6.3 introduces the migration methodology based on an uninformed search algorithm. Section 6.4 shows the results (expected NPVs and migration paths) of selected scenarios as well as the sensitivity analysis. We conclude the chapter with discussion and summary.

6.1. State-of-the-art Analysis

The authors of [44] undertake a cost-benefit analysis of various optical network technologies, assumed to be deployed as Fiber-To-The-Home (FTTH), shown in Figure 2.10. However, the possible benefits of Fiber-To-The-Building (FTTB) and Fiber-To-The-Cabinet (FTTCab) deployments are not covered. Also, the lack of granularity in Operational Expenditures (OpEx) calculations as well as the use of geometric models instead of geographical models for the network deployment, leads to unpredictable TCO under- and over-estimations [64]. Another work applied to FTTH (i.e., without the possibility to choose the final migration state) is proposed by [40]. The authors contribute to planning of multi-step migration, when multiple technologies are present. The output is then an optimal migration path, which considers migration window as well as holding time in every intermediate technology. However, the solution does not deal with the environment uncertainties such as user churn.

Over the years, tree based Artificial Intelligence (AI) algorithms have emerged as a front-runner to solve problems, in which complete information is not available. In the case of network migrations, this maps to NPs making strategic decisions on when and how many migration steps are needed in order to maximize the profits, keeping in mind an uncertain number of subscribers, variations on revenues and also associated TCO. The solution proposed in this study is based on the Expectimax Search algorithm [54], which is commonly used in AI-based applications and for the first time it has been applied to the network migration problem in our published study [9]. Here, we follow closely the published study [9].

These tree based AI algorithms usually consist of (i) agents, which execute an action based on the environment, and (ii) an environment which changes based on agent's actions. Any agent which takes an action in order to maximize its performance metric, is said to be a Rational Agent [55].

The use of AI based heuristic search in access network migration planning is studied in the work done by [34] and [41]. The problem statement defined in that work is to optimize the migration process from Very high speed Digital Subscriber Line (VDSL) to FTTCab GPON in an urban access network, undertaken in a pre-defined migration period. However, no evidence is provided if this optimization suffices for multi-step migration when different migration options are present.

Another approach to identify the best network migration was undertaken by [36] using strategic analysis of a Real Options Approach [46]. In the studied business case of a FTTx migration from a full copper deployment, this translates to options like the size of cabinets to deploy, the services to be provided to subscribers, etc., where all the options form a decision tree. However, the authors focus on a specific case study and model the probability based on assumptions made about the per-cabinet take up rate, which cannot be generalized.

With this analysis, we have identified the need in a migration model, which provides the flexibility of choosing different access network deployment options in various scenarios, while catering for revenue uncertainty. To tackle this, we use the Expectimax Search [54], which is a simplified uninformed adversarial search tree used to model sequential games. This search method is different from informed or deterministic searches, like MinMax search [54], because it considers the uncertainty arising from input parameters for which complete information is not available. In our work, we prefer an uninformed search over a deterministic search, because it allows us to model subscriber uncertainty.

6.2. Problem formulation, Assumptions and Input

This Subsection introduces the problem formulation, lists and explains the assumptions and necessary input for the model. Further, this section introduces the economic

parameters used to evaluate the results.

6.2.1. Problem Formulation

For better understanding, we explain the migration problem on a realistic example: migration from copper based Asymmetric Digital Subscriber Line 2+ (ADSL2+) network to PON. As has been already defined in the chapter introduction, migration of access networks is a multi-dimensional and complex process and gives the network operator multiple options to explore.

With no loss of generality, to limit the scope of the study we concentrate on the business model of the Vertically Integrated Operator (VIO) [61]. We define the VIO to be the only Internet provider in a given area, who owns the physical infrastructure (fiber, ducts, remote nodes), network (OLTs, ONUs, splitters) and as well as the services (Internet, television, telephony). The VIO assumes to have copper based technologies already deployed in an area and looks to migrate to any PON based technology, shown in Figure 6.1, since these are now mature and affordable to deploy [37, 53]. The complete migration is limited in time, which is referred as migration window T_{mig} [40]. However, the cost and revenue calculations take the network life-cycle into account (usually longer than T_{mig}), which is denoted by T_{NW}.

The business model also involves the inclusion of different types of subscriber demands, such as Residential, Business and Public ITS LTE Macro Base Stations (MBSs). With these, we create two different planning scenarios, namely *pure residential* (i.e., connecting residential users) and *converged* (i.e., connected residential, business and ITS MBSs demands). In the converged planning scenario, we ensure that the ITS MBSs are assigned separate wavelengths to support their backhaul traffic for high bandwidth and security purposes.

For different PON technologies, deployments can vary based on how far the fiber drop point is from the Central Office (CO). As shown in Figure 2.10, FTTCab has ONU placed at street cabinets, whereas FTTB has a fiber drop point directly inside the building. This invokes a difference in civil works cost, which as described in further sections, is an important cost driver. Another important cost driver is the cost of active equipment at the CO, depending on which the same PON deployment (same trenches, ducts, cables and passive equipment) can achieve higher data rates.

We look into the following technologies [37]: Gigabit Passive Optical Network (GPON), 10-Gigabit Passive Optical Network (XGPON), **UDWDM-PON!** (**UDWDM-PON!**) and Hybrid Passive Optical Network (HPON). Each of these technologies have different network equipment costs.

PON architectures can offer subscribers data rates of 25 Mbps, 50 Mbps and 100 Mbps as shown in Figure 6.1. The data rate can be increased incrementally by adding more

active equipment at the CO, making use of the dark fiber and by blowing additional fiber through a duct, which was assumed to be less expensive as compared to digging and closing the ducts again [56].

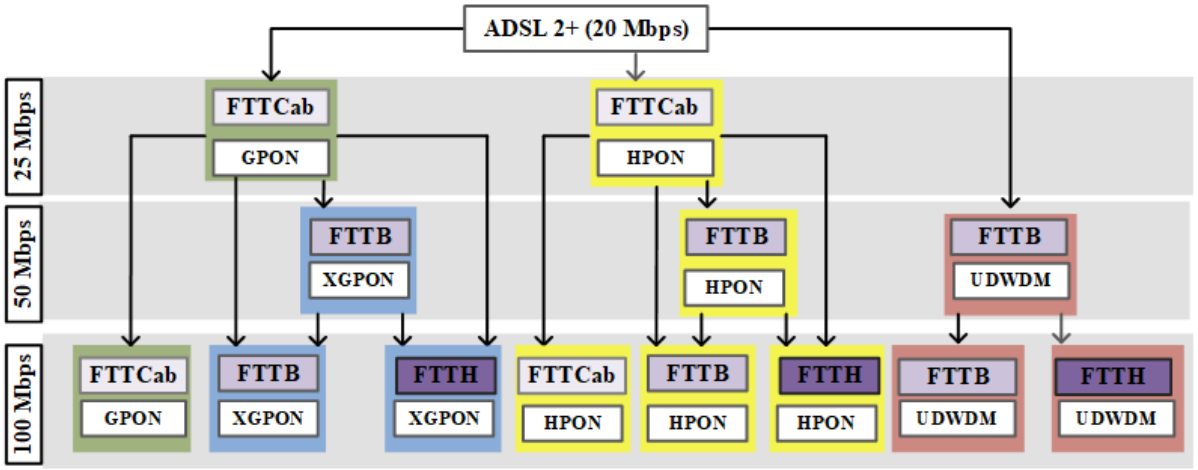

Figure 6.1.: Schematics of the allowed migrations starting from an Asymmetric Digital Subscriber Line 2+ (ADSL2+) solution offering 20 Mbps to different solutions offering 100 Mbps, differing in the Fiber-To-The-X (FTTx) architectures, data rates and technology. ©IEEE/OSA 2019

For consistency, each scenario is referred as FTTx_technology_bitrate. For example, FTTCab_GPON_25 refers to the FTTCab solution using GPON and offering 25 Mbps to the end users. This way, using the migration tree shown in Figure 6.1, we look into 13 possible PON deployments, for example, FTTB_XGPON_50 or FTTB_UDWDM_100.

Figure 6.1, also defines allowed migration paths to achieve 100 Mbps deployment for residential users, business users and ITS MBSs. Some migrations, for example, migrating from FTTCab_GPON_25 to FTTH_UDWDM_100 or FTTB_UDWDM_50 to FTTB_XGPON_100 are restricted. This arises from our assumption that GPON and XGPON based technologies need a two-stage deployment (at least two remote nodes), to provide 100 Mbps to users, whereas Ultra Dense Wavelength Division Multiplexing (UDWDM) technologies can satisfy the same requirement using a single stage deployment [3, 37]. Migrations involving changes in deployment types would lead to a higher TCO and thus shall be restricted.

In this study, we evaluate two scenarios, both of which have to provide at least 100 Mbps per user at the end of the migration period [38]:

1. **Benchmark scenario: FTTH as fixed migration goal**
   As most of the state-of-the-art papers consider FTTH as a fixed final state, e.g., [40] and [44]; we take it as our comparison scenario. This scenario considers only FTTH PON providing the end user with 100 Mbps. The profitability is maximized only within FTTH technologies.

2. **Proposed scenario: flexible migration goal, where any FTTx that maximizes the profitability can become a migration goal**
   Any FTTx architecture, i.e., FTTCab, FTTB or FTTH; can become migrations final state. The main criteria are that the final state provides the subscribers with 100 Mbps connection and maximizes the project profitability.

Comparing the results of these two scenarios, we evaluate the influence of the final state, i.e., fixed (only FTTH) or flexible (any FTTx) final state, when it is chosen only based on the maximum NPV at the end of the network Life-cycle. As NPV calculation requires a cost modeling of each of the different kinds of deployments, we need to find the TCO and define a revenue model, which is an input to the migration algorithm.

6.2.2. Total Cost of Ownership and Revenue Model

In order to make any business decisions, the cost of each option has to be evaluated. The TCO of the network consists of Capital Expenditures (CapEx) and Operational Expenditures (OpEx), see Chapter 2. This study is neither focused on the TCO calculation nor the cost modeling, but on the migration modeling and evaluation. However, as the TCO is crucial to select the best migration scenario, we introduce the used models, values and methodology. We closely follow the approach in [44] and supplement it with values from [37, 52].

The CapEx, in this study, is split into two major cost categories: civil work and equipment cost. The civil work cost is driven by the duct lengths and cost per meter of trenching and laying ducts. To find the costs of the network components, the respective electronic (Optical Line Terminal (OLT)) card, Power Splitter (PS), Digital Subscriber Line Access Multiplexer (DSLAM), Optical Network Unit (ONU), etc.) and non-electronic (fiber lengths, cabinets, Heating Ventilation and Air Conditioning (HVAC)) components are dimensioned based on the demands of the subscribers and the capacity of each component. The Operational Expenditures (OpEx) includes energy, fault management, network operation, marketing and rent. A detailed CapEx and Operational Expenditures (OpEx) calculation used in this study is presented in [3]. It is important to note that throughout this work, we present all costs and revenues in Cost Unit (C.U.), where 1 C.U.. is fixed at the price of a single GPON ONU in the year 2013 [37].

The lengths of fibers and ducts for each of the deployments are obtained using the Automated Map-Based Strategic Fixed Network Planning Tool (AMS) [1, 8]. The AMS is presented in Section 2.2. The planning details are out of the scope of this study but presented in detail in [3].

We model the subscriber behavior with three different penetration curves, as proposed in [53]: "conservative", "realistic", and "aggressive", which differ on the subscriber joining rates. These joining rates are then used to derive the number of subscribers connected to the network in every year, which is helpful in finding the yearly

revenue generated in an area. Figure 6.2 shows the percentage of households connected in a pure residential scenario at a given year. Readers may note that we limit the techno-economic calculations to 20 years, since projects in a given area last between 5-10 years and the remaining years are used to recover costs.

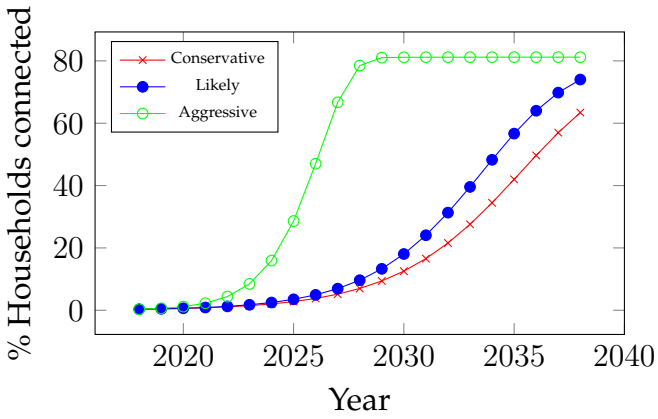

Figure 6.2.: Percentage of yearly connected residential subscribers based on the penetration curves from [53]. ©IEEE/OSA 2019

Table 6.1.: Yearly ARPU Summary, based on [35]. ©IEEE/OSA 2019

Data rate, Mbps	**Residential, C.U./year**	**Business, C.U./year**	**ITS, C.U./year**
20 Mbps	3.6	3.6	-
30 Mbps	7.2	36	-
50 Mbps	10.8	84	84
100 Mbps	13.2	110	110

Average Revenue Per User (ARPU), shown in Table 6.1, reflect the real optical access market tariffs [42]. For business and ITS subscribers, the yearly generated revenues are assumed to be higher since these subscribers need separate hardware and wavelengths for better security and faster fault reparation [35]. Since the subscriber pays for the data rate, the ARPU does not change across different technologies offering the same data rate.

Every year, apart from the number of subscribers joining the network, a certain number of the total connected subscribers leave it due to marketing, costs, other requirements, etc. This variation in the total number of connected subscribers is called user churn c and can change depending on the market, existing competitors, etc. The user churn is defined as a Bernoulli process; the success probability defining if the churn

occurs. As the trials in each year are independent from each other, the overall process in the migration is memoryless and thus Markovian.

The level of churn is assumed to be 10% [56]. This user churn leads to lower revenue for the same operational expenditures, since the services or the connection to the subscriber exists, but there is no monetary benefit out of it. We do not consider the ITS MBSs as a part of churn, since we assume that once connected, the public ITS provider does not leave the network. With this assumption, the operator revenue in a single year t is defined as:

$$R_t(\gamma_t) = \sum_{q \in Sub} (1-c)^{\gamma_t} n_{q,t}.R_q \ , \tag{6.1}$$

where $Sub \in \{Residential, Business\}$ and takes values from Table 6.1, $n_{q,t}$ is the number of subscribers of type q who are connected to the network at year t (calculated from the penetration curves shown in Fiure. 6.2), R_q is the per subscriber yearly revenue of type q, $0 \leq c \leq 1$ is the yearly churn rate of the subscribers and γ_t is a binary variable, which is defined as follows:

$$\gamma_t = \begin{cases} 1 & \text{if churn occurs,} \\ 0 & \text{otherwise.} \end{cases} \tag{6.2}$$

6.3. Expectimax based Migration Algorithm

This section introduces the proposed AI-based migration algorithm. Here we define the migration decision metric. Then, we introduce the modified Expectimax algorithm and apply it on a simple example. Like the Expectimax algorithm, we also used three different nodes (maximizer, chance and terminal).

6.3.1. Proposed Decision Metric and Utility Function

In this work, we choose the Net Present Value (NPV) [62] as our decision making metric. NPV is an economic metric, which shows the time value of money to valuate long-term projects, or project-profitability and it is defined in Chapter 2, Eq. (2.1) and Eq. (2.2). The revenue of the project is defined in Eq. (6.1).

In case migrations occur in an given year, we need to model the CapEx part of the investments. For this, we define an additional fixed cost inherent to migrating from technology s to technology s' as:

$$M_{s,s'} = \kappa_{i,j}\Delta_{CW_{s,s'}} + \upsilon_{p,q}\Delta_{Equip_{s,s'}}, \ \forall \ s, s' \in \{\text{Possible\_Technologies}\}, s \neq s' \ , \tag{6.3}$$

where $\Delta_{CW_{s,s'}}$ is the difference in civil work (CapEx) when there is a change of architecture, provided by the binary variable $\kappa_{i,j}$ defined in Eq. (6.4); and $\Delta_{Equip_{s,s'}}$ is the difference in CapEx equipment when there is an upgrade of the delivered bandwidth, provided by the binary variable $\upsilon_{p,q}$ defined in Eq. (6.5). These two CapEx values $\Delta_{CW_{s,s'}}$ and $\Delta_{Equip_{s,s'}}$ follow the TCO cost modeling in [44].

These binary variables $\kappa_{i,j}$ and $\upsilon_{p,q}$ distinguish which network upgrades have to be conducted: civil work, equipment or both.

$$\kappa_{i,j} = \begin{cases} 1 & \text{if } i \neq j \;\forall\; i,j \in \{\text{FTTCab, FTTB, FTTH}\} \\ 0 & \text{otherwise} \end{cases} \tag{6.4}$$

$$\upsilon_{p,q} = \begin{cases} 1 & \text{if } p \neq q \;\forall\; p,q \in \{20, 25, 50, 100\}\ Mbps \\ 0 & \text{otherwise} \end{cases} \tag{6.5}$$

Based on the definitions above, we define our utility function U for a current technology s at year t given a user churn γ_t, as follows:

$$U(s,t,\gamma_t) = \begin{cases} \sum_{i=t}^{T_{NW}} \frac{R_i(\gamma_i) - OPEX_i}{(1+d)^{T_{start}-i}} & \text{if terminal node} \\ \max_{s'} \left[H(s', t+1) \right. & \\ \quad \left. + \frac{R_t(\gamma_t) - OPEX_t}{(1+d)^{T_{start}-t}} - \mu_t \cdot M_{s,s'} \right] & \text{if maximizer node,} \end{cases} \tag{6.6}$$

where $R_i(\gamma_i)$, $OPEX_i$ and $M_{s,s'}$ are the revenue, yearly OpEx and migration CapEx respectively. γ_i is a binary variable ($\gamma_i = 1$ when user churn has occurred; $\gamma_i = 0$ otherwise). s is the current technology and s' is the technology to be migrated to, T_{start} is the starting year of the migration window, d is the discount rate of the project, μ_t is a binary variable ($\mu_t = 1$ when migration takes place in year t; $\mu_t = 0$ otherwise). The network life-cycle is T_{NW}, which can be any period of years longer than T_{mig}. $H(s', t+1)$ is the expected present value generated by the child maximizer nodes at depth $t+1$ for the next technology s'.

At the maximizer nodes, the subtraction of $\mu_t \cdot M_{s,s'}$ implies CapEx required for the migration. The value at the chance nodes is the weighted average of the value of its children, given by Eq. (6.7).

$$H(s,t) = \sum_{\gamma_t \,\in\, \{0,1\}} Pr(\gamma_t) \;\cdot\; U(s,t,\gamma_t), \tag{6.7}$$

where $H(s,t)$ is the value of the chance node of state s at depth t. Looking at Eq. (6.6) and Eq. (6.7), it is evident that the algorithm is recursive in nature.

To model the uncertainty of churn, we define $Pr(\gamma_t)$ as a two state Markov Chain with steady-state probabilities as defined in Eq. (6.8).

$$Pr(\gamma_t) = \begin{cases} 0.9 & \text{if } \gamma_t = 0 \\ 0.1 & \text{if } \gamma_t = 1 \end{cases} \tag{6.8}$$

6.3.2. Proposed Search Tree Algorithm

To explain the algorithm, let us use a simple example of a migration from ADSL2+ (20 Mbps) involving two technologies (see Figure 6.1): FTTCab_GPON_25 (referred as PON1) and FTTB_XGPON_100 (referred as PON2). The migration window T_{mig} is set to three years and the network life-cycle T_{NW} is set to five years. The final goal of the VIO is to find a technology, which provides it with the maximum profitability across the entire T_{NW}. Every year, for every possible migration, we have a maximizer node (blue rectangles with solid outlines in Figure 6.3) and chance node (red rectangle with dashed outline). For subsequent years, there can be either terminal nodes (green rectangles with dotted outline) or maximizer nodes again. We first discuss how the tree is built and then move to its evaluation using the utility function defined in Subsection 6.3.1.

Building the search tree At the beginning of the migration period, a maximizer node is present and indicates the current state of migrations (no migrations). Each of its child nodes (chance nodes), is assigned a new technology, to which migration is possible. For each chance node, there are two possibilities, namely $Churn$ and No_Churn, both having different utilities (refer Eq. (6.7) and Eq. (6.8)). Figure 6.3 shows that PON2 Churn and No Churn in 2019 are terminal nodes instead of maximizer nodes. This happens because PON2 satisfies the goal of the VIO to provide 100 Mbps to its subscribers.

Also, in 2019, PON1 has an option to migrate to either PON2 or not migrate at all. In the final year, all the technologies result in a terminal node, since the tree reaches the end of the migration window. The flow of tree building is a recursive approach and is implemented according to the pseudo-code provided in Algorithm 2.
Evaluating the search tree After the tree is built, the evaluation finds the migration path with the highest expected utility value. For explaining this evaluation, we refer to Figure 6.4. The algorithm always starts from the terminal nodes and then traverses its way up. The values stored at the terminal nodes are the NPV values from that year to end of T_{NW} (using Eq. (6.6)), assuming no further churn occurs and the subscriber penetration follows the "realistic" curve. The chance nodes find the expected value of its children, which translates to the expected NPV from the current year to the end of the network life-cycle (using Eq. (6.7)).

At every maximizer node, migration costs are subtracted from the accumulated NPV,

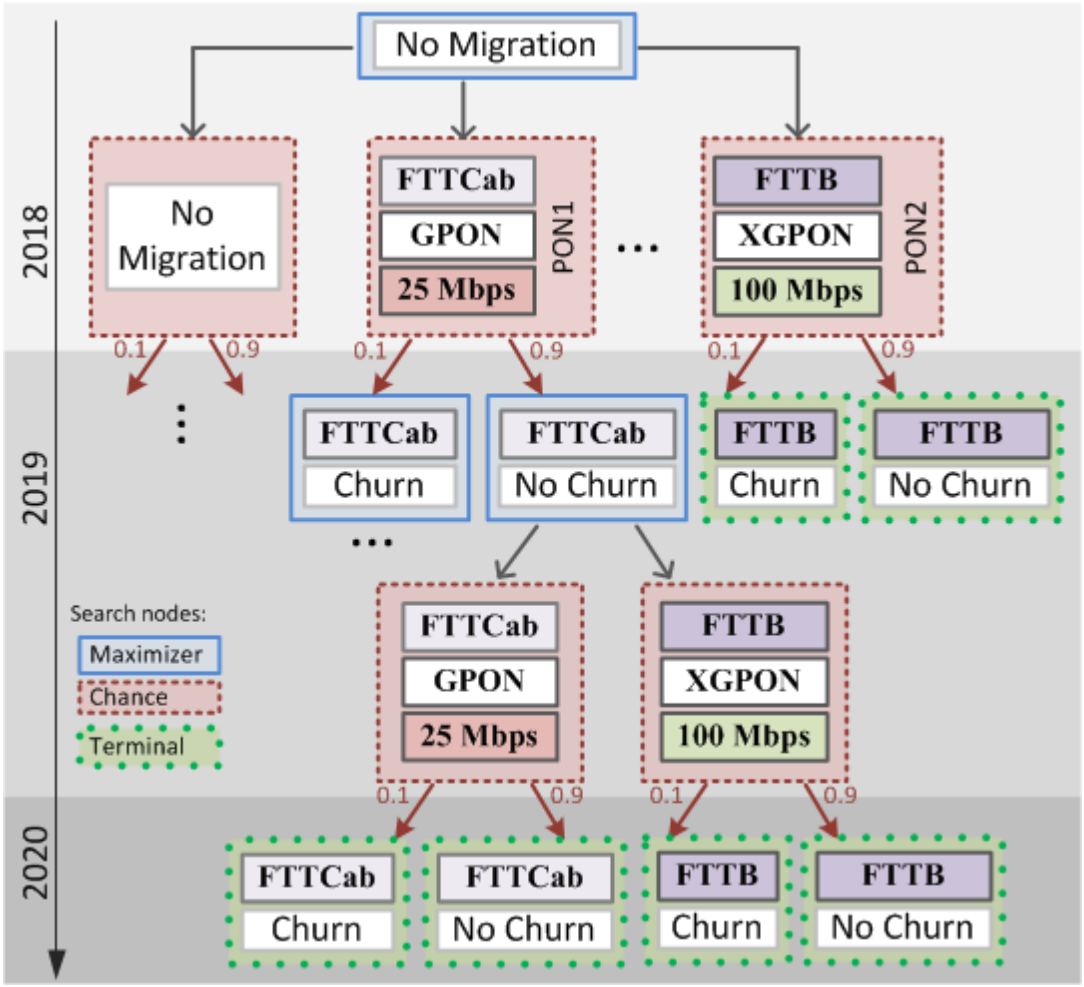

Figure 6.3.: Top down building of search tree of depth three years and two technology choices. The tree is built recursively till a terminal condition is satisfied. ©IEEE/OSA 2019

which can be seen from the PON1 maximizer node in year 2019. This is repeated till the the top-most maximizer node is reached, where the node with the maximum accumulated NPV is chosen. This leads to the search tree choosing the migration path as PON1 in 2019 and PON2 in 2020 as the most profitable decision, with an accumulated NPV of 381 C.U. Algorithm 1 shows how a built tree is evaluated, based on the current node being evaluated.

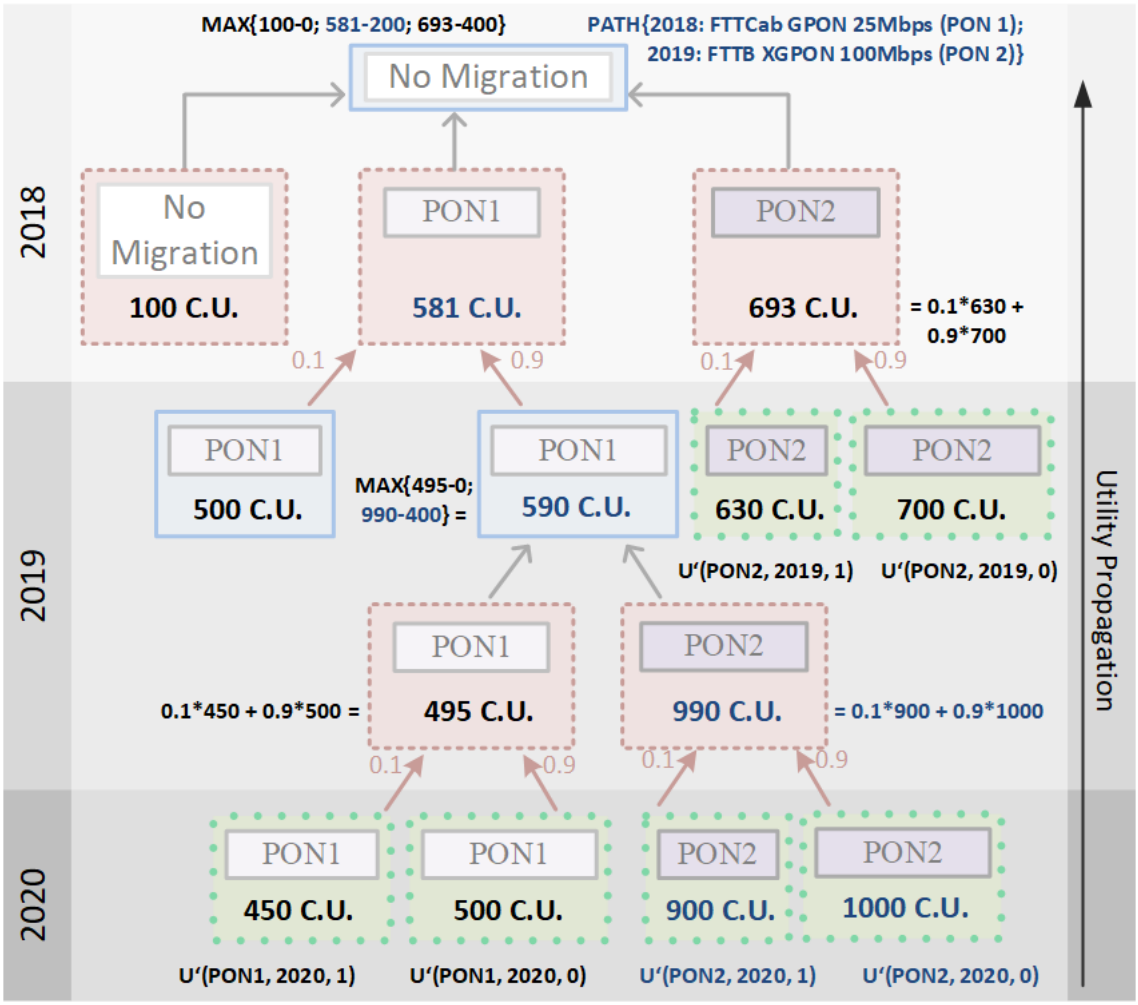

Figure 6.4.: Bottom up evaluation of utility function in search tree reveals migration path (in blue), which provides the highest Net Present Value (NPV) at the end of the network life-cycle. ©IEEE/OSA 2019

Algorithm 1 Evaluating the Expectimax tree. ©IEEE/OSA 2019

Ensure: $curr\_year \leq T_{mig}$
  function UTIL_FN($node\_type, year, tech, churn$)
    if $node\_type$ is $Terminal$ **then**
      return $U(tech, year, churn)$
        ▷ Ref. Eq. (6.6) with node type terminal
    else
      $children = possible\_migrations(tech)$
      return $\max_{children}[U(child, year + 1, churn)]$
        ▷ Ref. Eq. (6.6) with node type maximizer
    end if
  end function

Algorithm 2 Building the Expectimax tree. ©IEEE/OSA 2019

Ensure: $curr\_year \leq T_{mig}$
  procedure ADD_MAX($curr\_year, curr\_tech, type$)
    for $child$ in $possible\_migrations(curr\_tech)$ **do**
      ADD_CHANCE($child, curr\_year + 1$)
    end for
  end procedure

  procedure ADD_CHANCE($tech, curr\_year$)
    if $tech.data\_rate$ is $100\ Mbps$ **then**
      ADD_TERMINAL($tech, curr\_year$)
    else if $curr\_year$ is T_mig **then**
      ADD_TERMINAL($tech, curr\_year$)
    else
      ADD_MAX($curr\_year, curr\_tech, Churn$)
      ADD_MAX($curr\_year, curr\_tech, No\_Churn$)
    end if
  end procedure

  procedure ADD_TERMINAL($tech, curr\_year$)
    BEGIN_EVAL($tech, curr\_year$)
  end procedure

6.4. Evaluation of the Proposed Migration Algorithm

In our work, we have evaluated the performance of the proposed migration algorithm in a number of case studies. We looked into three types of deployment areas: dense urban (New York), urban (Munich), and suburban (Ottobrunn) [51].

As already mentioned, three demand types have been considered: residential, business and public ITS MBSs. The residential demands are defined by the buildings positions and the number of households per building, whereas the business demands are defined by the building positions and the density of the businesses in that area. For added security purposes, the business and ITS demands need to be sent on different wavelengths, which is supported by UDWDM and HPON technologies.

Here, we present only selected results of the urban deployment scenario in Munich (Germany). All the other results have been showcased and thoroughly discussed in Chapter 6 of [3]. An interested reader can also reproduce these results using the source code and input excel files (including migration matrices) provided in [146].

In case of Munich, each building is a Multiple Dwelling Unit (MDU), which consists on average of 6-8 potential residential or business subscribers [49, 50]. These subscribers have been divided into residential and business subscribers using the fixed percentage of business subscribers in a city [57, 44]. In Munich, 7% of the total buildings are considered to be business buildings [36]. The considered demands for the converged migration are: 27213 residential, 2049 business and two ITS MBSs.

All the presented results refer to the following scenario: area of 7 km^2 in the center of Munich, migration starting in T_{start}=2018 and ending in 2027 (i.e., T_{mig}=10 years), the network lifetime T_{NW} is set to 20 years, churn rate of c=10% and churn probability $Pr(\gamma_t)$=0.1. The technological scenario in our case was migration from the existing copper, i.e., ADSL2+, network to a future-proof PON architecture [42, 56].

The migration goal for the residential and business subscribers is to offer at least 100 Mbps per household or business by 2025. This requirement was dictated by the EU Broadband Regulation Policy on Digital Single Market [38]. The ITS MBSs, although not governed by any EU regulatory policy, have a technical requirement of at least 50 Mbps data rate, to support current Public ITS demands [8]. However, a higher data rate of 100 Mbps was assumed to be favorable in case of future increase in Public ITS traffic.

Pure Residential Migration

Here, we consider a purely residential scenario, where all the demands in the network are residential subscribers, i.e., households, whose tariffs are provided in Table 6.1.

Out of the 13 different PON technologies, which can be derived from the migration tree shown in Figure 6.1; Figure 6.5 shows the per subscriber CapEx in C.U. of selected technologies, all of which satisfy the 100 Mbps requirement. The CapEx costs are divided into components like civil work, fiber laying costs and equipment costs at various locations like CO, RNs and buildings. We observed that FTTH technologies are more expensive than non-FTTH ones, with FTTH_XGPON_100 being the most

expensive technology to deploy (11.18 C.U. per subscriber). Due to a single stage deployment and a high subscriber density in urban areas, UDWDM based FTTB/FTTH technologies have lower civil work cost as compared to XGPON based FTTB/FTTH.

From Figure 6.6, we see that FTTH technologies have the least OpEx, around 0.6 C.U. per subscriber. In FTTH case the user equipment (ONU) are located at the subscribers premises, thus subscribers pay for the rent and energy costs of the ONU. The highest OpEx of about 1 C.U. per subscriber per year is from FTTB_UDWDM_100, since the energy and rent costs of expensive UDWDM ONUs are borne by the VIO. To supplement the migration algorithm, we fix the per subscriber OpEx in ADSL2+ (copper) to 0.25 C.U. The OpEx calculations in our work are based on the model and data provided in [37]. The results of the expected NPV and the migration path for each of the different subscriber penetration curve is shown in Table 6.2.

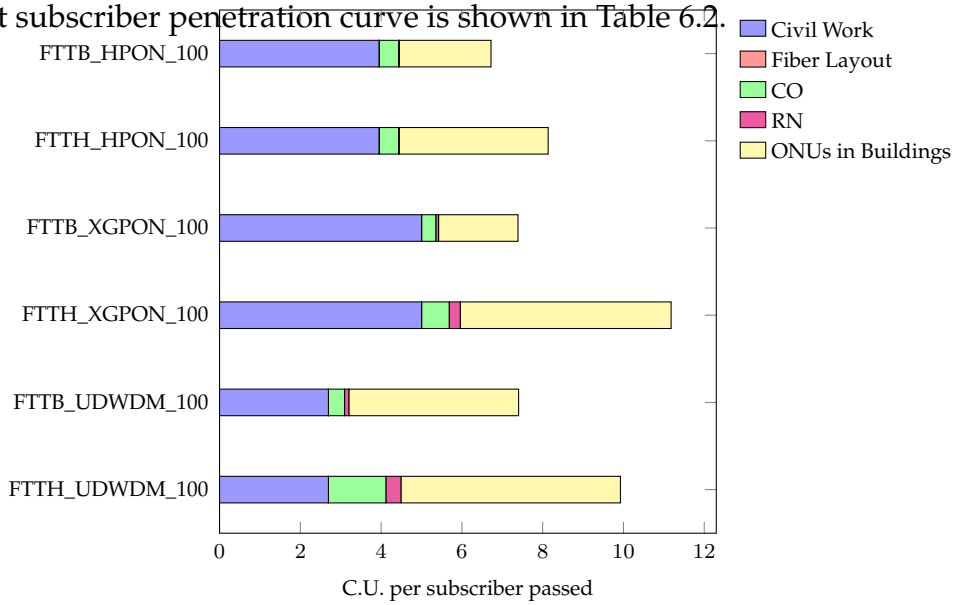

Figure 6.5.: Capital Expenditures (CapEx) categories of selected deployments in Munich pure residential scenario offering 100 Mbps to subscribers. ©IEEE/OSA 2019

From the results in Table 6.2, we observe that due to low ARPU for residential subscribers, the VIO cannot have a higher NPV in a purely residential deployment, unless the subscriber penetration is aggressive. We see that when only FTTH technologies provide 100 Mbps, the NPV is 20-50% lower because non-FTTH technologies with 100 Mbps (like FTTB_UDWDM_100) have a higher return on investment. We also observe that the algorithm suggests migrations in the beginning of the migration window, in order to get more revenue from the subscribers. This behavior is also recorded by the heuristic optimization models of [41].

Overall, in the worst case of a conservative subscriber penetration rate, coupled with only FTTH technologies providing 100 Mbps data rates, early migrations to a hybrid PON optical architecture result in at least a minimally positive NPV.

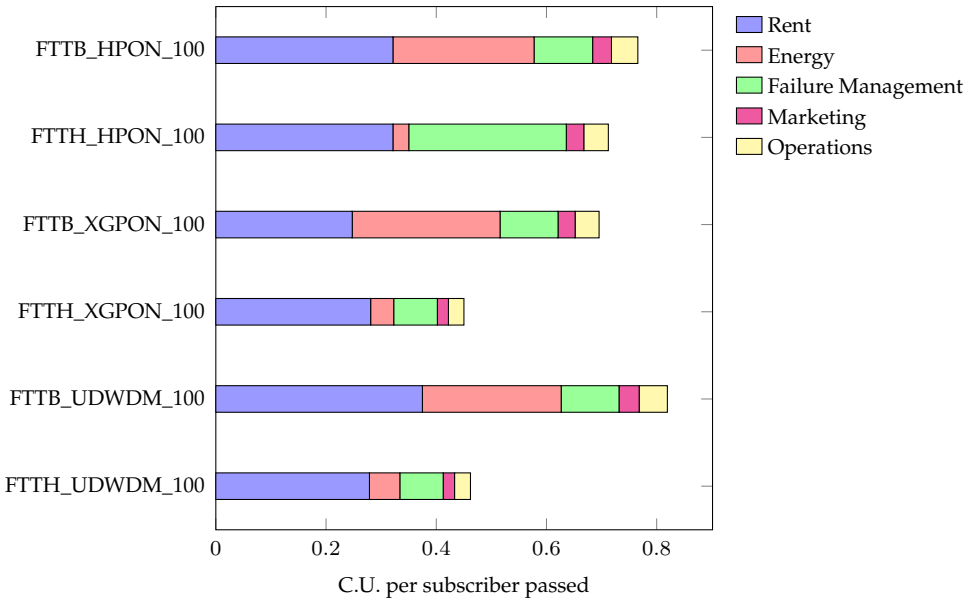

Figure 6.6.: Operational Expenditures (OpEx) categories of selected deployments in Munich pure residential scenario offering 100 Mbps to subscribers in year 2018. ©IEEE/OSA 2019

Table 6.2.: Resulting migration paths for Munich pure residential scenario. ©IEEE/OSA 2019

FTTCab/FTTB/FTTH provide 100 Mbps		
Penetration Curve	**FTTx Migration Path**	**Net Present Value, C.U.**
Conservative	2019: FTTB_UDWDM_50 2020: FTTB_UDWDM_100	**93837**
Realistic	2019: FTTB_UDWDM_50 2020: FTTB_UDWDM_100	**180161**
Aggressive	2019: FTTB_UDWDM_100	**886778**
Only FTTH provide 100 Mbps		
Penetration Curve	**FTTH Migration Path**	**Net Present Value, C.U.**
Conservative	2019: FTTH_HPON_100	**13313**
Realistic	2019: FTTH_HPON_100	**100679**
Aggressive	2019: FTTH_HPON_100	**815178**

Converged Migration

A converged scenario features heterogeneous demands: residential, business as well as public ITS MBSs. First, the planning and cost evaluation are performed and the results show that both CapEx and OpEx for every architecture in the converged scenario, are between 5-10% higher than in the pure residential scenario. While deploying the network, it is made sure that the business subscribers and residential subscriber do not share equipment for security reasons [35].

To visualize better a converged network deployment, we focus on the example of FTTH_HPON_100, which has been depicted in Figure 6.7. To meet the demands, every 10 Gbps card at the OLT is connected to a single Array WaveGuide (AWG) at the first RN. This device splits the optical signal from feeder fiber to up to 80 different wavelengths which can be either split further into 100 Mbps connections at the second RNs or can be connected directly to ITS LTE MBS.

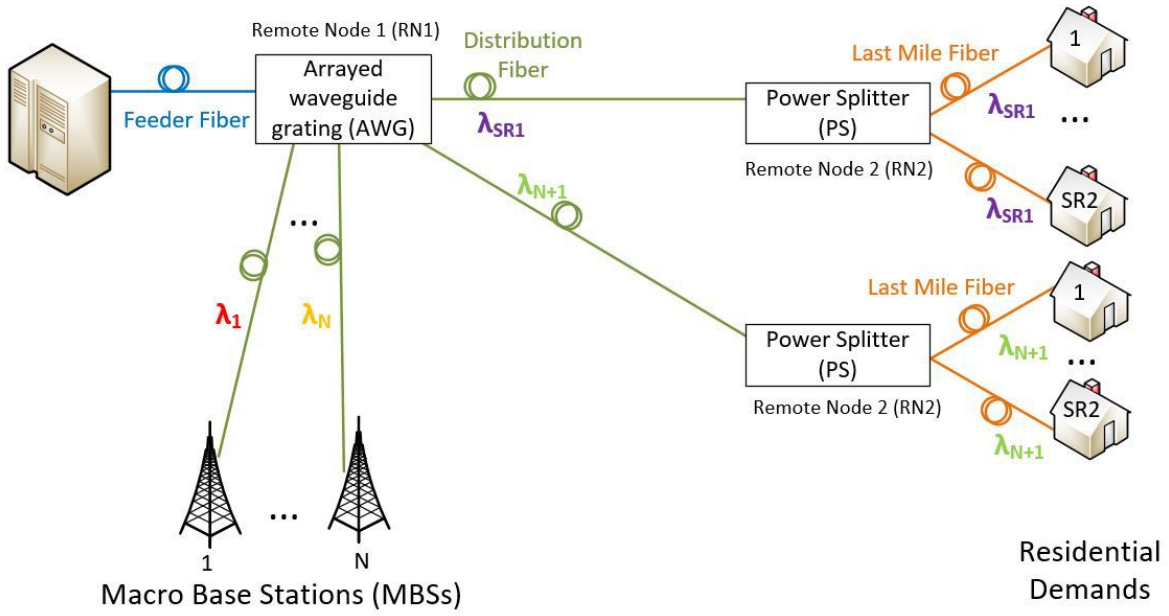

Figure 6.7.: Example deployment of a two-stage FTTH_HPON_100 with a 1:80 Array WaveGuide (AWG) at RN1 and 1:16 Power Splitters at RN2 in a converged scenario. ©IEEE/OSA 2019

In this deployment, additional infrastructure and equipment was added in order that each business building (consisting of 6-8 business subscribers) gets its own wavelength, in accordance with the SLAs that justify the higher price [35]. Due to these factors, the NPV is on an average 1.6 to 7.5 times higher for the converged case in all different scenarios, as compared to a pure residential scenario. The results from the migration algorithm are shown in Table 6.3.

In case migrations to FTTx technologies are allowed, FTTB_HPON_100 is preferred due to its highest NPV. Compared to the pure residential scenario, the algorithm selects HPON for "conservative" penetration curves, since they are more cost effective for converged scenario as compared to GPON and UDWDM technologies. Among FTTH technologies, migration to FTTH_UDWDM_100 is preferred because the high operational costs are offset by charging a higher tariff from business and ITS subscribers. FTTH_HPON_100, which was the preferred technology in the residential scenario, loses out marginally to FTTH_UDWDM_100 in this case, due to higher ONU costs in the hybrid PON technology.

Table 6.3.: Resulting migration paths for Munich converged scenario. ©IEEE/OSA 2019

FTTCab/FTTB/FTTH provide 100 Mbps		
Penetration Curve	**FTTx Migration Path**	**Net Present Value, C.U.**
Conservative	2019: FTTB_HPON_50 2020: FTTB_HPON_100	**190069**
Realistic	2019: FTTB_HPON_50 2020: FTTB_HPON_100	**325132**
Aggressive	2019: FTTB_UDWDM_100	**1429279**
Only FTTH provide 100 Mbps		
Penetration Curve	**FTTH Migration Path**	**Net Present Value, C.U.**
Conservative	2019: FTTH_UDWDM_100	**99885**
Realistic	2019: FTTH_UDWDM_100	**236452**
Aggressive	2019: FTTH_UDWDM_100	**1352004**

Sensitivity Analysis

The sensitivity analysis has been applied to the converged planning scenario of Munich (urban) area. The other scenarios have been also implemented, tested and found to behave in the same way as the one presented in this section. Here we chose a scenario with no constraints on when or to which technology to migrate. Since different studies have different units of currency, like Pounds (GBP), Euros and Cost Unit, we converted all the currencies into cost units using the current currency conversion. Here 1 C.U. is fixed at 50 Euros or 44.97 GBP.

Component Costs Techno-economic studies depends on the input cost models, different cost models yield different expected NPVs. In this study, we took the costs mentioned in three different studies, namely Rokkas [57] (deploying GPON based technology in a generic urban area), Phillipson [58] (deploying HPON based technology in a Dutch city) and BSG [47] (FTTCab based deployment in London). As a further contribution, we collected data from each of these different studies and undertook the cost modeling for all the different deployment technologies. We then compared all the technologies with each other and with also the base case, which are the values taken from OASE [37].

Table 6.4.: Per Unit Component Costs from OASE [56], Phillipson [58] Rokkas [57], BSG [47]. ©IEEE/OSA 2019

Component	OASE, C.U.	Phillipson, C.U	Rokkas, C.U.	BSG, C.U.
Duct /m	1.12	0.54	0.7	1.42
Fiber /m	0.02	0.006	0.006	0.192
GPON OLT Card	40	50	70	288
XGPON OLT Card	80	55*	200	300*
WDM OLT Port Card	8.8	60*	200	350*
Power Splitter	1.8	2*	10	1.4*
AWG	2.2	2*	12*	2*
DSLAM+Cabinet	124	220	300	294
GPON ONU	1	5	2	1.6
XGPON ONU	1.8	5*	4	1.8*
WDMPON ONU	2.3	5*	5*	2.3*
HPON ONU	3.1	5.5*	5	3.1*

* Assumed according to model trends.

For each of the four studies, we run the migration algorithm and find the expected NPV and the migration steps. Both [57] and [58] are comparable in terms of cost to the OASE base model [56]. Table 6.4 gives a list of major component costs from each of the studies. Since not all the components used in our work were mentioned in every study, we assumed these components to follow the general model trends.

Figure 6.8 shows the per subscriber CapEx in cost units for selected 100 Mbps deployments in a converged scenario. It is clear that three of the four studies have comparable costs, with the only exception being BSG.

We see that as the component costs increases, the NPV decreases, which is the expected behavior. As seen in Table 6.5, except the OASE base case, the other components choose FTTB_HPON_100 as the final technology and prefer early migrations to reap maximum benefits. The only exception to this is the BSG costs in conservative and realistic scenarios, which suggests not undertaking any migrations. This is be-

cause of the high costs involved and no change in the ARPU. Since the BSG study was done for an expensive and densely populated city like London, it is possible that the ARPU would be higher than what is used in our analysis.

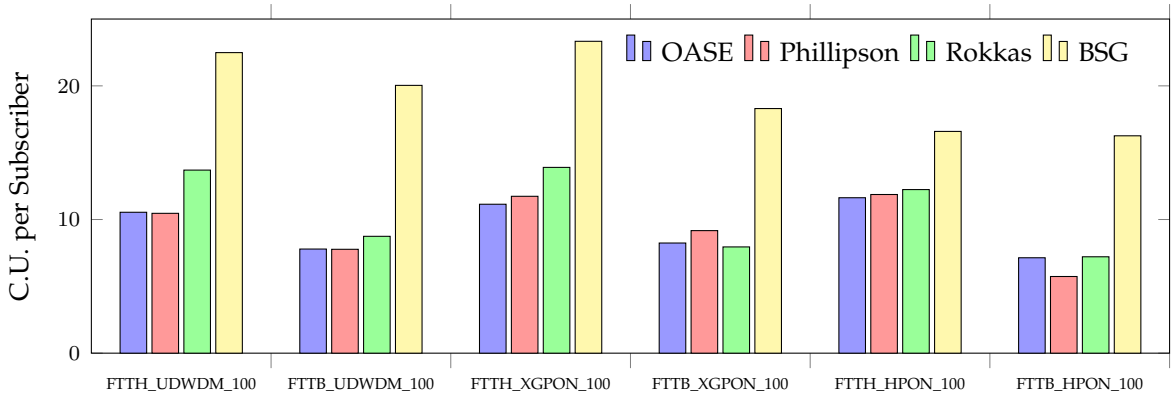

Figure 6.8.: CAPEX of selected deployments for different component costs in a converged scenario (OASE [56], Phillipson [58], Rokkas [57], BSG [47]).©IEEE/OSA 2019

Operational Expenditures

The final part of the sensitivity analysis includes an OpEx study. In many techno-economic works including [44] and [36], OpEx is considered as a fractional quantity of CapEx, which was originally modeled in [63]. This is because techno-economic researchers do not have access to component specific data like mean time to repair, energy consumption, component footprint and technician salaries.

Here, we choose two different OpEx models. The base model is already defined in Section 6.2. The percentage based OpEx model is taken from [36], where the OpEx of a technology t is defined as follows.

$$OPEX_t = 0.1 * C_{Elec_t} + 0.01 * C_{CW_t}, \tag{6.9}$$

where C_{Elec_t} and C_{CW_t} are the electronic and the civil works CapEx of a technology t, respectively.

As seen in Eq. (6.9), the OpEx is directly proportional to the CapEx values shown in Figure 6.5. For most technologies, the percentage based OpEx is cheaper per subscriber connected. However, in the case of FTTH based technologies, the newer OpEx model is between 0.25-1 C.U. higher, for every subscriber connected. Hence, the benefits of OpEx savings due to lower energy costs in FTTH architectures is not considered in this fraction based model.

From Table 6.6 we can infer that for a rough analysis, a percentage based OpEx model could be considered, keeping in mind the risk of underestimating the cost factors of various technologies.

Table 6.5.: Migration results of different component costs. ©IEEE/OSA 2019

OASE[56]		
Penetration Curve	**FTTx Migration Path**	**Net Present Value, C.U.**
Conservative	2019: FTTB_HPON_50 2020: FTTB_HPON_100	**190069**
Realistic	2019: FTTB_HPON_50 2020: FTTB_HPON_100	**325132**
Aggressive	2019: FTTB_UDWDM_100	**1429279**
Phillipson[58]		
Penetration Curve	**FTTx Migration Path**	**Net Present Value, C.U.**
Conservative	2019:FTTB_HPON_100	**122363**
Realistic	2019:FTTB_HPON_100	**221742**
Aggressive	2019:FTTB_HPON_100	**1055627**
Rokkas[57]		
Penetration Curve	**FTTx Migration Path**	**Net Present Value, C.U.**
Conservative	2019:FTTB_HPON_100	**75805**
Realistic	2019:FTTB_HPON_100	**175184**
Aggressive	2019:FTTB_HPON_100	**1009069**
BSG [47]		
Penetration Curve	**FTTx Migration Path**	**Net Present Value, C.U.**
Conservative	No Migrations	**37421**
Realistic	No Migrations	**53510**
Aggressive	2019: FTTB_HPON_100	**769030**

Table 6.6.: Migration results for different OPEX models. ©IEEE/OSA 2019

Base OpEx Model		
Penetration Curve	**FTTx Migration Path**	**Net Present Value, C.U.**
Conservative	2019: FTTB_HPON_50 2020: FTTB_HPON_100	**152401.51**
Realistic	2019: FTTB_HPON_50 2020: FTTB_HPON_100	**272726.55**
Aggressive	2019: FTTH_UDWDM_100	**1282631.54**
Percentage OpEx Model		
Penetration Curve	**FTTx Migration Path**	**Net Present Value, C.U.**
Conservative	2019: FTTB_HPON_50 2020: FTTB_HPON_100	**216007.47**
Realistic	2019: FTTB_HPON_50 2020: FTTB_HPON_100	**359372.65**
Aggressive	2019:FTTH_UDWDM_100	**1535318.70**

6.5. Summary and Discussion

In this chapter, we have looked at the converged network planning in the perspective of network evolution over time, i.e., migrations. We have put the overall (at the end of the life time) realistic network profitability as our main migration goal, leaving the final technology and architecture choice flexible. The final migration state is now chosen solely based on the maximal NPVs. It has shown interesting results, that the FTTH (commonly targeted as the final migration goal) often is less profitable as FTTB given the existing copper infrastructure. Further, we have accounted for the user uncertainty, i.e., user churn, by applying a rational agent (early stage AI) algorithm.

7. Conclusions

This chapter summarizes our conclusions on the dissertation. Here, we discuss our observations, results and their practical applications. The chapter is concluded with the outlook of the open research topics and possible future work.

7.1. Summary and Discussion

In this dissertation, we have looked into strategic network planning for converged ODNs, specifically for optical access and mobile backhaul convergence. As introduced in Chapter 1 and defined in Chapter 2, we have identified four main areas of interest of network planning: planning methodology, reliable communications, energy consumption minimization, network migration.

For the planning methodology, we have identified reproducibility and generality as two main issues that limit the contribution of strategic network planning studies and prevent the application of the research results to other use cases and generic studies. With our Automated Map-Based Strategic Fixed Network Planning Tool (AMS) [1], we allow reproducible network planning for a wide range of ODN scenarios from GPON to HPON (see Table 2.1 and Section 2.2 in Chapter 2) with and without link-disjoint protection, for homo- and heterogeneous demands. Geographic maps as the input for network planning result in not generalizable case studies. Geometric models lead to unpredictable cost under- and overestimations. We solve these problems with application of graph-based road topologies models [2], see Chapter 3.

Ultra-reliable communications require the average connection availabilities of not less than five nines. We address these requirements in Chapter 4. First, we look into fixed access network protection options [6] and wireless network protection options [7]. For the fixed access network, our reliability analysis shows that the bottlenecks of the connection availability are the serial components and the ODN connection availability with the investigated protection schemes is at least eight nines. For the heterogeneous wireless access network protection, we show on the implemented testbed and respective availability analysis that by switching between wireless technologies the five nine connection availability is achievable.

Energy consumption minimization is required from the ecological (reduce CO2 emissions) and economical (reduce costs) perspectives. We first look into the benefits of taking into account the activity patterns of heterogeneous demands, i.e., residential optical access and mobile backhaul (see Chapter 5). We show (as in [6]) that putting the equipment to sleep and dooze modes does not only save energy, but with the ap-

propriate protection scheme does not violate the delay requirements and does not significantly decrease the reliability. We also provide the measurements on the network-initiated equipment wake-ups over the state-of-the-art mobile network [5].

Finally, in Chapter 6 we have investigated network migration planning under user churn uncertainty with the goal of guaranteeing the project's profitability. Here, we have applied a rational agent based algorithm that maximizes the NPV and flexibly chooses the final migration state. This study was published in [9].

7.2. Outlook

There are multiple possible directions for the future work. First, in this dissertation we rely on the planning methodology from [43]. It is a heuristic, and a possible future study could be benchmarking the heuristic performance to the optimization. It could also include the problem of migrating from the microwave backhaul to the optical for different 5G RAN configurations, i.e., planning the x-haul.

The energy consumption studies could be improved with studies on the waking-up of the optical and ITS equipment. The studies could be further expanded to included generic ITS and not only the public transport. For the wireless reliability, it is important to define what constitutes a wireless failure and how to include the switching time in the availability analysis.

Finally, for the migration analysis other AI algorithms could be investigated and additional criteria as reliability and cost per Mbps can be take into account. An important aspect here is user adoption model and this could be another direction of investigation. A common problem for the NPs is the lack of new business models that would compensate for the declining revenues from the infrastructure.

A. OSM Clean-up Process

In this appendix, we describe the steps to clean-up an OSM map in ArcGIS. It is partially automated and we do not go in the code details. However, an interested reader can refer to [2] for the code implementation. Figure A.1 summarizes the OSM cleaning-up process. We follow this work flow in the description below.

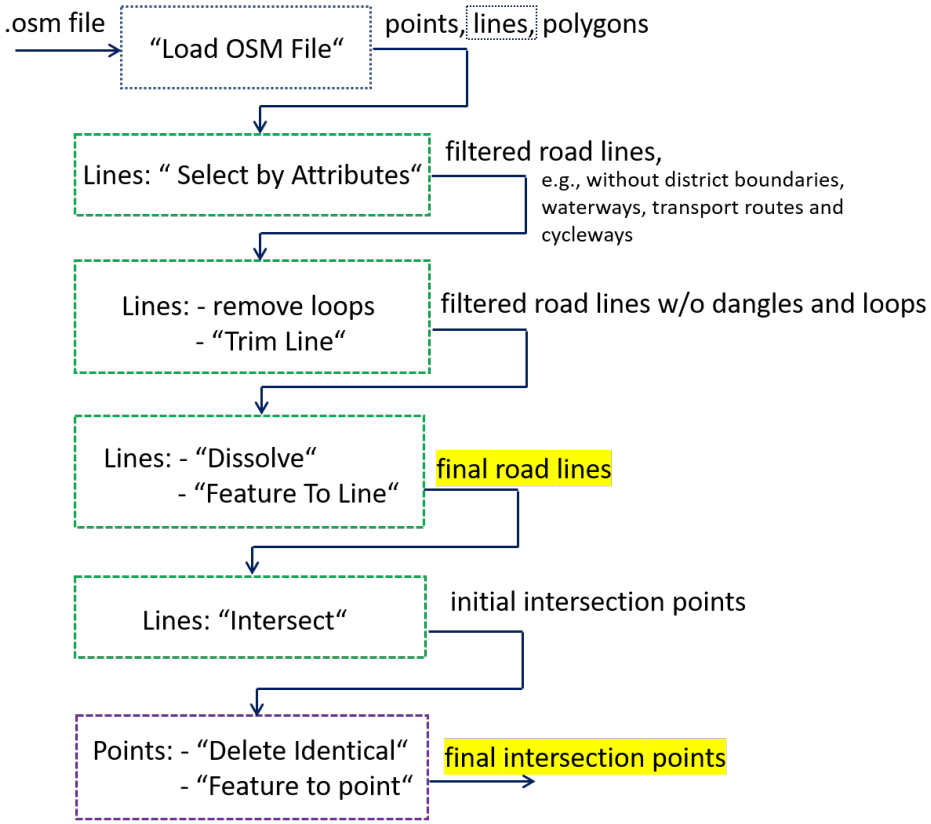

Figure A.1.: OSM clean-up process.

In Figure A.1, we use the following notation:

- Between the quotation marks we show the name of the used ArcGIS Tool, i.e., "ArcGIS Tool".
- On the left we show the type of input for the step and the box outline shows the processing steps with the same input type, e.g., lines input is used in the steps with the dashed green outline.

- On the right we show the output of the processing step. The highlighted in yellow outputs are the final outputs of the cleaning-up process.

First, an OSM map is loaded to the ArcMap (desktop application of ArcGIS) with a toolbox that has to be pre-installed. Figure A.2 shows the OpenStreetMap Toolbox as it is listed in ArcCatalog. The option "Load OSM File" imports from the .osm file the raw data (points, lines, polygons as shown in Figure 2.3 of Chapter 2).

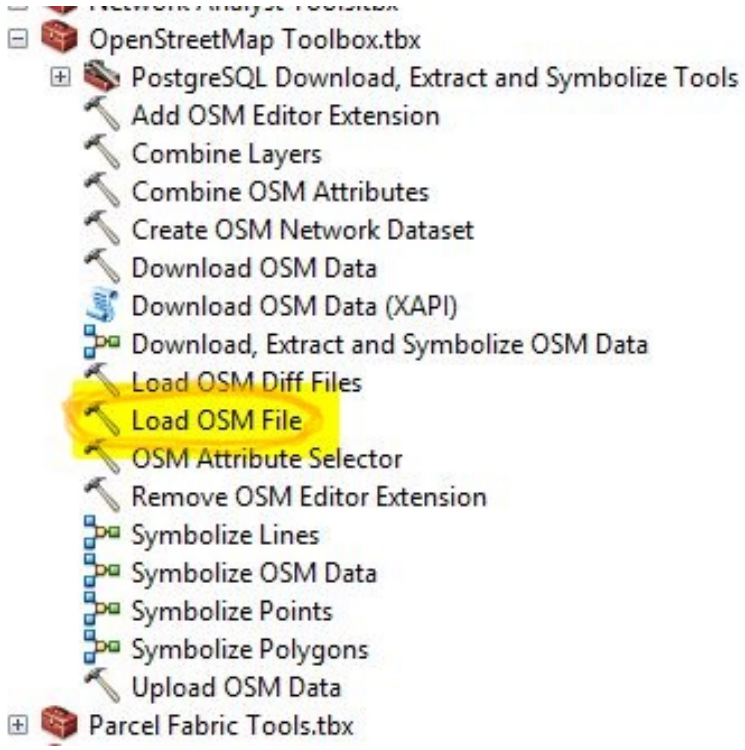

Figure A.2.: OpenStreetMap Toolbox for loading the .osm data to ArcMap. The highlighted in yellow "Load OSM File" option is used to load data from the .osm file. The loading result is shown in Figure 2.3 of Chapter 2.

From the loaded raw data, for the road modeling we use the lines (put in the frame in Figure A.1). The raw line data has all the information of the maps that is shown in lines. It includes district boundaries, waterways, transport routs (on- and underground), temporary ways, service roads, cycleways, etc. For the planning, only the road information is needed. This is why the lines data has to be filtered.

One of the pluses of ArcGIS is that it allows working with the map data as with the SQL-data base. Thus, when the structure of the data is known (how the road data is referred to), an SQL-query can be used to filter the needed data. The challenge here is in knowing the data structure as OSM is open source and generally not very consistent. So, for example, the expression for Munich looks different to Berlin. If not checked manually, this can result in unconnected road topology. Figure A.3 shows an example of initial data filtering with a simple SQL-query for the line data using the tool "Select by Attributes".

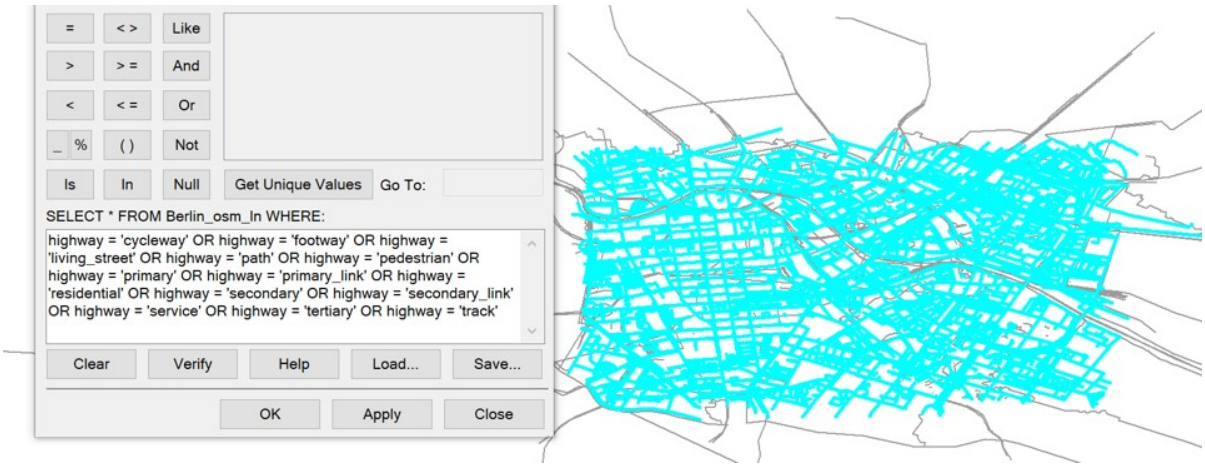

Figure A.3.: Example of "Select by Attributes" tool usage on line data: SQL-query and the selection visualization. The underlying thin gray lines are all the lines imported from .osm file. The thick turquoise lines are the selected in accordance with the SQL-query.

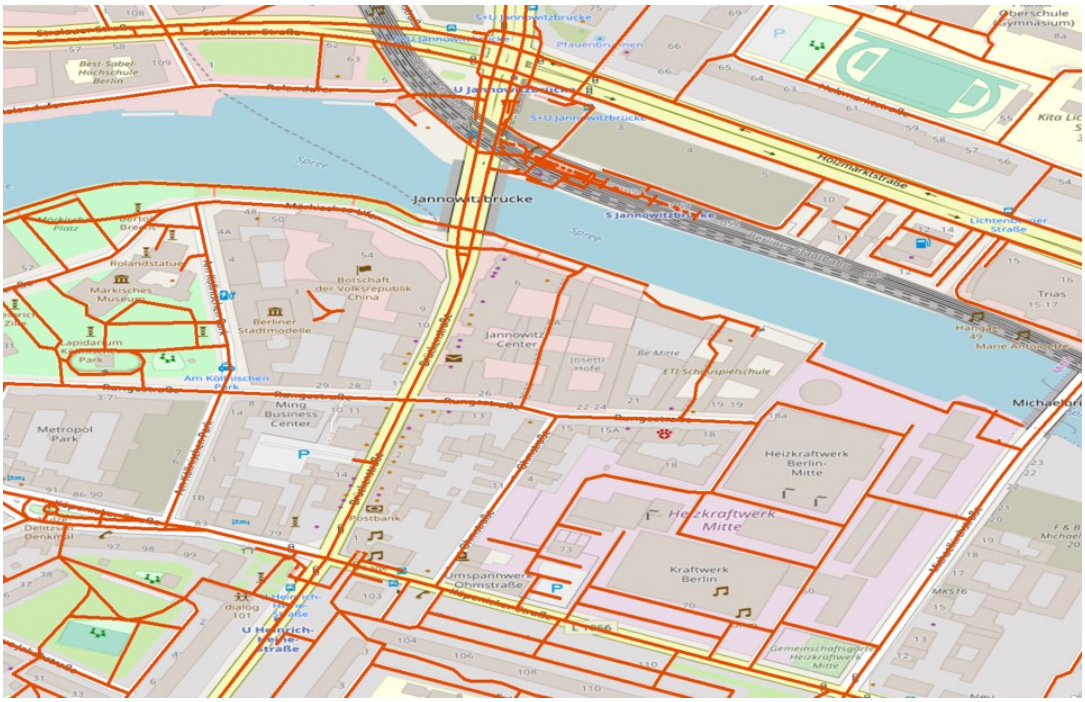

Figure A.4.: Close look on the selected line data with the underlying OSM visualization. Although it consists only of the lines that are marked as roads (red lines), the data is too noisy to be used for the strategic network planning: there are dangles, loops and other inconsistencies.

The results of the selection queries are controlled manually. The queries can be saved and then loaded to the selection tool later. The selection step can also be automated with Python, when there is no need in manual control, e.g., for a known dataset. Figure A.4 shows the resulting roads (thick red lines) after the selection from Figure A.3. We observe dangles, loops and free standing features.

After the selection, the dangles and free standing features are trimmed with a "Trim Line" tool and some of the lines removed manually according to the underlying graphical map representation. The loops in the topologies are either removed manually or with the script as presented in [2]. Figure A.5 shows the cleaned-up lines from Figure A.4. Here, we chose to remove the ways in historic parks and the roads that are less than 5 m apart. Note that there could be a number of alternative topology clean-up methods and rules of thumb. This is why for reproducibility it is important to include the underlying road topology model, as we do in [2].

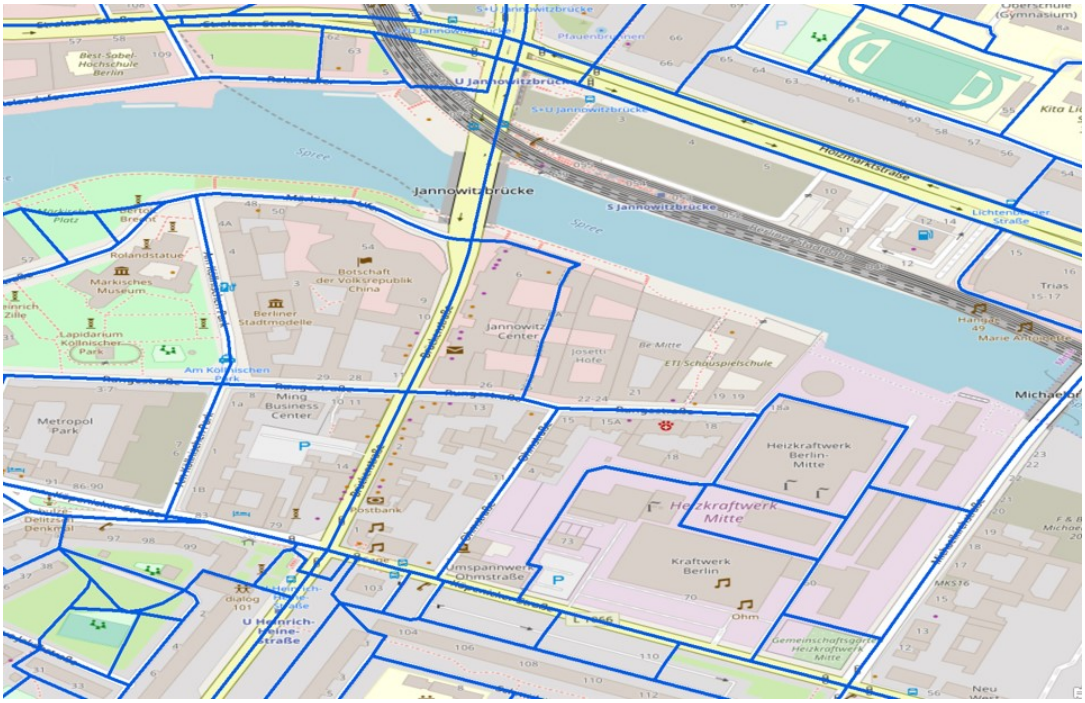

Figure A.5.: Close look on the cleaned-up line data: consistent road segments. The dangles, loops and inconsistencies were removed, the data can be used for strategic network planning.

Although the lines in Figure A.5 look consistent, there is one more step of processing. We illustrate this step with Figure A.6. In the left part of the figure, we see the resulting lines of the previous step and the automatically detected intersection. With the turquoise highlight we show a road segment, i.e., a line between two intersection points. When applying the tools "Dissolve" (creates a single part from the lines) and then "Feature to Line" (breaks single lines at intersections only), we obtain the road

segments with the break point only at the intersections as shown in the right part of the Figure A.6. Finally, we find all the intersection points of the cleaned-up road segments with the "Intersect" tool. We delete all the created duplicates with "Delete identical" tool and save the new point data class with "Feature to point" tool. These are our final road lines and final intersection points, see Figure A.1.

Figure A.6.: Close look on the cleaned-up line data: consistent road segments. The dangles, loops and inconsistencies were removed, the data can be used for strategic network planning.

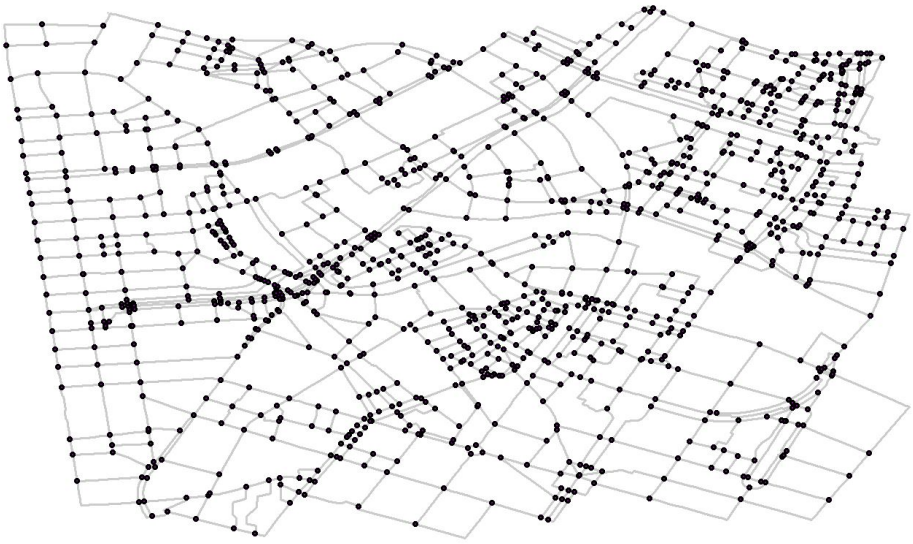

Figure A.7.: OSM data example that is used for strategic network planning.

Figure A.7 illustrates the cleaned-up OSM data ready for ArcGIS planning. Here, we show the result with a manual OSM clean-up, where there are no loops left. Figure 2.7

in Chapter 2 showed the BSs demands in the automatically cleaned-up from dangles and loops area (filtering was always manually controlled) and there are some loops left as some of them have intersections and thus are hard to distinguish automatically from the road segments.

Clean-up of the OSM maps is not the focus of the dissertation and is described here for completeness. In general, we use consistent OSM topologies that are published [2] for comparison purposes and possible further use.

List of Figures

List of Tables

Bibliography

Publications by the author

Cited in the dissertation:

[1] E. Grigoreva, "Automated Fixed Network Planning Tool," 2019.

[2] E. Grigoreva and S. K. Patri, "Abstract City Topologies Generation," 2019.

[3] S. K. Patri, E. Grigoreva, and C. Mas Machuca, "Converged Network Migration Planning," tech. rep., Elektrotechnik und Informationstechnik, 2018.

[4] E. Grigoreva, S. K. Patri, W. Kellerer, and C. Mas Machuca, "Evaluation of Graph-Based Road Topology Models for Strategic Network Planning," *submitted to IEEE/OSA Journal of Optical Communications and Networking*, 2019.

[5] E. Grigoreva, J. Xu, and W. Kellerer, "M2M Wake-Ups over Cellular Networks: Over-The-Top SIP," in *Proceedings of the 5th Workshop on All Things Cellular: Operations, Applications and Challenges*, ATC '16, pp. 37–42, ACM, 2016.

[6] E. Grigoreva, E. Wong, M. Furdek, L. Wosinska, and C. Mas Machuca, "Energy Consumption and Reliability Performance of Survivable Passive Optical Converged Networks: Public ITS Case Study," *IEEE/OSA Journal of Optical Communications and Networking*, vol. 9, pp. C98–C108, Apr 2017.

[7] E. Grigoreva, D. Shrivastava, C. Mas Machuca, W. Kellerer, J. Dittrich, H. Wilk, and H. Zimmermann, "Heterogeneous Wireless Access Network Protection for Ultra-Reliable Communications," in *2017 IEEE Vehicular Networking Conference (VNC)*, pp. 17–22, Nov 2017.

[8] E. Grigoreva, C. Mas Machuca, and W. Kellerer, "Optical Backhaul Network planning for DSRC-based Public Intelligent Transportation System: a Case Study," in *2016 18th International Conference on Transparent Optical Networks (ICTON)*, pp. 1–4, July 2016.

[9] S. K. Patri, E. Grigoreva, W. Kellerer, and C. Mas Machuca, "Rational Agent-Based Decision Algorithm for Strategic Converged Network Migration Planning," *IEEE/OSA Journal of Optical Communications and Networking*, vol. 11, no. 7, pp. 371–382, 2019.

Other publications:

[10] E. Grigoreva, M. Laurer, M. Vilgelm, T. Gehrsitz, and W. Kellerer, "Coupled Markovian Arrival Process for Automotive Machine Type Communication Traffic Modeling," in *2017 IEEE International Conference on Communications (ICC)*, pp. 1–6, May 2017.

[11] E. Wong, E. Grigoreva, L. Wosinska, and C. Mas Machuca, "Enhancing the Survivability and Power Savings of 5G Transport Networks Based on DWDM Rings," *IEEE/OSA Journal of Optical Communications and Networking*, vol. 9, pp. D74–D85, Sept 2017.

[12] E. Grigoreva, V. Grigoryev, I. Khvorov, Y. Raspaev, and W. Kellerer, "Techno-Economic Case Study on Dedicated RAN for an Intelligent Transportation System: Impact of the Legislation-Driven Costs," *NETNOMICS: Economic Research and Electronic Networking*, vol. 18, pp. 23–41, May 2017.

[13] I. Dlas, E. Grigoreva, C. Mas Machuca, L. Wosinska, and E. Wong, "Delay-Constrained Framework for Road Safety and Energy-Efficient Intelligent Transportation Systems," in *43rd European Conference on Optical Communication, ECOC 2017, Gothenburg, Sweden, 17 September 2017 through 21 September 2017*, pp. 1–3, Institute of Electrical and Electronics Engineers (IEEE), 2018.

General publications

[14] European Telecommunications Network Operators' Association, "The State of Digital Communications 2019: Ideas, facts and figures on the sector," 2019.

[15] A. Khan, W. Kellerer, K. Kozu, and M. Yabusaki, "Network sharing in the next mobile network: Tco reduction, management flexibility, and operational independence," *IEEE Communications Magazine*, vol. 49, no. 10, pp. 134–142, 2011.

[16] M. Grötschel, C. Raack, and A. Werner, "Towards optimizing the deployment of optical access networks," *EURO Journal on Computational Optimization*, vol. 2, no. 1-2, pp. 17–53, 2014.

[17] S. Verbrugge, S. Pasqualini, F.-J. Westphal, M. Jäger, A. Iselt, A. Kirstädter, R. Chahine, D. Colle, M. Pickavet, and P. Demeester, "Modeling Operational Expenditures for Telecom Operators," in *Proceedings of Conference on Optical Network Design and Modeling*, pp. 455–466, 2005.

[18] M. Jaber, M. A. Imran, R. Tafazolli, and A. Tukmanov, "5G Backhaul Challenges and Emerging Research Directions: A Survey," *IEEE access*, vol. 4, pp. 1743–1766, 2016.

[19] J. M. Simmons, *Optical Network Design and Planning*. Springer, 2014.

[20] Conservation, GPON Power, "ITU-T G-Series Recommendations-Supplement 45 (G. sup45)," *ITU-T*, 2009.

[21] P. Monti, S. Tombaz, L. Wosinska, and J. Zander, "Mobile backhaul in heterogeneous network deployments: Technology options and power consumption," in *2012 14th International Conference on Transparent Optical Networks (ICTON)*, pp. 1–7, July 2012.

[22] British Standard, "BS 4778 (1991): Glossary of terms used in quality assurance (including reliability and maintainability)," *British Standards Institution, London*.

[23] S. Gosselin, A. Pizzinat, X. Grall, D. Breuer, E. Bogenfeld, S. Krauß, J. A. T. Gijón, A. Hamidian, N. Fonseca, and B. Skubic, "Fixed and Mobile Convergence: Which Role for Optical Networks?," *Journal of Optical Communications and Networking*, vol. 7, no. 11, pp. 1075–1083, 2015.

[24] Z. Pi and F. Khan, "System Design and Network Architecture for a Millimeter-Wave Mobile Broadband (MMB) System," in *34th IEEE Sarnoff Symposium*, pp. 1–6, May 2011.

[25] G. Chen, G. Esch, P. Wonka, P. Müller, and E. Zhang, "Interactive Procedural Street Modeling," in *ACM transactions on graphics (TOG)*, vol. 27, p. 103, ACM, 2008.

[26] FTTH Council, "FTTH Handbook. Version 7 of February 2016," 2016.

[27] T. Delmarcelle and L. Hesselink, "The Topology of Symmetric, Second-Order Tensor Fields," in *Proceedings of the conference on Visualization*, pp. 140–147, IEEE Computer Society Press, 1994.

[28] K. R. Gabriel and R. R. Sokal, "A New Statistical Approach to Geographic Variation Analysis," *Systematic zoology*, vol. 18, no. 3, pp. 259–278, 1969.

[29] D. W. Matula and R. R. Sokal, "Properties of Gabriel Graphs Relevant to Geographic Variation Research and the Clustering of Points in the Plane," *Geographical analysis*, vol. 12, no. 3, pp. 205–222, 1980.

[30] D. Maniadakis and D. Varoutas, "Incorporating Gabriel Graph Model for FTTx Dimensioning," *Photonic Network Communications*, vol. 29, no. 2, pp. 214–226, 2015.

[31] D. Gardan, A. Zaganiaris, A. Madani, R. Madigou, and D. Machon, "Techno-Economics of Advanced Optical Subscriber Networks," in *Global Telecommunications Conference and Exhibition'Communications Technology for the 1990s and Beyond'(GLOBECOM), 1989. IEEE*, pp. 1335–1339, IEEE, 1989.

[32] B. Jobard and W. Lefer, "Creating Evenly-Spaced Streamlines of Arbitrary Density," in *Visualization in Scientific Computing'97*, pp. 43–55, Springer, 1997.

[33] C. Raack, J. M. Garcia, and R., "Centralised versus Distributed Radio Access Networks: Wireless Integration into Long Reach Passive Optical Networks," in *Telecommunication, Media and Internet Techno-Economics (CTTE), 2015 Conference of*, pp. 1–8, IEEE, 2015.

[34] S. Türk, J. Noack, R. Radeke, and R. Lehnert, "Strategic Migration Optimization of Urban Access Networks Using Meta-Heuristics," *2014 26th International Teletraffic Congress, ITC 2014*, 2014.

[35] FTTH Council, "FTTH Business Guide," tech. rep., Fiber-to-the-Home Council Europe, 2016.

[36] M. Tahon, S. Verbrugge, D. Colle, M. Pickavet, P. J. Willis, and P. Botham, "Migration to Next Generation Access Networks: A Real Option Approach," *16th Annual International Conference on Real Options, Proceedings*, pp. 1–11, 2012.

[37] OASE, "Technical Assessment and Comparison of Next-Generation Optical Access System Concepts," *Deliverable 4.2. 1*, pp. 40–68, 2011.

[38] European Commission on Digital Single Market, "Strategy & Policy on Broadband Europe: Digital Single Market," 2014.

[39] R. Zhao, L. Zhou, and C. Mas Machuca, "Dynamic Migration Planning Towards FTTH," *Proceedings of 2010 14th International Telecommunications Network Strategy and Planning Symposium, Networks 2010*, 2010.

[40] R. Romero Reyes, R. Zhao, and C. Mas Machuca, "Advanced Dynamic Migration Planning towards FTTH," *IEEE Communications Magazine*, vol. 52, pp. 77–83, Jan 2014.

[41] S. Türk, X. Liu, R. Radeke, and R. Lehnert, "Particle Swarm Optimization of Network Migration Planning," *GLOBECOM - IEEE Global Telecommunications Conference*, pp. 2230–2235, 2013.

[42] FTTH Council Europe, "Case Studies Collection," no. February, 2015.

[43] A. Shahid and C. Mas Machuca, "Dimensioning and Assessment of Protected Converged Optical Access Networks," *IEEE Communications Magazine*, vol. 55, no. 8, pp. 179–187, 2017.

[44] S. Van der Merwe, C. Gruber, Y. Grigoreva, and T. Kessler, "A Model-Based Techno-Economic Comparison of Optical Access Technologies," *GLOBECOM Workshops, 2009 IEEE*, pp. 1–6, 2009.

[45] J. Chen, L. Wosinska, C. Mas Machuca, and M. Jaeger, "Cost vs. Reliability Performance Study of Fiber Access Network Architectures," *IEEE Communications Magazine*, vol. 48, no. 2, pp. 56–65, 2010.

[46] J. Mun, "Real Options Analysis versus Traditional DCF Valuation in Layman's Terms," *Managing Enterprise Risk: What the Electric Industry Experience Implies for Contemporary Business*, pp. 75–106, 2006.

[47] Analysys Mason, "The Costs of deploying Fibre-based Next-generation Broadband Infrastructure," *Final report for the Broadband Stakeholder Group, Ref: 12726-371*, no. September, 2008.

[48] C. Mas Machuca, "Lecture slides in Techno-economic Analysis for Telecommunication Networks," October 2017.

[49] Jones Lang Lassalle GmbH, "Residential City Profile Munich," Tech. Rep. 1, 2016.

[50] Government of New York City, "New York City Mandatory Inclusionary Housing," tech. rep., 2018.

[51] A. Mitcsenkov, M. Kantor, K. Casier, B. Lannoo, K. Wajda, J. Chen, and L. Wosinska, "Geographic Model for Cost Estimation of FTTH deployment: Overcoming Inaccuracy in Uneven-populated areas," *2010 Asia Communications and Photonics Conference and Exhibition, ACP 2010*, pp. 397–398, 2010.

[52] K. Casier, *Techno-economic Evaluation of a Next Generation Access Network Deployment in a Competitive Setting*. PhD thesis, Ghent University, 2009.

[53] M. Van der Wee, S. Verbrugge, M. Tahon, D. Colle, and M. Pickavet, "Evaluation of the Techno-Economic Viability of Point-to-Point Dark Fiber Access Infrastructure in Europe," *Journal of Optical Communications and Networking*, vol. 6, no. 3, p. 238, 2014.

[54] D. Klein, "Lecture Notes in CS 188: Artificial Intelligence Fall 2010 Expectimax Search," 2010.

[55] S. J. Russell and P. Norvig, *Artificial Intelligence: A modern approach*. Pearson Education, Inc., 3 ed., 2010.

[56] OASE, "OASE Value Network Evaluation Deliverable 6.3," tech. rep., OASE, 2013.

[57] T. Rokkas, "Techno-Economic Analysis of PON Architectures for FTTH deployments: Comparison between GPON, XGPON and NG-PON2 for a Greenfield Operator," in *Telecommunication, Media and Internet Techno-Economics (CTTE), 2015 Conference of*, pp. 1–8, IEEE, 2015.

[58] F. Phillipson, C. Smit-Rietveld, and P. Verhagen, "Fourth Generation Broadband Delivered by Hybrid FTTH Solution – A Techno-economic Study," *Journal of Optical Communications and Networking*, vol. 5, no. 11, pp. 1328–1342, 2013.

[59] K. McMahon and P. Salant, "Strategic planning for telecommunications in rural communities," *Rural Development Perspectives*, vol. 14, pp. 2–7, 1999.

[60] M. Rahman, C. Mas Machuca, K. Grobe, and W. Kellerer, "Advantages of Joint Access Network Planning in Dense Populated Areas," in *19th European Conference on Network and Optical Communications, NOC 2014*, June 2014.

[61] M. Forzati, C. Mattsson, K. Wang, and C. P. Larsen, "The Uncaptured Value of FTTH Networks," in *2011 13th International Conference on Transparent Optical Networks*, pp. 1–4, June 2011.

[62] D. S. Remer and A. P. Nieto, "A Compendium and Comparison of 25 Project Evaluation techniques. Part 1: Net Present Value and Rate of Return Methods," *International Journal of Production Economics*, vol. 42, no. 1, pp. 79–96, 1995.

[63] S. Verbrugge, D. Colle, M. Pickavet, P. Demeester, S. Pasqualini, A. Iselt, A. Kirstädter, R. Hülsermann, F.-J. Westphal, and M. Jäger, "Methodology and Input Availability Parameters for Calculating OpEx and CapEx costs for Realistic Network Scenarios," *Journal of Optical Networking*, vol. 5, no. 6, pp. 509–520, 2006.

[64] A. Mitcsenkov, M. Kantor, K. Casier, B. Lannoo, K. Wajda, J. Chen, and L. Wosinska, "Geometric Versus Geographic Models for the Estimation of an FTTH Deployment," *Telecommunication Systems*, vol. 54, no. 2, pp. 113–127, 2013.

[65] C. Mas Machuca, J. Chen, and L. Wosinska, "Cost-EfficientPprotection in TDM PONs," *IEEE Communications Magazine*, vol. 50, no. 8, pp. 110–117, 2012.

[66] 3GPP, "TS 23.682: Architecture enhancements to facilitate communications with packet data networks and applications," tech. rep., March 2015.

[67] 3GPP, "TS 03.40: Technical realization of the Short Message Service (SMS)," tech. rep., May 2003.

[68] D. Boswarthick, O. Elloumi, and O. Hersent, eds., *M2M Communications: A Systems Approach, Section 6.3*. Wiley, 2012.

[69] J. Rosenberg, "SIMPLE Made Simple: An Overview of the IETF Specifications for Instant Messaging and Presence Using the Session Initiation Protocol (SIP)," tech. rep., April 2013.

[70] B. Campbell, J. Rosenberg, H. Schulzrinne, C. Huitema, and D. Gurle, "Session Initiation Protocol (SIP) Extension for Instant Messaging," tech. rep., Network Working Group, 2002.

[71] Y. Agarwal, R. Chandra, A. Wolman, P. Bahl, K. Chin, and R. Gupta, "Wireless Wakeups Revisited: Energy Management for VoIP over Wi-Fi Smartphones," in *Proceedings of the 5th International Conference on Mobile Systems, Applications and Services*, MobiSys '07, pp. 179–191, ACM, 2007.

[72] T. Pering, Y. Agarwal, R. Gupta, and R. Want, "CoolSpots: Reducing the Power Consumption of Wireless Mobile Devices with Multiple Radio Interfaces," in *Proceedings of the 4th International Conference on Mobile Systems, Applications and Services*, MobiSys '06, pp. 220–232, ACM, 2006.

[73] E. Shih, P. Bahl, and M. J. Sinclair, "Wake on Wireless: An Event Driven Energy Saving Strategy for Battery Operated Devices," in *Proceedings of the 8th Annual International Conference on Mobile Computing and Networking*, MobiCom '02, pp. 160–171, ACM, 2002.

[74] Nokia, "Nokia LTE M2M: Optimizing LTE for the Internet of Things," tech. rep., 2014.

[75] R. Pries, T. Hobfeld, and P. Tran-Gia, "On the Suitability of the Short Message Service for Emergency Warning Systems," in *Vehicular Technology Conference, 2006. VTC 2006-Spring. IEEE 63rd*, vol. 2, pp. 991–995, May 2006.

[76] N. Maskey, S. Horsmanheimo, and L. Tuomimäki, "Latency analysis of LTE network for M2M applications," in *Telecommunications (ConTEL), 2015 13th International Conference on*, pp. 1–7, July 2015.

[77] I. Demirkol, C. Ersoy, and E. Onur, "Wake-up Receivers for Wireless Sensor Networks: Benefits and Challenges," *IEEE Wireless Communications*, vol. 16, pp. 88–96, August 2009.

[78] N. M. Pletcher, S. Gambini, and J. M. Rabaey, "A 2GHz 52 μW Wake-Up Receiver with -72dBm Sensitivity Using Uncertain-IF Architecture," in *2008 IEEE International Solid-State Circuits Conference - Digest of Technical Papers*, pp. 524–633, February 2008.

[79] M. Starsinic, A. S. I. Mohamed, G. Lu, D. Seed, B. Aghili, C. Wang, S. Palanisamy, and P. Murthy, "An IP-based Triggering Method for LTE MTC Devices," in *2015 Wireless Telecommunications Symposium (WTS)*, pp. 1–6, April 2015.

[80] C. Gessner and O.Gerlach, "Voice and SMS in LTE." White paper, 2014.

[81] B. Ford, P. Srisuresh, and D. Kegel, "Peer-to-peer Communication Across Network Address Translators," in *Proceedings of the Annual Conference on USENIX Annual Technical Conference*, ATEC '05, pp. 13–13, 2005.

[82] C. Schwartz, T. Hossfeld, F. Lehrieder, and P. Tran-Gia, "Angry Apps: The Impact of Network Timer Selection on Power Consumption, Signalling Load, and Web QoE," *Journal of Computer Networks and Communications*, 2013.

[83] R. Urata, C. Lam, H. Liu, and C. Johnson, "High Performance, Low Cost, Colorless ONU for WDM-PON," in *National Fiber Optic Engineers Conference*, pp. 1–3, Optical Society of America, 2012.

[84] C. Lange, R. Hülsermann, D. Kosiankowski, F. Geilhardt, and A. Gladisch, "Effects of network Node Consolidation in Optical Access and Aggregation Networks on Costs and Power Consumption," in *Optical Metro Networks and Short-Haul Systems II*, vol. 7621, p. 76210F, International Society for Optics and Photonics, 2010.

[85] M. Forzati, A. Bianchi, J. Chen, K. Grobe, B. Lannoo, C. Mas Machuca, J.-C. Point, B. Skubic, S. Verbrugge, E. Weis, *et al.*, "Next-generation optical access seamless evolution: Concluding results of the European FP7 project OASE," *IEEE/OSA Journal of Optical Communications and Networking*, vol. 7, no. 2, pp. 109–123, 2015.

[86] A. Shahid, C. Mas Machuca, L. Wosinska, and J. Chen, "Comparative Analysis of Protection Schemes for Fixed Mobile Converged Access Networks Based on Hybrid PON," in *Telecommunication, Media and Internet Techno-Economics (CTTE), 2015 Conference of*, pp. 1–7, IEEE, 2015.

[87] E. Wong, C. Mas Machuca, and L. Wosinska, "Survivable Hybrid Passive Optical Converged Network Architectures Based on Reflective Monitoring," *Journal of Lightwave Technology*, vol. 34, no. 18, pp. 4317–4328, 2016.

[88] E. Wong, C. Mas Machuca, and L. Wosinska, "Survivable Architectures for Power-Savings Capable converged Access Networks," in *2016 IEEE International Conference on Communications (ICC)*, pp. 1–7, IEEE, 2016.

[89] K. Dar, M. Bakhouya, J. Gaber, M. Wack, P. Lorenz, *et al.*, "Wireless Communication Technologies for ITS Applications," *IEEE Communications Magazine*, vol. 48, no. 5, pp. 156–162, 2010.

[90] Z. H. Mir and F. Filali, "LTE and IEEE 802.11 p for Vehicular Networking: a Performance Evaluation," *EURASIP Journal on Wireless Communications and Networking*, vol. 2014, no. 1, p. 89, 2014.

[91] J. Harding, G. Powell, R. Yoon, J. Fikentscher, C. Doyle, D. Sade, M. Lukuc, J. Simons, and J. Wang, "Vehicle-to-Vehicle Communications: Readiness of V2V Technology for Application," tech. rep., 2014.

[92] R. Bera, J. Bera, S. Sil, S. Dogra, N. B. Sinha, and D. Mondal, "Dedicated Short Range Communications (DSRC) for Intelligent Transport System," in *Wireless and Optical Communications Networks, 2006 IFIP International Conference on*, pp. 5–pp, IEEE, 2006.

[93] E. Wong, M. Mueller, M. P. I. Dias, C. A. Chan, and M. C. Amann, "Energy-Efficiency of Optical Network Units with Vertical-Cavity Surface-Emitting Lasers," *Optics express*, vol. 20, no. 14, pp. 14960–14970, 2012.

[94] ITU, "Recommendation G.775 (10/98): Loss of Signal (LOS), Alarm Indication Signal (AIS) and Remote Defect Indication (RDI) defect detection and clearance criteria for PDH signals," 1998.

[95] C. Mas Machuca, E. Wong, M. Furdek, and L. Wosinska, "Energy Consumption and Reliability Performance of Survivable Hybrid Passive Optical Converged Networks," in *Photonic Networks and Devices*, pp. NeTu3C–2, Optical Society of America, 2016.

[96] J. Gozálvez, M. Sepulcre, and R. Bauza, "IEEE 802.11 p Vehicle to Infrastructure Communications in Urban Environments," *IEEE Communications Magazine*, vol. 50, no. 5, 2012.

[97] M. Rausand, "Introduction to Reliability Engineering," *Risk and reliability in marine technology,(Ed. CG Soares)*, pp. 371–381, 1998.

[98] S. McGettrick, F. Slyne, N. Kitsuwan, D. B. Payne, and M. Ruffini, "Experimental End-to-End Demonstration of Shared N: M Dual-Homed Protection in SDN-Controlled Long-Reach PON and pan-European Core," *Journal of Lightwave Technology*, vol. 34, no. 18, pp. 4205–4213, 2016.

[99] ETSI, TCITS, "Intelligent Transport Systems (ITS); Vehicular Communications; Basic Set of Applications; Definitions," tech. rep., Tech. Rep. ETSI TR 102 638, 2009.

[100] E. Wong and K.-L. Lee, "Characterization of Highly-Sensitive and Fast-Responding Monitoring Module for Extended-Reach Passive Optical Networks," *Optics express*, vol. 20, no. 8, pp. 9019–9030, 2012.

[101] M. Vogt, R. Martens, and T. Andvaag, "Availability Modeling of Services in IP Networks," in *Design of Reliable Communication Networks, 2003.(DRCN 2003). Proceedings. Fourth International Workshop on*, pp. 167–172, IEEE, 2003.

[102] A. Dixit, B. Lannoo, D. Colle, M. Pickavet, and P. Demeester, "Wavelength swichted hybrid tdma/wdma pon: A flexible next generation optical access solution [invited]," *in Proc. of Transparent Optical Networks (ICTON)*, 2014.

[103] J. Chen and L. Wosinska, "Analysis of protection schemes in pon compatible with smooth migration from tdm-pon to hybrid wdm/tdm-pon," *Journal of optical networking*, vol. 6, no. 5, pp. 514–526, 2007.

[104] N. Nadarajah, A. Nirmalathas, and E. Wong, "Self-protected ethernet passive optical networks using coarse wavelength division multiplexed transmission," *Electronics letters*, vol. 41, no. 15, pp. 866–867, 2005.

[105] M. A. Esmail and H. Fathallah, "Fiber fault management and protection solution for ring-and-spur wdm/tdm long-reach pon," in *2011 IEEE Global Telecommunications Conference-GLOBECOM 2011*, pp. 1–5, IEEE, 2011.

[106] A. Shahid, C. Mas Machuca, L. Wosinska, and J. Chen, "Comparative Analysis of Protection Schemes for Fixed Mobile Converged Access Networks Based on Hybrid PON," in *2015 Conference of Telecommunication, Media and Internet Techno-Economics (CTTE)*, pp. 1–7, IEEE, 2015.

[107] A. Shahid and C. Mas Machuca, "Enhanced dimensioning and comparative analysis of different protection schemes for hybrid pon converged access networks (hpcan)," 2015.

[108] J. Baliga, R. Ayre, K. Hinton, W. V. Sorin, and R. S. Tucker, "Energy consumption in optical ip networks," *Journal of Lightwave Technology*, vol. 27, no. 13, pp. 2391–2403, 2009.

[109] E. Wong, M. Mueller, M. P. Dias, C. A. Chan, and M. C. Amann, "Energy-efficiency of optical network units with vertical-cavity surface-emitting lasers," *Optics express*, vol. 20, no. 14, pp. 14960–14970, 2012.

[110] M. N. Dilber, R. Sajjad, and S. Mohammad, "Comparative Analysis of Traditional Telephone and VoIP Systems," *Journal of Independent Studies and Research*, vol. 12, no. 1, p. 25, 2014.

[111] P. Stavroulakis, *Terrestrial Trunked radio-TETRA: a global security tool*. Springer Science & Business Media, 2007.

[112] A. K. Salkintzis, "Evolving Public Safety Communication Systems by Integrating WLAN and TETRA Networks," *IEEE Communications Magazine*, vol. 44, no. 1, pp. 38–46, 2006.

[113] A. P. Avramova, L. Dittmann, and S. Michail, "MIH based Mobility for TETRA-LTE Network," in *Proceedings of ICT Innovations*, 2013.

[114] A. Amditis, A. Oliveira, C. A. Grazia, C. Katsigiannis, D. Kanakidis, E. Sdongos, H. Gierszal, J. Jackson, K. Romanowski, M. Casoni, M. Klapez, N. Patriciello, P. Simplicio, and S. Sonander, "Integration between Terrestrial and Satellite Networks: the PPDR-TC Vision," in *2014 IEEE 10th International Conference on Wireless and Mobile Computing, Networking and Communications (WiMob)*, pp. 77–84, 2014.

[115] A. Pigni, F. Arreghini, P. Danielli, and R. Agrone, "Heterogeneous Network Testbed for Tactical Communication in Shore Scenario," in *MILCOM 2015 - 2015 IEEE Military Communications Conference*, pp. 483–488, 2015.

[116] B. Canberk, G. A. Shah, O. B. Akan, and O. Ergul, "Adaptive and Cognitive Communication Architecture for Next-Generation PPDR Systems," *IEEE Communications Magazine*, vol. 54, no. 4, pp. 92–100, 2016.

[117] M. A. Alamoud and W. Schütz, "Okumura-Hata Model Tuning for TETRA Mobile Radio Networks in Saudi Arabia," in *2nd International Conference on Advances in Computational Tools for Engineering Applications (ACTEA)*, pp. 47–51, 2012.

[118] A. Bavarva, A. Dave, A. Singh, and H. Soni, "MATLAB Simulation Based Various Path Loss Prediction Model," pp. 1157–1160, 2015.

[119] Hytera, "TETRA Hand-Held Radio," tech. rep., Hytera Mobilfunk GmbH, Bad Münder, Germany, 2014.

[120] National Telecommunications and Information Administration, "The Equipment Characteristics for LTE FDD Transmitters and Receivers," tech. rep., Washington, DC, 2017.

[121] Alcatel Lucent, "BB 400 Solution LTE Practical Training," tech. rep., 2017.

[122] Airbus Defense and Space, "TETRA System Release 7.0," tech. rep., 2016.

[123] R. Gandhi, *Empirical Path Loss Model for Outdoor 802.11b Wireless Links*. PhD thesis, IIT Kanpur, 2003.

[124] H. Aida, K. Rojviboonchai, and T. Osuga, "R-M/TCP: Protocol for Reliable Multi-Path Transport over the Internet," in *19th International Conference on Advanced Information Networking and Applications (AINA'05) Volume 1 (AINA papers)*, vol. 1, pp. 801–806, March 2005.

[125] M. Rentschler and P. Laukemann, "Performance Analysis of Parallel Redundant WLAN," in *Proceedings of 2012 IEEE 17th International Conference on Emerging Technologies Factory Automation (ETFA 2012)*, pp. 1–8, September 2012.

[126] P. Popovski, "Ultra-reliable communication in 5G wireless systems," in *1st International Conference on 5G for Ubiquitous Connectivity*, pp. 146–151, November 2014.

[127] E. Wong, M. P. I. Dias, and L. Ruan, "Predictive Resource Allocation for Tactile Internet Capable Passive Optical LANs," *Journal of Lightwave Technology*, vol. 35, pp. 2629–2641, July 2017.

Cited websites

[128] Redlands, CA: Environmental Systems Research Institute (ESRI), "Algorithms used by the ArcGIS Network Analyst extension," 2019.

[129] Redlands, CA: Environmental Systems Research Institute, (ESRI), "Arcgis desktop: Release 10.3.1."

[130] iqgeo, "myWorld Fiber Planning - Communications."

[131] Redlands, CA: Environmental Systems Research Institute, (ESRI), "Planning Fiber-to-the-Home Construction in Three Hours."

[132] 3-gis, "Fiber Network Management Solutions: Built for information, Engineered for performance."

[133] comsof, "Software for FTTx Network Planning and Design, formerly FIBERPLANIT."

[134] vetrofibermap, "Fiber Management: From Strategy to Splice."

[135] OpenStreetMap contributors, "Planet dump retrieved from https://planet.osm.org4," 2017.

[136] Huawei, "Huawei ME909u-521 - 4G/LTE - Mini PCI Express - EU/ASIA."

[137] "AT&T reiterates previous plans to shut down its GSM-based 2G network by end of 2016, citing need to refarm spectrum."

[138] "VoLTE: Voice over LTE; Alles über "echte" Telefonie via 4G Mobilfunknetze."

[139] Tarifverbund, Münchner Verkehrs- und Tarifverbund, "Journey planner: Timetable page," 2018.

[140] B. Berry, D. Satterwhite, S. Jury, S. Ratliff, and R. Taylor, "Internet-Draft Dynamic Link Exchange Protocol (DLEP)," 2017.

[141] G. Combs, "Wireshark."

[142] H. Rogge, "http://www.olsr.org/."

[143] B. A. Mah, J. Dugan, J. Poskanzer, K. Prabhu, and S. Elliott, "iperf3."

[144] premiertek.net, "WLAN Specifications (Long Distance)."

[145] Cassidian Communication GmbH, "HPM Description and Interfaces," 2014.

[146] S. K. Patri, "ExpectiMigPlan: An AI-based Network Planning tool," 2018.